

CHARACTERIZATION OF BAINITIC AND MARTENSITIC
MICROSTRUCTURES IN BEARING STEELS

A THESIS SUBMITTED TO
THE GRADUATE SCHOOL OF NATURAL AND APPLIED SCIENCES
OF
MIDDLE EAST TECHNICAL UNIVERSITY

BY

ECE NAZ YURTSEVEN

IN PARTIAL FULFILLMENT OF THE REQUIREMENTS
FOR
THE DEGREE OF MASTER OF SCIENCE
IN
METALLURGICAL AND MATERIALS ENGINEERING

SEPTEMBER 2019

Approval of the thesis:

**CHARACTERIZATION OF BAINITIC AND MARTENSITIC
MICROSTRUCTURES IN BEARING STEELS**

submitted by **ECE NAZ YURTSEVEN** in partial fulfillment of the requirements for
the degree of **Master of Science in Metallurgical and Materials Engineering**
Department, Middle East Technical University by,

Prof. Dr. Halil Kalıpçılar
Dean, Graduate School of **Natural and Applied Sciences**

Prof. Dr. Cemil Hakan Gür
Head of Department, **Metalurji ve Malzeme Mühendisliği**

Prof. Dr. Bilgehan Ögel
Supervisor, **Metalurji ve Malzeme Mühendisliği, METU**

Examining Committee Members:

Prof. Dr. Ali Kalkanlı
Metalurji ve Malzeme Mühendisliği, METU

Prof. Dr. Bilgehan Ögel
Metalurji ve Malzeme Mühendisliği, METU

Prof. Dr. Rıza Gürbüz
Metalurji ve Malzeme Mühendisliği, METU

Assist. Prof. Dr. Mert Efe
Metalurji ve Malzeme Mühendisliği, METU

Prof. Dr. Nuri Durlu
Makine Mühendisliği, TOBB

Date: 09.09.2019

I hereby declare that all information in this document has been obtained and presented in accordance with academic rules and ethical conduct. I also declare that, as required by these rules and conduct, I have fully cited and referenced all material and results that are not original to this work.

Name, Surname: Ece Naz Yurtseven

Signature:

ABSTRACT

CHARACTERIZATION OF BAINITIC AND MARTENSITIC MICROSTRUCTURES IN BEARING STEELS

Yurtseven, Ece Naz
Master of Science, Metallurgical and Materials Engineering
Supervisor: Prof. Dr. Bilgehan Ögel

September 2019, 98 pages

Bainitic transformations in steels is a well-known phenomenon for more than 60 years. However, in recent years, the lower bainite in high carbon steels gained importance due to their superior mechanical properties since bainitic transformation takes place at very low temperatures, i.e. 160°C -200 °C.

In this study, the morphology and mechanical properties of lower bainite are studied after applying different heat treatment procedures. The study covers SAE 52100 grade bearing steel. The specimens are austenitized at either 825°C, 875°C or 1000°C. As austenitization temperature increases the time required for obtaining 100% bainite increases also. All the bainitic specimens yielded hardness values in the range 595HV-645HV whereas the hardness of the as-quenched specimens yielded hardness values in the range 670HV-780HV. As far as the retained austenite contents are concerned, the amount of retained austenite in bainitic samples are always lower than 10%. However, the retained austenite content of austenitized and quenched specimens are in the range 10%-55%, such that an increase in austenitization temperature yields higher amount of austenite. For conditioning this retained austenite a tempering operation at 235°C is needed so that the retained austenite can transform to martensite upon cooling to room temperature.

The bainitic specimens which are transformed to bainite after austenitizing at 1000°C showed brittle behavior and their tensile testing could not be performed. The bainitic specimens yielded UTS values higher than 2000MPa.

Keywords: Bainite, Martensite, Martensite Start, Retained Austenite, Hardness, XRD

ÖZ

RULMAN ÇELİKLERİNDE BEYNİTLİ VE MARTENSİTLİ YAPILARIN KARAKTERİZE EDİLMESİ

Yurtseven, Ece Naz
Yüksek Lisans, Metalurji ve Malzeme Mühendisliği
Tez Danışmanı: Prof. Dr. Bilgehan Ögel

Eylül 2019, 98 sayfa

Çeliklerde beynit dönüşümleri 60 yıldan fazladır bilinen bir fenomendir, fakat son yıllarda üstün mekanik özelliklerinden dolayı yüksek karbonlu çeliklerde alt beynit dönüşümü daha çok önem kazandı. Yüksek karbonlu çeliklerde, beynit dönüşümleri 160 °C - 200 °C gibi oldukça düşük sıcaklıklarda gerçekleşebilmektedir bu da alt-beynitli yapı oluşumuna, dolayısıyla üstün mekanik özelliklere sebebiyet verir.

Bu çalışmada farklı ısıl işlemlerden sonra oluşan alt beynit yapısının morfolojisi ve mekanik özellikleri incelenir. Bu çalışma SAE 52100 sınıfı rulman çeliğini kapsar. Numuneler 825°C, 875°C ve 1000°C’de östenitlenir. Östenitleme sıcaklığı arttıkça, 100% beynit elde etmek için gereken zaman artar. Tüm beynitli numuneler 595 HV30 ve 645 HV30 arasında değişen sertlik değerleri gösterirken, yağda su verilmiş numunelerin sertlik değerleri 670 HV30 ve 780 HV30 arasında değişmektedir. Kalıntı östenit içeriği ele alınırsa, beynitli numunelerin kalıntı östenit oranı her zaman %10’dan azdır. Lakin, östenitlenmiş ve yağda su verilmiş numunelerin kalıntı östenit içeriği %10 ila %55 arasında değişmektedir. Öyle ki östenitleme sıcaklığındaki artış, kalıntı östenit oranında bir artışa sebep olur. Bu kalıntı östenitin kullanılabilmesi için, numunenin 235°C’de menevişlenmesi gerekmektedir; böylece menevişleme sıcaklığından oda sıcaklığına soğuma sırasında kalıntı östenit martensite dönüşebilir.

1000°C’de östenitlemeden sonra oluşan beynitli numuneler, kırılğan bir karakter gösterdi ve çekme tesleri uygulanamadı. Beynitli numuneler 2000MPa’dan daha fazla azami gerilme gücü gösterdi.

Anahtar Kelimeler: Beynit, Martensit, Martensit Başlangıç, Kalıntı Östenit, Sertlik, XRD

To My Precious Family and All the Independent Women, I Have Ever Known...

ACKNOWLEDGEMENTS

First and foremost, I would like to express my deepest gratitude to my supervisor Prof. Dr. Bilgehan Ögel who guided me throughout this work with his valuable comments, supports, understanding and patience. One simply could not wish for a better or friendlier supervisor.

I would like to express my thanks to ORS Bearing Inc. for SAE 52100 steel provision.

I would like to express my thanks to Zeren Özgeneci (engineer in ORS Bearings Inc.) for provision of SAE 52100 steel.

I would like to express my appreciation to Dr. Süha Tirkeş for his valuable advices and generous support.

I extend my sincere gratitude to my manager Seda Sayılğan Ebetürk, for her support, encouragement, interest and patience. She will be always an inspiration and exemplary character to me. Without her, I would not be able to write this thesis.

I would specially thank to Serkan Yılmaz for his friendship and helps in SEM analysis.

I would also extend my thanks to Yusuf Yıldırım, Cemal Yanardağ and Nilüfer Özel for their helps in metallography laboratory, mechanical workshop and XRD analysis.

I also would like to express my gratitude to my primary school teacher, Ayla Muharremođlu, for raising me to become a responsible and self-confident person.

I also owe my deepest gratitude to my coworkers Erdi Kandemir, Didem ŐimŐek, and Mehmet etin, for their support and hold down the fort in the factory when I took time off for this study.

I am grateful to Erdem Erkin Erdođan, Dilan Őahiner and Mertcan Narin for helping me in my experiments when I worked overtime. Especially Mertcan Narin makes this thesis study much more joyful with endless laughter and cheering and has guided me with his infinite knowledge about metallurgy.

Special thanks to my lifelong friends Gizem Yeđenođlu, Ecem Gungör, Elvin Uysal for their support during this research. I have been blessed with their love and cheerful friendship throughout my life.

I also would like to thank my precious friends Aylin Dedeođlu, and Bersu BaŐtuđ Azer for their priceless and unique friendship making my life full of joy and gossip.

I thank my fellow lab mates Zeynep Öztürk, Sena Okay, Gülten Kılı, Simge Bakır and Zeynep Öztürk for their genuine support, common sharing and fun.

Finally, I am indebted to my parents Türkan Yurtseven and Ayhan Yurtseven for their love, effort, patience, guidance, understanding and wisdom throughout my entire life. I would be nothing if they were not my parents. I am proud of to be their daughter.

TABLE OF CONTENTS

ABSTRACT	v
ÖZ.....	vii
ACKNOWLEDGEMENTS.....	x
TABLE OF CONTENTS	xii
LIST OF TABLES.....	xv
LIST OF FIGURES	xvi
LIST OF ABBREVIATIONS.....	xx
LIST OF SYMBOLS	xxii
CHAPTERS	
1. INTRODUCTION.....	1
2. THEORY AND LITERATURE REVIEW	3
2.1. SAE52100 Steel	3
2.1.1. Introduction	3
2.1.2. Microstructure	4
2.1.3. Mechanical Properties of SAE52100	5
2.2. Microstructures	7
2.2.1. Martensite.....	7
2.2.2. Bainite	14
2.2.2.1. Upper Bainite.....	18
2.2.2.2. Lower Bainite	20
2.2.3. Retained Austenite	22
2.3. Transformation Mechanisms of Bainite.....	23

2.4. Heat Treatment of Bainite Formation	27
2.4.1. Austempering.....	27
2.4.2. Tempering	29
2.5. Kinetics of Bainite Transformation	31
2.6. Alloying Elements	33
3. MATERIALS AND METHODS.....	35
3.1. Material	35
3.1.1. Spectral Analysis	35
3.2. Heat Treatment Processes	35
3.2.1. Heat Treatment Equipment.....	35
3.2.2. Heat Treatment Parameters.....	37
3.3. Microstructural Characterization.....	39
3.4. Image Analysis	40
3.5. X-Ray Diffraction Analysis.....	40
3.6. Hardness Measurement	43
3.7. Tensile Testing	44
4. RESULTS	45
4.1. Transformation Mechanism of Bainite in 100Cr6 Steel	45
4.2. Microstructural Characterization.....	48
4.2.1. Microstructural Development in Oil Quenched Samples	48
4.2.2. Microstructural Development in Isothermally Heat-Treated Samples	51
4.2.2.1. Microstructural Development in Isothermally Heat-Treated Samples Austenitized at 825 °C	51

4.2.2.2. Microstructural Development in Isothermally Heat-Treated Samples Austenitized at 875 °C	54
4.2.2.3. Microstructural Development in Isothermally Heat-Treated Samples Austenitized at 1000 °C	57
4.2.3. Microstructural Development in Tempered Specimens	60
4.3. Quantitative Analysis of Undissolved Alloy Carbides	66
4.4. Retained Austenite Measurements	68
4.4.1. Retained Austenite Analysis of Quenched Specimens	70
4.4.2. Retained Austenite Analysis of Isothermally Heat-Treated Specimens ..	72
4.4.3. Retained Austenite Analysis of Tempering Effect	76
4.5. Mechanical Characterization	78
4.5.1. Hardness Measurements	78
4.5.2. Tensile Tests	83
5. DISCUSSION	85
5.1. Microstructural Characterization	85
5.1.1. Microstructural Characterization of As-quenched Specimens	85
5.1.2. Microstructural Characterization of Isothermally-Treated Specimens	86
5.1.3. Microstructural Characterization of Tempered Specimens	88
5.2. Retained Austenite Measurements	88
5.3. Mechanical Characterization	90
5.3.1. Hardness Measurements	90
5.3.2. Tensile Test	91
6. CONCLUSION	93
REFERENCES	95

LIST OF TABLES

TABLES

Table 1.1. Chemical Composition of SAE52100 (100Cr6) [9]	2
Table 3.1. Chemical composition of 100Cr6 raw material used.....	35
Table 3.2. Process flows and sample identifications.....	38
Table 3.3. The data for calculation of retained austenite volume fraction of 1000A-Q	43
Table 4.1. The information gathered from the TTT diagrams constructed by JMatPro	47
Table 4.2. Quantitative Analysis of Undissolved Alloy Carbides Constructed by ImageJ	67
Table 4.3. Planes and Peak Angles of Ferrite and Austenite Peaks.....	68
Table 4.4. Retained Austenite Analysis Results of All Samples	69
Table 4.5. Undissolved Carbides and Retained Austenite Volume Fractions of Oil Quenched Samples	70
Table 4.6. Sample identifications, heat treatment procedure, resultant morphologies and the hardness values of all specimens	78
Table 4.7. Tension test results of the specimens	83

LIST OF FIGURES

FIGURES

Figure 2.1. Isothermal Transformation Diagram(TTT) of (a) a plain carbon steel 1035 and (b) an alloy steel 52100 [15]	6
Figure 2.2. Iron- Iron Carbide Equilibrium Phase Diagram[4]	8
Figure 2.3. Crystal structures. (a) Austenite (FCC). (b) Ferrite (BCC). (c) Martensite (BCT) [6]	9
Figure 2.4. Morphology of martensite (a) lath (b) plate type morphology [6]	11
Figure 2.5. Micrograph of (a) lath type morphology (b) plate type morphology of martensite [20]	11
Figure 2.6. Ms versus carbon content. Also the range of compositions in which the various types of martensite exist [6]	12
Figure 2.7. The effect of carbon on the hardness and thereby the strength of martensite and austenite[13].....	13
Figure 2.8. Isothermal Transformation Diagram(TTT) of SAE 52100, bainite transformation region marked [15]	15
Figure 2.9. Microstructures in a eutectoid steel: (a) pearlite formed at 720°C, (b) bainite obtained by isothermal transformation at 290°C, (c) bainite obtained by isothermal transformation at 180°C (d) martensite[21].....	15
Figure 2.10.Schematic illustration of the morphology of a sheaf [22].....	16
Figure 2.11. TTT for 1080 steel, pearlite and bainite regions, their strength and hardness are shown. Also isothermal cooling paths (a) for obtaining upper bainite (b) for obtaining lower bainite are shown. [17].....	17
Figure 2.12. An illustration of the growth of bainite and the development of upper or lower bainite.[24].....	19
Figure 2.13. Electron microscope images of (a) upper bainite and (b) lower bainite. [17].....	19

Figure 2.14. Effect of transformation temperature on bainitic steel strength [26].....	21
Figure 2.15. Effect of carbon content on the volume fraction of martensite and the amount of retained.....	22
Figure 2.16. Schematic representation of ledge mechanism (hocam bunu okuduklarımdan yorumlayıp daha anlaşılır olması açısından ben çizdim o yüzden referansım yok)	24
Figure 2.17. Definition of T_0 curve [25]	26
Figure 2.18. Typical austempering heat treatment path[27]	28
Figure 2.19. Graphical representation of effect of tempering time and temperature on hardness.[2]	30
Figure 2.20. Comparison in between the Luzginova's experiments and calculated bainite fractions for different isothermal holding times[42]	32
Figure 3.1. Heat treatment equipment used in this study (a) Protherm muffle furnace, (b) Protherm salt bath, (c) Dry heat oven.....	36
Figure 3.2. (a) the 100Cr6 bar and (b) the heat treatment specimen cut from it.....	36
Figure 3.3. Preparation of a metallographic specimen.....	39
Figure 3.4. The XRD measurement specimen of 100Cr6 from different angles	41
Figure 3.5. Tensile Test Specimen of 100Cr6 steel	44
Figure 4.1. TTT diagram of 100Cr6 austenitized at 825 °C constructed by using JMatPro.	46
Figure 4.2. TTT diagram of 100Cr6 austenitized at 875 °C constructed by using JMatPro.	46
Figure 4.3. TTT diagram of 100Cr6 austenitized at 1000 °C constructed by using JMatPro.	47
Figure 4.4. SEM image of the specimen (a) 825A-Q, (b) 875A-Q; undissolved carbides in martensitic matrix	49
Figure 4.5. (a) Optical micrograph of the specimen 1000A-Q. Martensite needles in retained austenite (white matrix) can be seen. (b) SEM image of specimen 1000A-Q. Austenite between the martensite needles can be resolved as light contrasted areas.	50

Figure 4.6. SEM image of 825A-1d, undissolved carbides in a matrix of bainite and martensite.....	52
Figure 4.7. SEM image of the specimen 825A-2d, undissolved carbides in a matrix of bainite and martensite	53
Figure 4.8. SEM image of the specimen 875A-1d, undissolved carbides in a matrix of bainite and martensite	55
Figure 4.9. SEM image of the specimen 875A-2d, undissolved carbides in a matrix of bainite and martensite	56
Figure 4.10. SEM image of the specimen 1000A-4d, bainite and martensite	58
Figure 4.11. SEM image of the specimen 1000A-6d, bainite and martensite	59
Figure 4.12. SEM image of the specimen (a) 825A-Q, undissolved carbides in martensite and (b) 825A-Q-180T, undissolved carbides in tempered martensite	61
Figure 4.13. SEM image of the specimen 825A-Q-235T, undissolved carbides in tempered martensite.....	62
Figure 4.14. SEM image of the specimen (a)875A-Q, undissolved carbides in martensite and (b) 875A-Q-180T, undissolved carbides in tempered martensite	63
Figure 4.15. SEM image of the specimen 875A-Q-235T, undissolved carbides in tempered martensite.....	64
Figure 4.16. SEM image of the specimen (a) 1000A-Q, martensite and (b) 1000A-Q-180T, tempered martensite	65
Figure 4.17. XRD data of oil quenched- untempered specimens: 825A-Q, 875A-Q, and 1000A-Q	71
Figure 4.18. Graphical Representation of Undissolved Alloy Carbide and Retained Austenite Percentages of as-quenched specimens	71
Figure 4.19. XRD data of untempered specimens of 825 °C austenitization: 825A-Q, 825A-1d and 825A-2d	72
Figure 4.20. XRD data of untempered specimens of 875 °C austenitization: 875A-Q, 875A-1d and 875A-2d	73
Figure 4.21. XRD data of untempered specimens of 1000 °C austenitization: 1000A-Q, 1000A-4d and 1000A-6d	74

Figure 4.22. Graphical Representation of Retained Austenite Percentages of as-quenched and isothermally treated specimens for series of 825 °C, 875 °C and 1000 °C of austenitization.....	75
Figure 4.23. Graphical Representation of Tempering Effect on Retained Austenite on as-quenched and isothermally heat-treated specimens for 1 day and 2 days for 825 and 875 °C of austenitization.....	76
Figure 4.24. Hardness values of as-quenched specimens with different austenitization temperatures and tempering effect on hardness values of as-quenched specimen	79
Figure 4.25. Hardness values of as-quenched and isothermally heat-treated specimens with different austenitization temperatures.....	80
Figure 4.26. Graphical Representation of Tempering Effect on Isothermally Heat-Treated Specimens of Different Austenitization Temperatures.....	81
Figure 4.27. The effect of double tempering and its comparison with the tempering effect on the oil quenched and isothermally treated specimens of different austenitization temperatures.....	82
Figure 4.28. Tensile test results of the specimen in every trial.....	83
Figure 4.29. Graphical representation of hardness and UTS relations of as quenched and tempered specimens of austenitization at 825°C and 875°C.....	84

LIST OF ABBREVIATIONS

ABBREVIATIONS

A_0 : initial cross-sectional area of the specimen

BCC: body centered cubic crystal

BCT: body centered tetragonal crystal

EL: elastic limit

FCC: face centered cubic crystal

HB: Brinell Hardness

HV: Vickers Hardness

HV30: Vickers Hardness under 30 kg load

L: initial length of tensile test specimen

M_f : martensite finish temperature

M_s : martensite start temperature

TS: Tensile Strength

TTT: isothermal transformation diagram: time temperature transformation diagram

ΔL : elongation

SAE: Society of Automotive Engineers

TRIP: transformation induced plasticity

ASTM: American Society for Testing and Materials

A: retained austenite

B: bainite

M: martensite

U.C.: undissolved alloy carbide

LIST OF SYMBOLS

SYMBOLS

γ : austenite

γ_R : retained austenite

α : ferrite

CHAPTER 1

INTRODUCTION

Steel is the most widely used metallic material in industry because it can be fabricated inexpensively and can be tailored easily therefore this material provides the wide range of properties. Moreover, there are variety of manufacturing techniques of steel which gives the precise final product. The properties of steel strongly depend on the microstructure and it is affected by composition of the constituents, volume fractions, size, morphologies of the constituent phases and production method. Heat treatment is an easy way to tailor the properties of steel. [1],[2]

Rolling element bearings can be produced from wide variety of steels. In this thesis SAE52100 (100Cr6) steel grade is focused because it is widely used in bearing applications. There are three reasons for that; the first one is that this steel grade can endure under higher contact stresses with respect to other bearing steels, the other one is it offer higher dimensional stability under temperature extremes, the last reason and the most valuable one for this thesis is that SAE52100 is heat treatable, especially it is very suitable to form bainitic structure due to its high carbon content. [1],[3]

Normally the purpose of heat treatment of steel is to obtain martensite which is the strongest, hardest but the most brittle morphology. However nowadays only strength is not enough. Lower bainite morphology provides the combination of high strength, high ductility and high fracture toughness, and this is because of the microstructure consist of very fine bainitic ferrite laths with retained austenite film between them. [4],[5]

Bainite morphology forms in the temperature range lower than that of pearlite formation and higher than that of martensite formation. That is why the kinetics does not allow all the carbon diffuses into retained austenite during bainite reaction. That is why some carbide precipitation occur in bainite sheaves. In the recent lower bainite

studies; the sheaves are expected to be in nanoscale for superior mechanical properties and the bainitic ferrite is expected to be carbide free because the presence of carbides limits the strength of microstructure. Moreover, if carbon is trapped into retained austenite, the strength of retained austenite increases and hinders the ferrite-austenite interface movement as a result of it the final bainite sheaves cannot grow more than a limiting size. Generally, to preserve these conditions, researchers who study on lower bainite designed new alloys. For example, aluminum and cobalt are added to improve kinetics since the transformation temperatures are chosen to be low to obtain fine microstructures. Another addition is approximately 1.5-2 wt% silicon to suppress carbide precipitation in ferrite. [6],[7],[8] Table 1.1 shows the chemical composition of SAE52100. It can be clearly seen the Si content is not enough to suppress carbide precipitation.

Table 1.1. *Chemical Composition of SAE52100 (100Cr6) [9]*

Composition in Wt%							
C%	Mn%	Si%	P%	S%	Cr%	Mo%	Cu%
0.93-1.05	0.25-0.45	0.15-0.35	0.025	0.015	1.35-1.60	0.10	0.30

In this thesis the main purpose is to obtain lower bainite with commercial ways. To achieve this first the austempering heat treatment was applied to the SAE52100 specimens. Microstructural characterization is processed with optical and scanning electron microscopy. Moreover, to predict mechanical behavior macro hardness measurements are completed then tensile test was applied to the suitable heat-treated specimens. For retained austenite measurements X-ray Diffraction method was used. Therefore, this thesis studies the microstructures and mechanical properties of martensite and lower bainite in SAE52100.

CHAPTER 2

THEORY AND LITERATURE REVIEW

2.1. SAE52100 Steel

2.1.1. Introduction

A bearing is described as a mechanical element that assists relative movement between moving parts, most importantly minimizes the friction between the parts. For a bearing operate properly, it should be able to sustain its shape stability and rotation accuracy under the condition of repeated high stress. In order to make a bearing by using steel one should consider couple of things. First, high hardness and hard yield strength is required since one of the working conditions is under high stress. Also, since this stress is repeated one should consider the fatigue resistance of the steel and finally wear resistance is another important property to produce bearings because the primary function of a bearing is reducing friction between the moving parts. SAE52100 is commonly used for bearing production because of its high carbon (approximately 1.0 %) and chromium (approximately 1.35-1.60 %) content. While high carbon content provides high hardness and high strength, high chromium content gives the property of wear resistance since it is a strong carbide former. Undoubtedly heat treatment procedure is very effective on these properties and on fatigue resistance. [9] SAE52100 grade is the name given according to ASTM A295 standard. Another grade is 100Cr6 which is given according to DIN 17230. The steel is also named as SUJ2 and EN31 according to JIS G4805 and BS 970 respectively. [10]

2.1.2. Microstructure

The purpose of conventional heat treatment of SAE52100 is to obtain martensitic microstructure which is the hardest and the strongest phase. Despite of its strength, martensite is very brittle and shows little toughness. To remedy this deficiency tempering process is vital. [4] In order to obtain fully martensitic microstructure, austenitization and quenching is required. Austenitization temperature and time are chosen according to specimen size and chemical composition. SAE52100 is fully austenitized at 1050 °C and then the specimen quenched to transform austenite into martensite. Then tempering is applied. During tempering process hardness and strength decreases while toughness and ductility increases. Tempering temperature is always below the eutectoid temperature. The temperature and time for tempering are chosen according to target mechanical properties of the final microstructure. At the end of these heat treatments the final microstructure is tempered martensite which compose of ferrite and cementite phases. [2], [6], [9], [11], [12]

Carbides should be present in the microstructure to increase wear resistance because bearings are exposed to high frictions during their service. Because of this, the aim of conventional heat treatment is not only to obtain fully martensitic microstructure but also keep carbides in the final microstructure. Stickles has found that up to 3-4 vol.% of carbides in the microstructure increases wear resistance. [12] It should be noted that during austenitization some or all of the carbides dissolve into the austenite depending on the temperature. The optimum austenitization temperature is determined as 840°C to keep approximately 3-4% volume carbides in the final microstructure. [11]

On the other side, when there is martensitic microstructure it is inevitable to have retained austenite beside martensite, unless cryogenic heat treatment is applied. In commercial heat treatment of 52100 oil which is in room temperature is used as quenching medium to avoid cracks. Therefore, there is always retained austenite in the final microstructure. [11] Certain amount of retained austenite is necessary to increase the service life of the bearings because it increases ductility and toughness. Moreover it increases fatigue resistance because the retained austenite transform into

martensite under stress/strain.[13] To conclude, the final microstructure of conventional heat treatment of SAE52100 steel consists of tempered martensite, undissolved carbides and retained austenite.

2.1.3. Mechanical Properties of SAE52100

While testing mechanical properties, hardness is the first test to do. There are several advantages to apply hardness test like simplicity or inexpensiveness. Hardness test is performed by forcing a small indenter into the surface of a material to be tested. The depth or size of the indentation gives hardness value. The softer the material, larger and deeper the indentation and results in lower hardness index number. There are four hardness scale used widely and they are grouped according to the shape and size of the indenter. The indenter of Brinell hardness scale is 10 mm sphere, on the other hand the indenter of Vickers and Knoop scale is diamond pyramid different in sizes. In Rockwell scale, the indenter is diamond cone. These four scales can be converted into each other through hardness conversion tables. [4]

The hardness values also give an idea about the other mechanical properties such as tensile strength. Hardness and tensile strength are proportional. The relation is linear, and the equation is given in Eq. 1 where *HB* is *Brinell Hardness* [4], [14] Generally at room temperature SAE52100 bearing steels have hardness in between 60 and 67 Rockwell. [10]

$$TS(MPa) = 3.45 \times HB$$

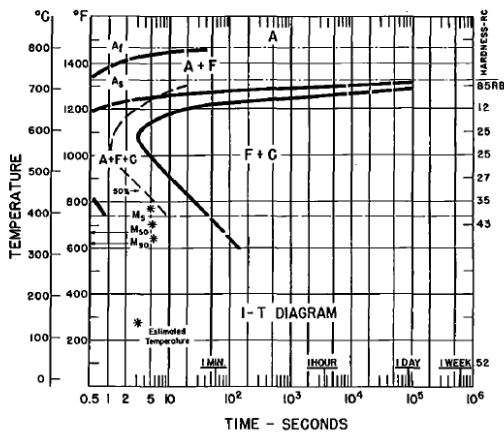
Eq. 1

The main aim of the heat treatment of steel is to reach the desired, adequate hardness. Hardenability is a property that determines the ability of an alloy to harden. Depth and distribution of the martensitic phase is concerned for steel. [1], [2], [13]

Alloying elements like chromium, molybdenum, nickel, silicon and manganese have high influence on increasing hardenability by delaying the austenite-ferrite and/or pearlite reactions therefore more martensite is allowed to form upon the same cooling rate. Delaying the reactions represented by shifting the nose of ferrite/pearlite in the isothermal transformation diagram, meaning time required to initiate the transformation reaction increased. [4] The chromium content of SAE52100 is in between 1.35-1.60 wt%. [9] This gives remarkable hardenability to the alloy. Two isothermal transformation curves which was derived from Atlas of Time-Temperature Diagram for Iron and Steels are present in Figure 2.1.

Type: 1035 Mod.

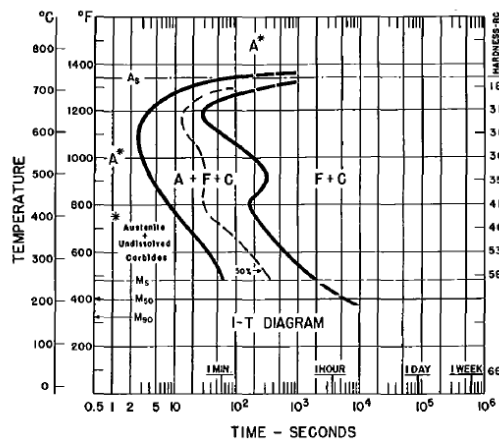
Composition: Fe - 0.35% C - 0.37% Mn Grain size: 75% 2-3, 25% 7-8 Austenitized at 843° C (1550°F)



(a)

Type: 52100

Composition: Fe - 1.02% C - 0.36% Mn - 0.20% Ni - 1.41% Cr Grain size: 9 Austenitized at 843° C (1550°F)



(b)

Figure 2.1. Isothermal Transformation Diagram(TTT) of (a) a plain carbon steel 1035 and (b) an alloy steel 52100 [15]

The first diagram belongs to 1035 plain carbon steel, ferrite transformation starts immediately as illustrated in Figure 2.1.a on the other hand SAE52100 bearing steel in Figure 2.1.b the ferrite transformation delayed remarkably. The difference in these steels are carbon and chromium composition. Chromium composition is effective on shifting the ferrite nose and hence increasing hardenability. The reason is that chromium is a strong carbide forming element.[1] Carbon is also effective increasing hardenability but not as much as the alloying elements mentioned above. The effect

of carbon is seen on martensite start temperature. Increasing carbon content lowers martensite start temperature (M_s). The difference of M_s of plain carbon steel and 52100 is nearly 270 °C, observed in Figure 2.1.

The ultimate tensile strength(UTS) of SAE52100 can be up to 2574 MPa depending on the production method. [10]

2.2. Microstructures

2.2.1. Martensite

Martensite is a metastable phase that transforms from austenite by rapid quenching to the low temperatures. The cooling rate must be rapid to avoid the nose of TTT diagram so that any other phase like ferrite does not form. As it is a non-equilibrium phase it is not seen in the equilibrium phase diagrams. Normally, in isothermal transformations, phase constituents reach equilibrium by diffusion-controlled transformation and hence these constituents like ferrite and cementite are seen on the equilibrium phase diagram of iron and iron carbide (Figure 2.2). The transformation of martensite is athermal (nonisothermal); the cooling rate for obtaining martensite is so high that, there is no chance for diffusion and hence all the carbon in the parent austenite is trapped in the structure eventually austenite lattice is distorted. Not having a chance for diffusion, martensite is a supersaturated solid solution of iron and carbon. [6], [13], [16], [17]

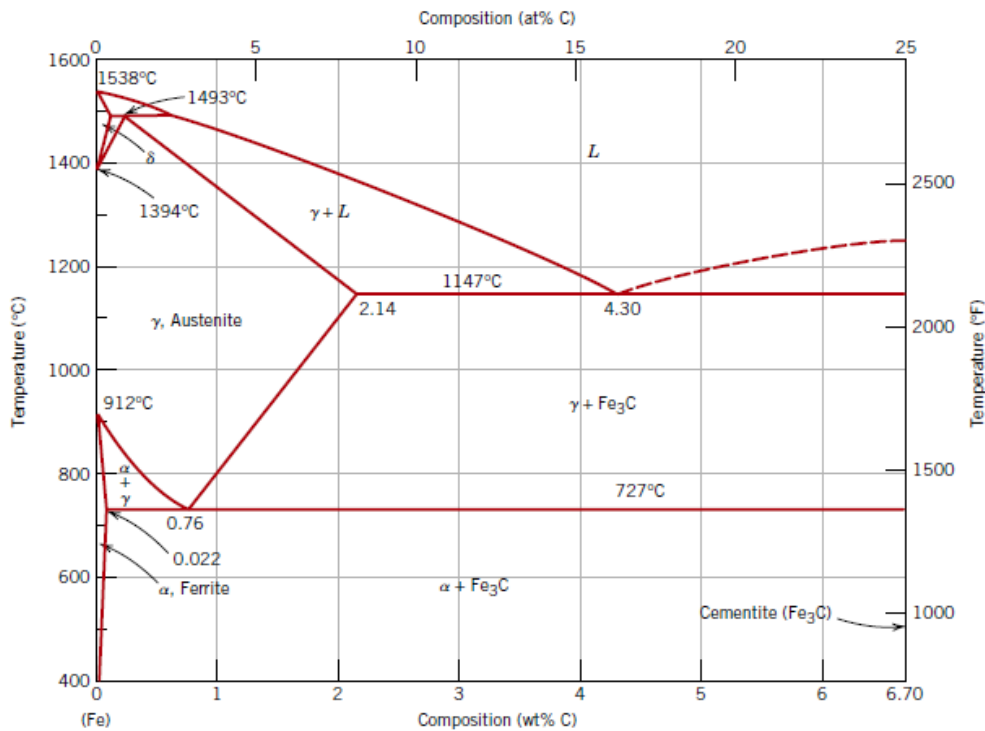


Figure 2.2. Iron- Iron Carbide Equilibrium Phase Diagram[4]

There are main distinctive features of martensitic transformations over other phase transformations. First of all, the transformation is diffusionless, the chemical composition of martensite and the parent phase are the same. The last feature is that atoms move cooperatively and the result is lattice structure change. [17]

Because of the deformation of parent austenite, shape change, shear and volume expansion of approximately 4%, at the end of the transformation the final crystal structure is body centered tetragonal instead of a cubic crystal. [6] The difference between the crystal structure and the entrapped carbon atoms which are the cause of this shape change can be seen clearly in Figure 2.3.

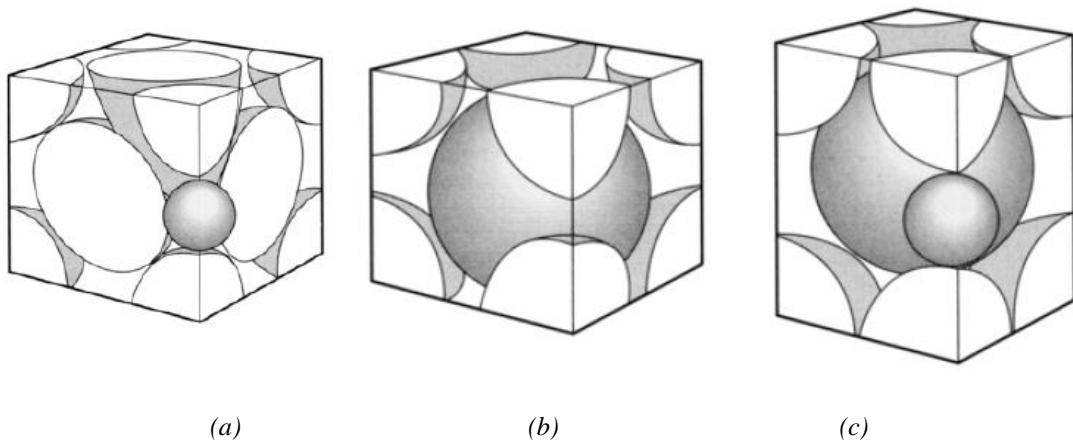


Figure 2.3. Crystal structures. (a) Austenite (FCC). (b) Ferrite (BCC). (c) Martensite (BCT) [6]

This diffusionless character lead to shape change and due to this shape change martensitic transformation is also called shear or displacive transformation. Bhadeshia[18] has believed that there are two proof for this diffusionless character; the first one is inconsistency of diffusion phenomenon and rapid cooling rate.[18] Martensitic phase can form at very low temperatures where diffusion is not imaginable even for the interstitial atoms over the long times. The second reason is the chemical composition of martensite is founded to be same with the parent austenite therefore no carbon diffusion has occurred.[18]

While obtaining martensitic structure temperature is the only concern. No matter how fast the cooling is, if necessary, undercooling is not provided martensitic transformation does not happen. The transformation begins at martensite start temperature (M_s) and ends at martensite finish temperature (M_f) and these temperatures are not constant for steels. The volume fraction of martensite depends on the temperature of the quenching medium. When the specimen reaches to M_f temperature the morphology is 100% martensite. If the temperature of the medium is exactly in the middle of M_s and M_f temperatures then the morphology is 50% martensite and the rest is retained austenite. [6], [17]

In this thesis, since the main aim is to study bainite and martensite morphology, some of the experiments are performed above the M_s temperature so this is very critical

temperature. As mentioned before, carbon decreases the martensite start temperature, but carbon is not the only element that have an influence on M_s too. Jacek Trzaska developed an M_s formula experimentally (Eq. 2) . [19] However in ASM Handbook of Heat Treating this formula is given as Eq. 3. [2]

$$M_s (\text{°C}) = 541 - 401 (\text{wt\% C}) - 36 (\text{wt\% Mn}) - 10.5 (\text{wt\% Si}) - 14 (\text{wt\% Cr}) \\ - 18 (\text{wt\% Ni}) - 17 (\text{wt\% Mo})$$

Eq. 2

$$M_s (\text{°C}) = 512 - 453 (\text{wt\% C}) - 16.9 (\text{wt\% Ni}) + 15 (\text{wt\% Cr}) - \\ 9.5 (\text{wt\% Mo}) + 217 (\text{wt\% C})^2 + 71.5 (\text{wt\% C})(\text{wt\% Mn}) - \\ 67.6 (\text{wt\% C})(\text{wt\% Cr})$$

Eq. 3

In ferrous martensite there are two types of microstructures. If carbon content is less than 0.6wt% lath morphology is observed. For greater carbon contents plate martensite morphology is observed. Laths are in the shape of long and thin plates. As illustrated in Figure 2.4.a, group of laths become packets. In each packet all the laths have the same crystallographic orientation. Adjacent packets are separated by high angle grain boundaries, indicating the orientation difference. Plate martensite is sometimes called acicular (needle like) martensite. The distinguishing morphology of plate martensite is the zig-zag pattern of smaller plates. The bigger plates seen on Figure 2.4.b are nucleated at the beginning of the martensitic transformation. The smaller plates following zig-zag pattern has formed the latter stages of the transformation. The main difference between lath and plate martensite beside their appearance is that the plates grow throughout the austenite grain while laths grow only throughout a subunit; blocks. [6], [17]

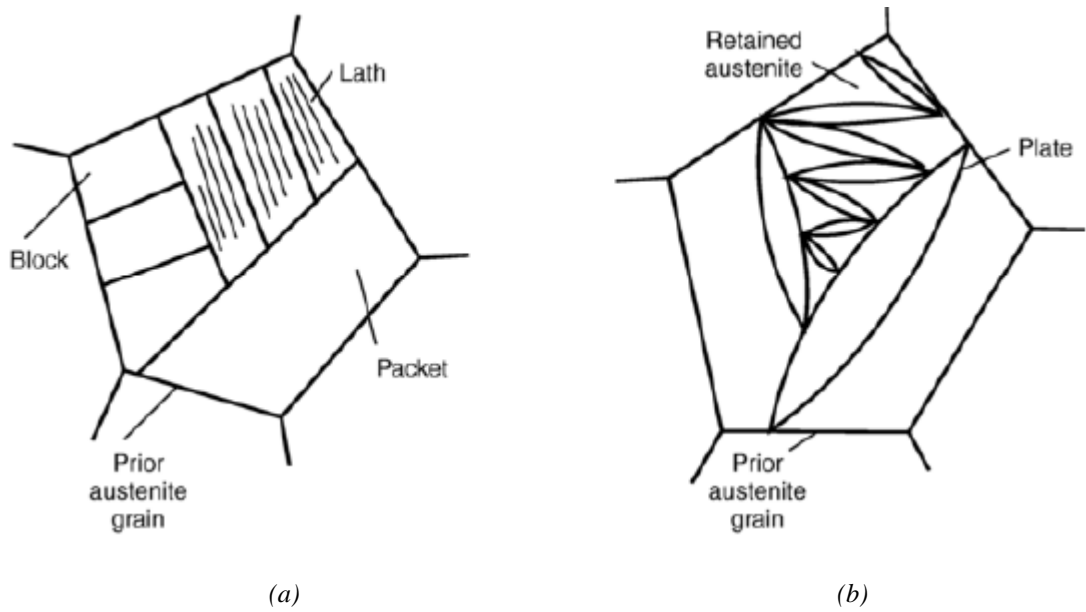


Figure 2.4. Morphology of martensite (a) lath (b) plate type morphology [6]

The difference between lath and plate type morphologies can be seen on micrographs in Figure 2.5. The carbon content of SAE 52100 is variable depending on the austenitization temperature meaning depending on the decomposition of carbides. It can be maximum 1wt%. So that the martensite morphology seen on the specimens are variable as in Figure 2.6.

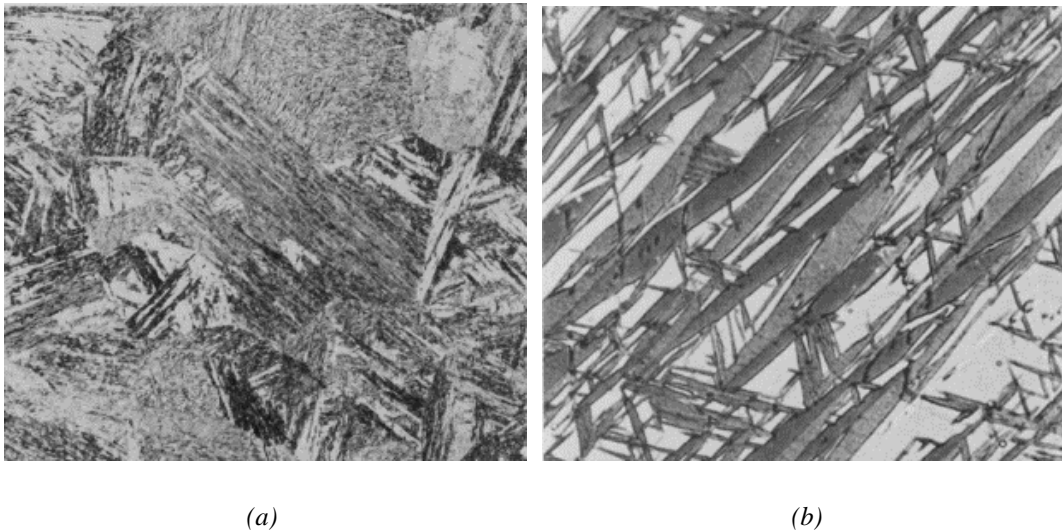


Figure 2.5. Micrograph of (a) lath type morphology (b) plate type morphology of martensite [20]

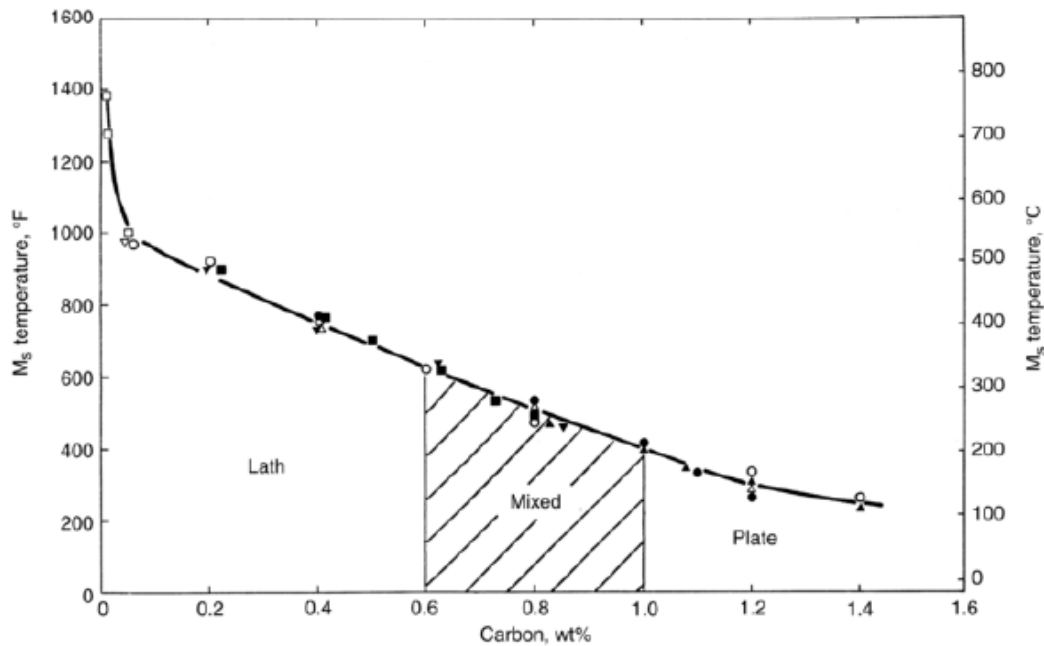


Figure 2.6. Ms versus carbon content. Also the range of compositions in which the various types of martensite exist [6]

As mentioned before, like austenite, the strength of martensite is directly related to the carbon content (Figure 2.7) As carbon content increases the strength of martensite increases. Also, transformation of martensite causes 4% volume increase this creates residual stresses in addition to the strains created by the misfit of carbon atoms. One can easily predict that as the carbon content increases misfit of interstitial atoms increases leading increasing strain and dislocation density. That is why martensite with high carbon content is stronger. Moreover at high carbon levels this residual stress becomes so severe that material cracks. [13], [21]

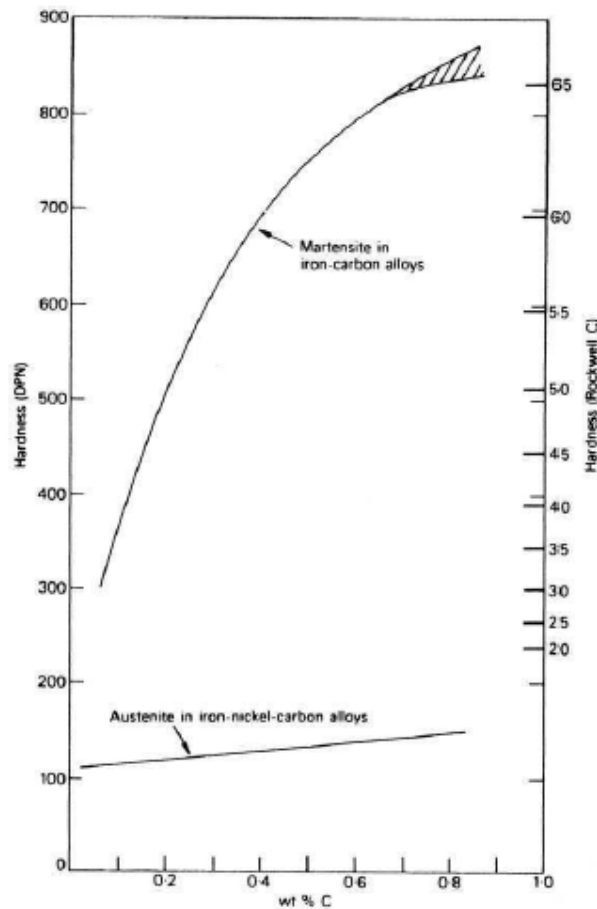


Figure 2.7. The effect of carbon on the hardness and thereby the strength of martensite and austenite[13]

These residual internal stresses are introduced to the steel upon quenching makes the morphology very brittle and poor in toughness in other word impossible to use. For stress relief tempering is essential. The steel is heated to a temperature below eutectoid temperature for a specified time. This mechanism depends on carbon diffusion and single-phase BCT martensite decomposes into ferrite and cementite. While martensite is metastable tempered martensite is stable, its constituents can be seen on equilibrium iron-iron carbide phase diagram. The tempering temperatures are ranging from 200°C to 650°C and the times are generally ranging from 30 minutes to 2 hours. By tempering toughness and ductility are enhanced as the strength and toughness decreases that is why time and temperature are chosen according to target properties. [4], [16]

2.2.2. Bainite

Like martensite, bainite is a non-equilibrium phase because it is obtained by relatively high cooling rates comparing to equilibrium phases. [16] The cooling rate is rapid enough to avoid pearlite formation and yet not rapid enough to form martensite. The difference is quenching is not the only heat treatment to form bainite, isothermal heat treatment is essential because bainite is actually a product of decomposition of austenite into ferrite and cementite therefore time is required for decomposition. It forms in a temperature range in between M_s and the pearlite transformation temperature range. The bainite formation range is marked on TTT of SAE 52100 in Figure 2.8 [6], [13], [21]

The difference between pearlite and bainite is the morphology. Pearlite is a product of reconstructive growth of ferrite and cementite therefore it has lamellar morphology. On the other hand, despite of diffusion-controlled mechanism of bainite, it has also a displacive character like martensite. Bainite does not develop a lamellar structure. Bainitic ferrite is needle like, similar to laths of martensite whereas the cementite particles are very fine and chunky. This very fine array of ferrite and cementite makes bainite stronger and tougher than pearlite. The microstructural differences can be seen in Figure 2.9. It should be noted in the figure the etching is different between martensite and bainite. The appearance of bainite is darker because it contains more cementite particles segregated. [16]–[18], [21]

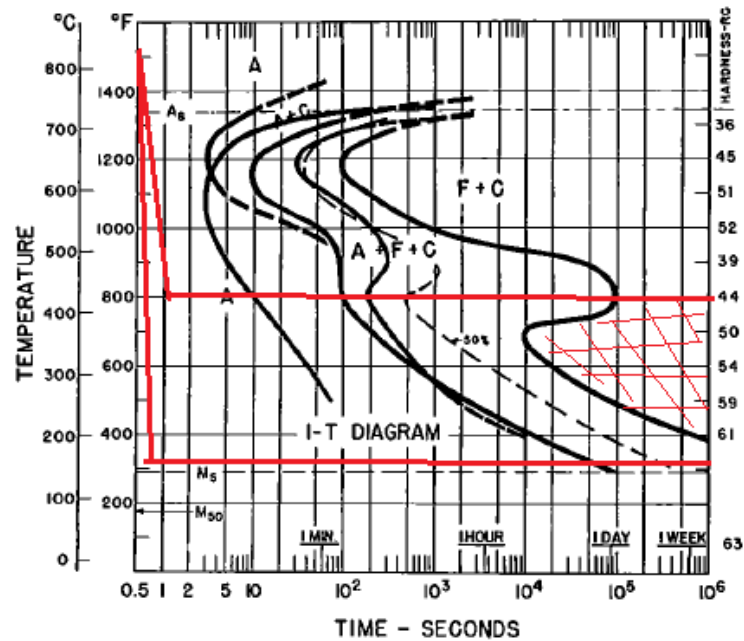


Figure 2.8. Isothermal Transformation Diagram(TTT) of SAE 52100, bainite transformation region marked [15]

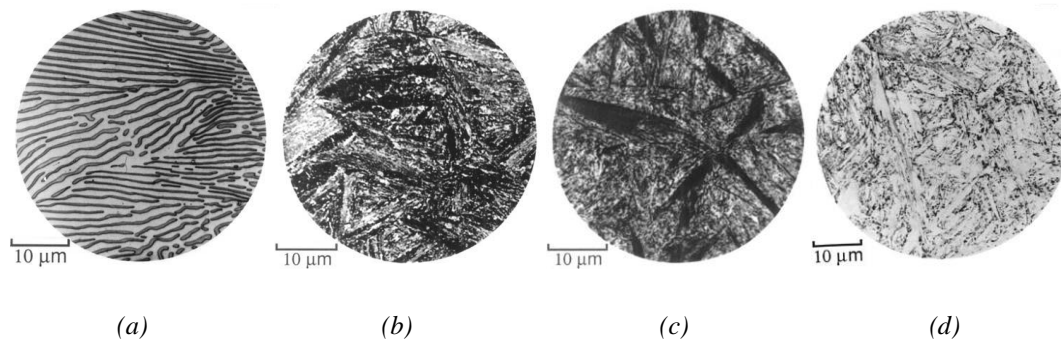


Figure 2.9. Microstructures in a eutectoid steel: (a) pearlite formed at 720°C, (b) bainite obtained by isothermal transformation at 290°C, (c) bainite obtained by isothermal transformation at 180°C (d) martensite[21]

Bainitic ferrite laths or platelets is the main constituent of the bainite phase, but residual phases should be considered. These residual phases are inevitable during bainite transformation and they can be cementite, martensite or untransformed, residual austenite. Ferrite needles are separated with these residual phases. The plate or lath of bainitic ferrite can be called as subunit and aggregates of subunits are called

sheaves. The platelets of a sheaf may not be completely isolated from each other by residual phases just like the sheaf in Figure 2.10. Here platelets are mostly adjacent, low orientation grain boundaries are formed along the contiguous surfaces. It might be deduced that all subunits grow in a common crystallographic orientation inside a sheaf. Moreover, platelets within a sheaf is approximately in the same size because each subunit has limited growth. Newly formed subunit nucleates at the tip of the existing subunit and this phenomenon gives the wedge shape of a sheaf. The larger end of the sheaf is the end where nucleation of ferrite started.[21], [22]

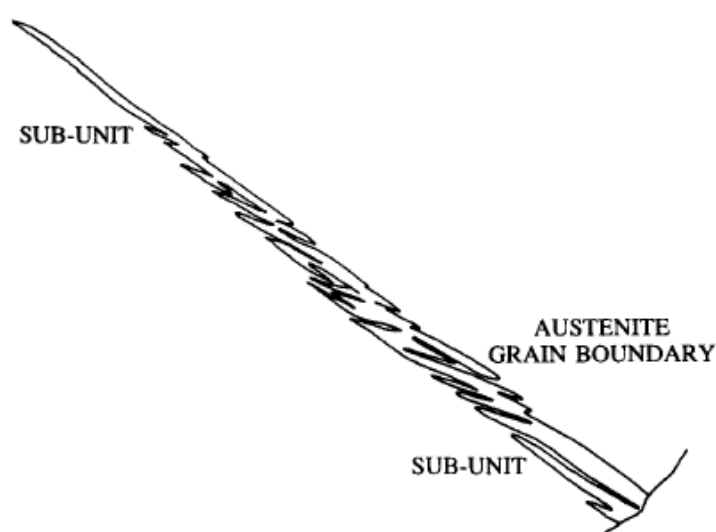


Figure 2.10. Schematic illustration of the morphology of a sheaf [22]

As mentioned before bainitic transformations have both diffusion-controlled character and displacive character. Growth of each plate creates shape deformation around the transformed region, and this creates large shear stresses around the growing ferrite. These shear stresses create strain on the austenite. This strain is named invariant-plane strain. This mechanism is similar to that of martensite however bainite sheaves form at much higher temperatures compared to martensitic transformation temperatures so that strains are relieved, and relief happens by plastic deformation of the contiguous austenite phase. Increasing dislocation density becomes a barrier for moving austenite/ferrite interface as a result growth of bainitic ferrite stops eventually. This

explains why bainite sheaves have certain size and these size are smaller than grain size while martensite sheaves having size of the grain diameter of parent austenite. [13]

The plate or lath morphology of ferrite are thought to be dependent upon the transformation temperature and carbon concentration as in the martensitic transformation. Bainite morphology is grouped into two; one is upper bainite mostly lath structure and the other is lower bainite mostly plate structure. In Figure 2.11 transformation temperature range of the phases and some of the mechanical properties are illustrated on isothermal transformation diagram of a plain carbon steel. [23]

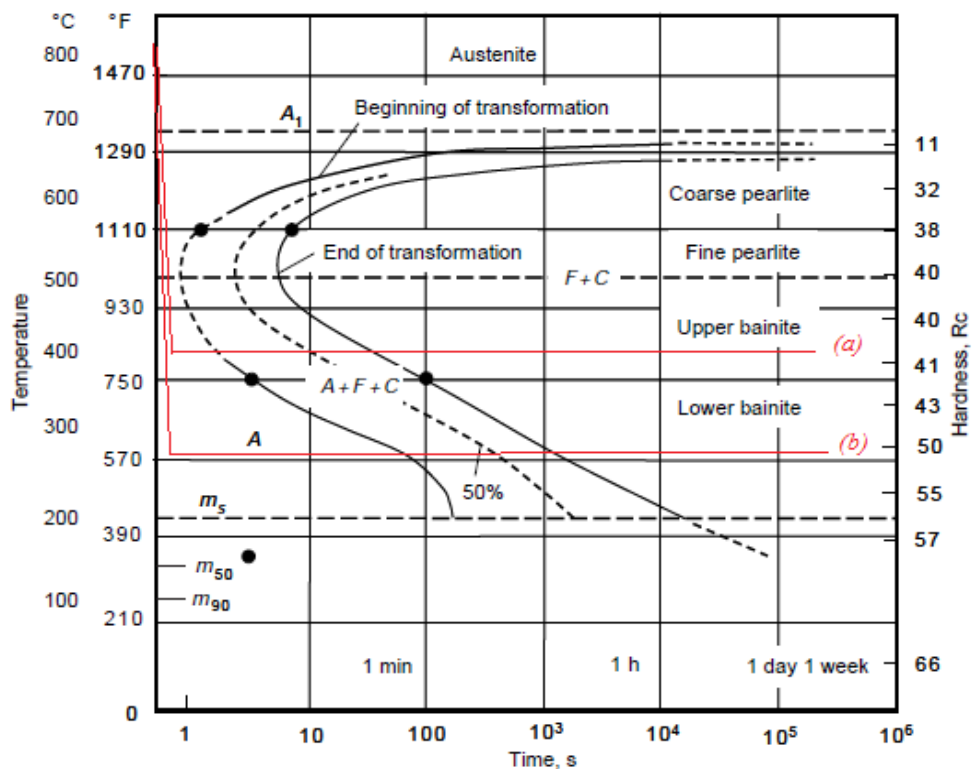


Figure 2.11. TTT for 1080 steel, pearlite and bainite regions, their strength and hardness are shown. Also isothermal cooling paths (a) for obtaining upper bainite (b) for obtaining lower bainite are shown. [17]

2.2.2.1. Upper Bainite

Upper bainite forms isothermally at higher temperatures with respect to lower bainite. The temperature range is just below the pearlite transformation zone and typically ranging from 400 °C to 550 °C. To obtain upper bainite, one should quench the austenitized steel rapid enough to avoid pearlite formation to the temperatures in between 400 and 550°C and isothermally hold the specimen for long enough to obtain bainitic structure. In Figure 2.11.a isothermal cooling path to produce upper bainite is illustrated. Both upper and the lower bainite have acicular morphology but the upper bainitic ferrites are coarser since high temperatures enhances the diffusion kinetics. While formation of upper bainite, first bainitic ferrite nucleates heterogeneously at the grain boundary of austenite and grows approximately parallel to each other. Ferrite has low solubility of carbon. During growing these supersaturated ferrite starts to eject excessive carbon. Because of this diffusion, austenite becomes carbon enriched and eventually cementite starts to form at the interface in between austenite and ferrite and necessarily grows the same direction as ferrite. Since diffusion is favored at high temperatures, all excessive carbon can be ejected from ferrite and no carbide precipitation seen in the upper bainite morphology. Therefore, at the end of the transformation the resultant morphology is clusters of platelets of carbide free ferrite in approximately identical crystallographic direction. (Figure 2.12 and Figure 2.13.b) Usually cementite particles lie along the ferrite platelets, the amount and continuity varies with carbon content of the steel. [6], [16]–[18], [23]

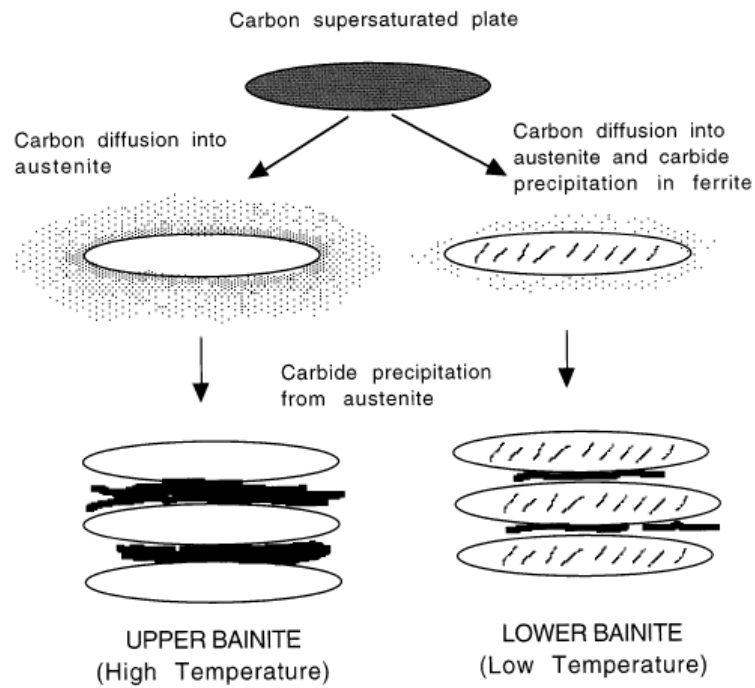


Figure 2.12. An illustration of the growth of bainite and the development of upper or lower bainite.[24]

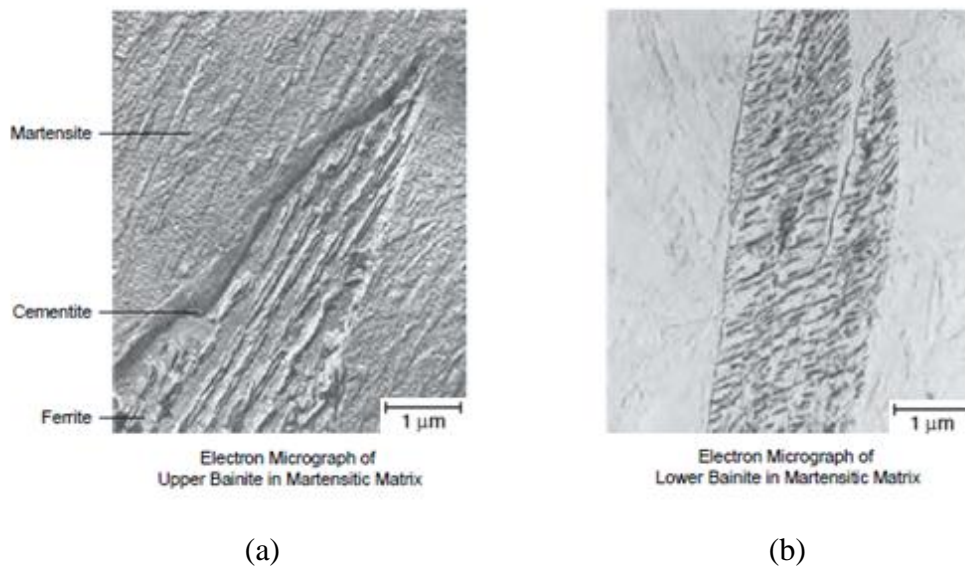


Figure 2.13. Electron microscope images of (a) upper bainite and (b) lower bainite. [17]

2.2.2.2. Lower Bainite

Lower bainite forms isothermally at lower temperatures with respect to upper bainite. The temperature range is just above the M_s and typically ranges from 200 °C to 400 °C. To obtain lower bainite, one should quench the austenitized steel rapid enough to avoid pearlite formation to the temperatures in between 200 and 400 °C and isothermally hold the specimen for long enough to obtain bainitic structure. In Figure 2.11.b isothermal cooling path to produce lower bainite is illustrated. The schematic representation of morphological difference between upper and lower bainite is seen Figure 2.12. Since transformation temperatures are lower, carbon diffusion kinetics are not favored unlike upper bainite. While formation of lower bainite, first bainitic ferrite nucleates heterogeneously at the grain boundary of austenite and grow nearly parallel to each other. The difference from the upper bainite is that since the temperatures are much lower there is more undercooling and hence more driving force therefore, in lower bainite more ferrite grains nucleate. This is the main reason why lower bainite has a finer microstructure than upper bainite. As supersaturated ferrite grows, it starts to eject excessive carbon to the neighboring austenite. However, since transformation temperatures are lower, carbon diffusion is not favored as much as upper bainite. That is why, only some of the carbon can enter the austenite and some of the carbon precipitate as cementite because austenite is still carbon enriched. Comparing the upper bainite, austenite is less carbon enriched, so the thickness of cementite precipitation is much lower. These thin film of cementite and ferrite layers makes lower bainite much tougher than upper bainite. [3], [7], [8], [9], [21], [22], [27], [29]

Due to lower diffusion kinetics there is some excess carbon trapped in the newly formed bainitic ferrite. These carbon atoms cannot be present in the solid solution thermodynamically. Therefore, to reduce carbon concentration of ferrite to the concentration of equilibrium phase diagram, carbides precipitates in the ferrite. This is the main difference seen in the morphologies of upper and lower bainites. (Figure 2.12 and Figure 2.13.b) Generally both cementite (Fe_3C) and ϵ -carbide ($Fe_{2.4}C$) form in the bainitic ferrite laths depending on the chemical composition and transformation

temperature while only cementite precipitates between the ferrite laths. Therefore, at the end of the transformation the resultant morphology is clusters of ferrites -more needle like than upper bainitic ferrite-, carbide precipitates inside of bainitic ferrite, finer and less in amount cementite precipitates. These increased surface area of ferrite/carbide/austenite interfaces because of fine microstructure, acts as a barrier for dislocations and hence increasing strength of the structure. That is why as transformation temperature decreases, strength increases as illustrated in Figure 2.14. Hence lower bainite is not only tougher than upper bainite but also stronger. [13], [17] Bainite derives its strength from its morphology whereas the strength of martensite is directly proportional to the dissolved carbon. [25] In this thesis, lower bainitic microstructure in SAE 52100 is focused.

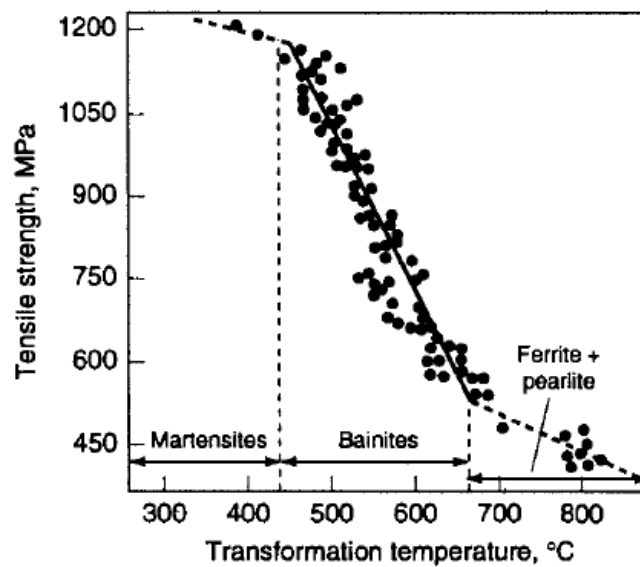


Figure 2.14. Effect of transformation temperature on bainitic steel strength [26]

2.2.3. Retained Austenite

When there is martensitic or bainitic transformation, the existence of retained austenite (γ_R) is inevitable. For martensitic transformations, generally the temperature of quenching medium or service temperature which is mostly room temperature is much higher than M_f . Therefore, some untransformed austenite remains in the morphology. For bainitic transformations, carbon partitioning takes place. As mentioned before, increasing carbon content decreases the M_s and thereby M_f . Accordingly, carbon partitioning directly affects the volume fraction of retained austenite. This carbon influence is shown in Figure 2.15. During carbon ejection from newly formed ferrite to adjacent austenite, the carbon content of the austenite gradually increases, thus martensitic transformation range gradually decreases. At some point, transformation temperature is not high enough to transform this austenite with new composition; so some austenite remains untransformed. [13], [16], [27]

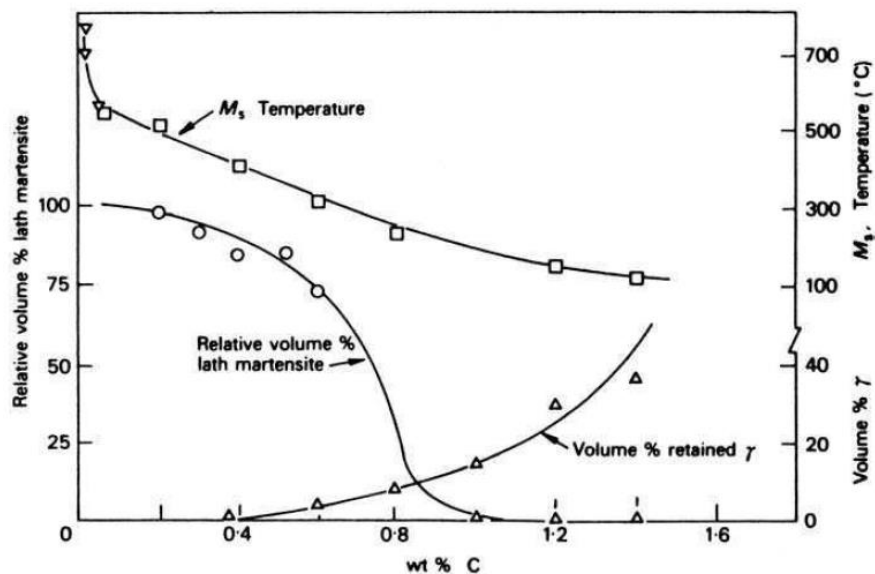


Figure 2.15. Effect of carbon content on the volume fraction of martensite and the amount of retained austenite in Fe-C alloys[13]

Retained austenite (γ_R) improves ductility because it has ability to transform martensite under strain. This effect is called transformation induced plasticity (TRIP).

This transition provides relaxation of the local stress concentration and further strain hardening of the material. There are two reasons for this additional strain hardening: the former is that transformation of retained austenite to martensite increases the volume fraction of the hard phase and the latter is transformation strains provides additional plastic deformation.[3], [28] Moreover, γ_R has a great positive influence on toughness. This transformation induced plasticity reduces stress concentration point. The existence of γ_R decelerate crack propagation by crack branching and crack blunting. [29]

Retained austenite can exist in two forms: blocky and film types. Blocky austenite is unstable, due to TRIP effect, it can cause catastrophic failures and has detrimental effects on dimensional stability of the product. On the other hand, film of γ_R is very desired in the final microstructure. In bainitic, especially lower bainitic, microstructures, thin film of retained austenite is located in between the fine bainitic ferrite plates and it is very stable due to carbon enrichment, meaning no further transformation is possible. This fine structure gives excellent strength and toughness balance. Moreover, TRIP effect works positively here because the martensitic transformation does not cause catastrophic failure since films are very thin. Also, the shape change caused by transformation is compensated by the neighboring ferrite.[25], [28], [30], [31]

2.3. Transformation Mechanisms of Bainite

There are ongoing uncertainties about transformation mechanism of bainite. Two main transformation mechanisms are proposed. The first view claims that newly formed ferrite nucleates and grows by short-range iron diffusion on the ferrite/austenite interface. The latter states that the first ferrite forms by diffusionless/displacive mechanism. [16], [27], [32]

Diffusive theory tells that both nucleation and growth have reconstructive mechanism. It is believed that growth rate of ferrite/austenite interface being slow with respect to

martensite is the evidence of diffusion controlled transformation.[16], [33] The diffusion during bainitic transformation occurs via ledge mechanism. An interface is illustrated in Figure 2.16. This interface is in between austenite and newly formed bainitic ferrite. Short range diffusion of substitutional atoms occurs at the ledges of this interface. Because of the diffusion, ledge moves through the austenite region meaning ferrite growing. According to Aaronson's observations the net movement of the interface is perpendicular to the direction of the ledge movement resulting in thickening. Unfortunately this ledge mechanism fails to explain plate morphology of bainite.[27], [34], [35]

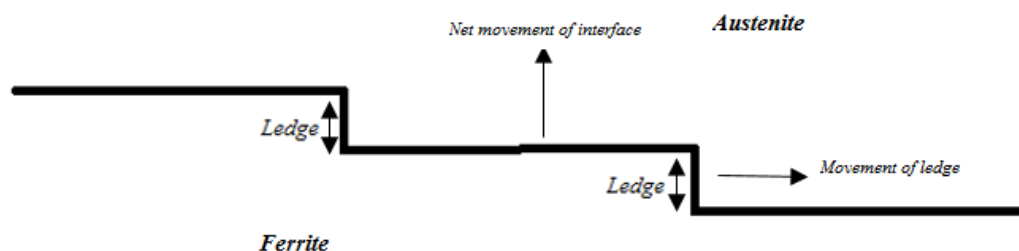


Figure 2.16. Schematic representation of ledge mechanism

Nevertheless longitudinal growth is remarkably greater than the latitudinal growth leading to feathery shape of the bainite morphology.[16]

Diffusionless theory, on the other hand, claims that bainitic ferrite forms by shear and carbides -in this case cementite- form as a secondary reaction, form consecutively rather than a reconstructive growth. [34], [35] In martensitic transformations both nucleation and growth happen via displacive mechanism. However for bainitic transformation, it is agreed on bainite nucleation is diffusion controlled because it happens via carbon partitioning.[34], [36] During displacive growth, atoms make a cooperative glide type movement but with little displacement compared to neighboring atoms. [16] Despite of his belief about diffusion controlled

transformation, Hultgren's atom-probe experiments have shown that alloy content of bainitic cementite is lower than that of pearlitic cementite in the same steel and this gives the idea that substitutional alloying elements do not participate in bainite reaction. [33], [34] Moreover, the substitutional alloy content of parent austenite is equal to that of bainitic ferrite. Therefore, Hultgren's experiments are supported, it is proven that iron and other substitutional atoms do not diffuse and this is considered as an evidence of diffusionless transformation. [22] To sum up displacive mechanism; bainite reaction happens by first paraequilibrium nucleation of ferrite in which only carbon diffusion takes place and then diffusionless, displacive growth. [3]

As mentioned before (in 2.2.2.Bainite) bainite sheaves have limited growth due to invariant-plane strain created by shear. [13] Also there is a kinetic reason for this limiting growth. Examining the carbon profile, the retained austenite carbon concentration is below that of the value seen on equilibrium phase diagram, indicating that bainite transformation ceases before the equilibrium is reached.[3], [33], [35], [37] The austenite to ferrite transformation occurs to lower free energy. As mentioned before as ferrite forms, carbon is rejected to the surrounding austenite and lowering the difference in free energies of ferrite and austenite. Further transformation means further increase in carbon content of the austenite and at some point, the free energies of ferrite and austenite will be equal and therefore transformation stops. The carbon concentration of austenite which represents the equal free energies is defined as the carbon concentration that coincide with T_0 curve. The free energy curves and the related part of the equilibrium iron-iron carbide phase diagram are represented in Figure 2.17. In other words, T_0 point is a locus point on temperature and carbon concentration diagram where austenite and ferrite of the same chemical composition have identical free energies. [7], [25], [37]

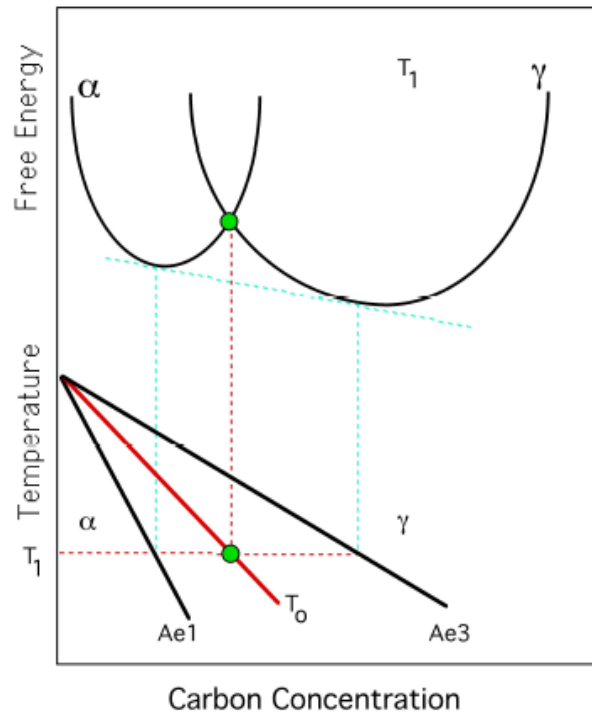


Figure 2.17. Definition of T_0 curve [25]

When carbon concentration of austenite reaches the locus point, bainite transformation stops. At that point, transformation is thermodynamically impossible. Since the carbon concentration is below than the equilibrium value of austenite this mechanism is called incomplete transformation phenomenon. However, there are some experiments that shows that carbon concentrations of retained austenite is in between the T_0 curve and the Ae_3 paraequilibrium line. These measurements performed by Bhadeshia and Waugh have indicated that the bainite transformation do not stop at the T_0 curve, on the contrary continues. Still residual austenite carbon concentration is well below than the equilibrium value (Ae_3), therefore these findings are suitable with the incomplete reaction phenomenon.[18], [37]

The bainite fraction can be calculated by Lever Rule on Figure 2.17. [25] There are three ways to increase the fraction of bainitic ferrite and hence three precaution to avoid blocks of retained austenite. The first one is adjusting the T_0 curve to higher carbon concentrations addition of substitutional alloying elements. The second one is

using a steel with high carbon concentration and the last one is lowering the transformation temperature so that further transformation can take place, so less retained austenite is obtained.[3]

Displacive and diffusive theories find a common ground that bainite forms above M_s and below B_s . These are the lowest and the highest transformation temperature limits respectively. Transformation temperature and the fraction of austenite undergoes transformation is inversely proportional. As transformation temperature is lowered under B_s , the fraction of bainitic ferrite is increased.[33], [36]

2.4. Heat Treatment of Bainite Formation

As mentioned before in the 2.2.2.Bainite on the page 14, in order to obtain a 100% bainitic morphology, first the steel must be fully austenitized and then cooled to a temperature above the martensite start and below the pearlite transformation temperatures of the steel. Cooling rate must be rapid enough to avoid formation of other phases like ferrite. Moreover, isothermal heat treatment is essential to give time austenite decomposition to ferrite. The period should be long enough to complete the transformation. However, no matter how long the time is, there will be always residual austenite due to incomplete transformation phenomenon. [4], [6], [18] This heat treatment is called austempering. [2]

2.4.1. Austempering

Austempering is an isothermal transformation of a ferrous alloy in a temperature range in between the pearlite and martensite transformation. It can be described as an interrupted quenching and remaining at a temperature above M_s for formation of bainite morphology. The cooling path of a typical austempering process is shown in Figure 2.18. Conventionally steels are quenched and tempered to form tempered martensite however austempering has several advantages over quenching and

tempering. For the same hardness value, austempered steels show increased ductility, toughness and strength. Since there is no martensite formation, dimensional change and hence additional machining is reduced. [2], [27]

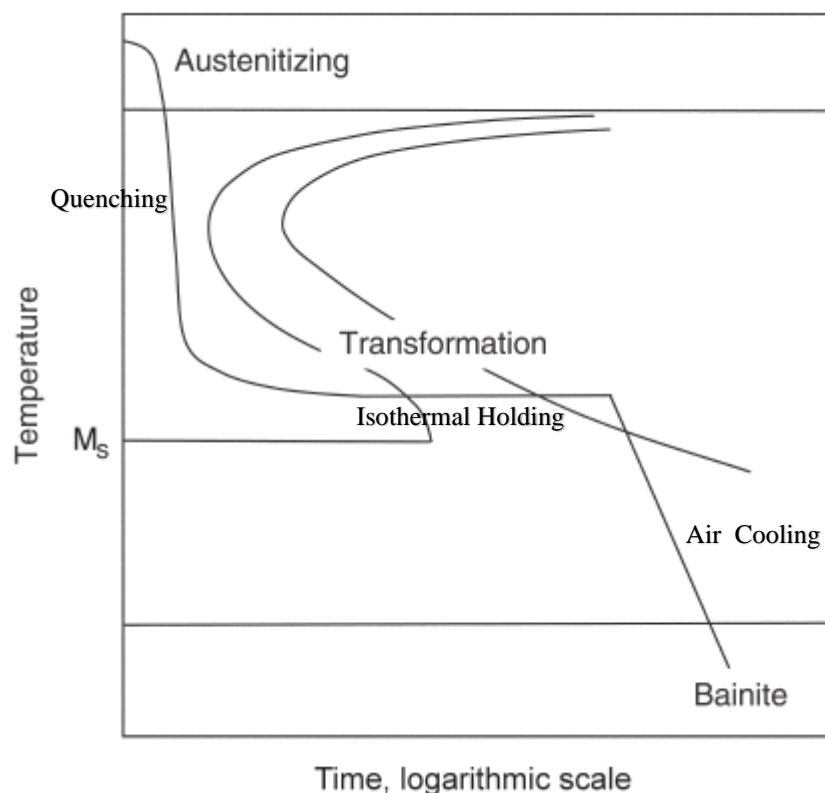


Figure 2.18. Typical austempering heat treatment path[27]

Austenitizing temperature is an important parameter in heat treatments because it controls the austenite grain size, hence the grain size of the final morphology. Moreover, in 100Cr6 austenitizing temperature affects the carbide dissolution and martensite start temperature by implication. Upon heating austenite starts to form at 775 °C however typical austenitization temperature is determined for 100Cr6 in between the range of 840 °C and 860 °C to keep approximately 3-4% volume carbides in the final morphology so that the product would be wear resistant. [2], [11] In this study, three different austenitization temperature 825 °C, 875 °C and 1000 °C are

selected to see the effect of different carbide dissolution on the microstructure and mechanical properties.

For quenching medium generally molten salt is used because of several reasons. First, it can maintain the selected temperature for long times and remains stable at operating temperature. It eliminates the vapor phase barrier during initial stage of quenching. Moreover, it can be easily removed from the specimen by water. The temperature is selected according to the steel and aimed morphology.[2]

For selection of isothermal time, aimed morphology and the transformation temperatures are the criterion. By austempering, transformation period must be long enough to crossing 1% bainite and 100% bainite times. Then the specimen is air cooled.

2.4.2. Tempering

Tempering is simply heating of a steel under a temperature lower than eutectoid temperature for a period to increase ductility and toughness and also, stress relief. Tempering temperature and time are chosen according to the hardness required. The temperature and time effect on hardness is seen on Figure 2.19. Tempering can be performed in convection furnaces, hot oil, salt bath and molten metal. The selection is done according to the working condition. In this thesis, two tempering temperature are selected: 180°C and 235°C for 90 minutes and suitable furnace is for these temperatures is convection furnaces. [2]

Tempering process has four stages; the temperature ranges of stage 1, stage 2, stage 3 and stage 4 are 20 to 100 °C, 100 to 200 °C, 200 to 350 °C and 250 to 700 °C respectively.[2] Due to the selection of temperatures, some of the tempered specimens will go through stages 1 and 2, some of the specimens will go through stages 1, 2 and 3.

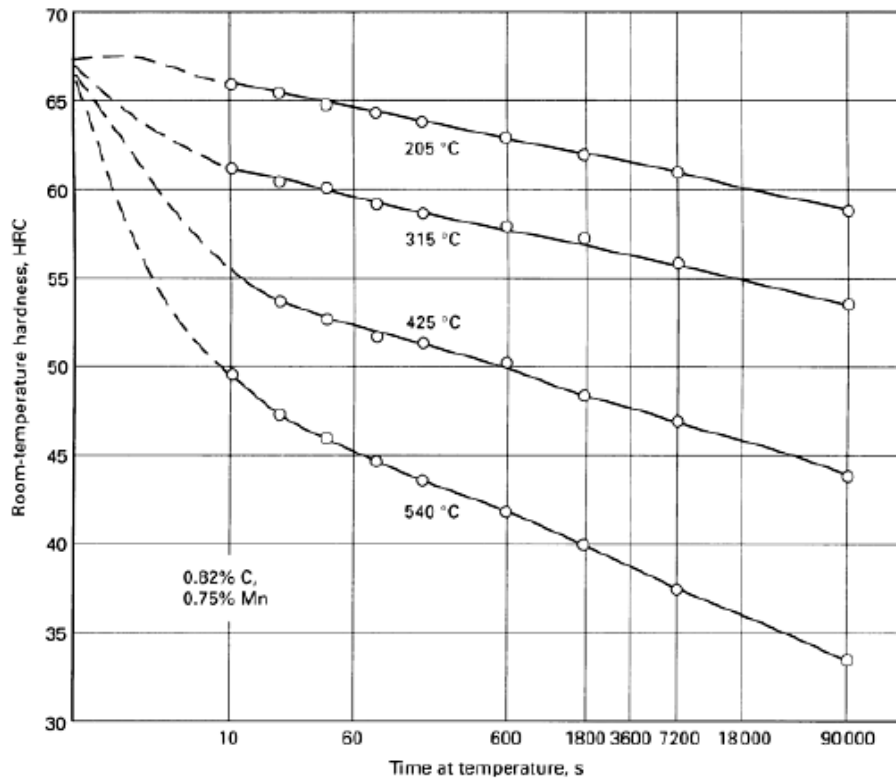


Figure 2.19. Graphical representation of effect of tempering time and temperature on hardness.[2]

In medium and high carbon steels (like 100Cr6), martensite formed is not stable at room temperature because carbon can diffuse in the martensite lattice at this temperature. Miller et al, has shown by atom probe experiments that up to 100 °C, during the stage 1 of tempering, due to short range diffusion of carbon atoms to dislocation and martensite plate boundaries, carbon clusters form.[2],[13],[38]

As temperature increases, the instability of carbon concentration increases because diffusion is more rapid at higher temperatures and eventually carbides (cementite (Fe_3C) and ϵ -carbide ($Fe_{2.4}C$)) start to precipitate. This corresponds to the stage 2 of tempering. Therefore, in medium or high carbon steels, an increase in hardness have been observed when temperature is around 100 °C and above which was related to the carbide precipitations. [2], [13]

In the stage 3 meaning temperature is above 200 °C, the retained austenite decomposes. As mentioned in the 2.3. Transformation Mechanisms of Bainite on the page 23, during austenite transformation to bainite, bainite reaction stops when the carbon content of retained austenite reaches to T_0 point instead of the equilibrium value. That is why austenite is not stable in a thermodynamic point of view. [39],[40] In most resources, it is indicated that at stage two of tempering, retained austenite decomposes into bainitic ferrite and cementite. [2],[13],[21] However, Talebi et. al. [39] has experimented that, during tempering some of the retained austenite transforms into lower bainite. Although this decomposition, there is still many untransformed retained austenite islands in the structure. These islands transforms into fresh martensite during cooling to ambient temperature. [39] Furthermore, Podder and Bhadeshia [41] has proved that by dilatometry, during first hour of tempering, ferrite formation does not appear however precipitation of carbides decreases the carbon concentration of austenite and hence lead to formation of fresh martensite during cooling cycle, identified by TEM. This phenomenon is described as conditioning.[41] In the stage 4 of tempering, precipitated carbides spheroidize.[2] In this study none of the samples are heat treated to stage 4.

2.5. Kinetics of Bainite Transformation

While investigating the rate of bainite reaction, more than nucleation and growth must be considered, like carbon diffusivity or undercooling. Sheaves of bainite normally nucleate at the austenite grain boundary and propagate towards the interiors by nucleation and growth of individual subunits. New subunits nucleate at the tips of previous subunits. The nucleation of subunits in adjacent positions happens in a much slower rate. Due to this interval between formation of subunits results in the overall lengthening rate of a sheaf is smaller than that of individual subunit. This process which is lengthening occurs in a constant rate. There are researches about that thickening rate is constant too however, Hehemann et. al. have found that thickening rate decreases with increasing thickness. [13],[22] This result is expected because if

bainitic ferrite forms by the diffusional mechanism, it can grow until the average carbon concentration of the phases reaches the equilibrium value. On the other hand, if bainitic ferrite develops by displacive mechanism, the thickness and length of the subunits is restricted by the neighboring austenite and in this case, thickening is limited by coherency of the ferrite austenite interface. [34]

Carbide precipitation also affects kinetics since by precipitation, carbon is removed from residual austenite or supersaturated ferrite. [13] Diffusion rate of carbon is smaller in austenite than ferrite so diffusivity of carbon are different in ferrite and austenite so rate of decarburization is directly affected.[22]

At lower temperatures, bainite nucleation is more rapid than its growth and so that finer grained structure forms at lower temperatures.[12] However, at lower temperatures transformation kinetics are low so that to complete bainite reaction time needs to be increased. The critical thing is decrease in temperature and increase in time are not proportional. According to Luzginova's experiments isothermal transformation temperature gets closer to the M_s , isothermal holding time should be increased more. Luzginova has compared her experiment with calculated bainite fractions according to literature and this comparison is shown in Figure 2.20. [42]

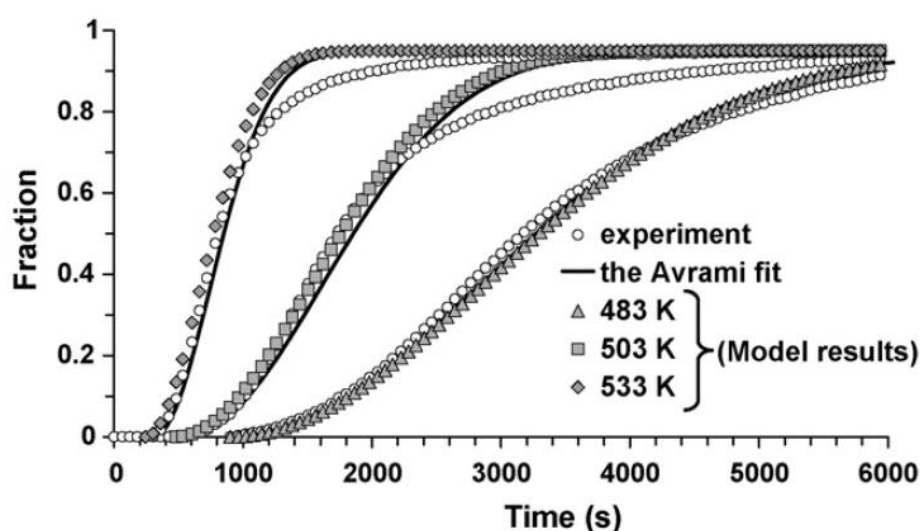


Figure 2.20. Comparison in between the Luzginova's experiments and calculated bainite fractions for different isothermal holding times[42]

2.6. Alloying Elements

All the elements that accelerate bainite reaction increase free energy difference between ferrite and austenite. [9]

Carbon has a large effect on suppressing not only the martensite start temperature (M_s) but also the bainite start temperature (B_s) for both upper and lower bainite. Like M_s , B_s is suppressed by other elements too (Eq. 4) but carbon is the most effective one.[13]

$$B_s(^{\circ}\text{C}) = 830 - 270C - 90Mn - 37Ni - 70Cr - 83Mo$$

Eq. 4

Moreover, the solubility of carbon in austenite is much higher than that of ferrite, and carbon itself is an austenite stabilizer so that it causes a general retardation of transformation kinetics.[13] Furthermore, increase in carbon concentration leads to decrease in sheave lengthening rate. [13], [21]

The addition of aluminum, silicon and cobalt can accelerate the bainite transformation kinetics by adjusting the free energies, however in 100Cr6 these elements are not present in appreciable amounts. Thus, chromium has a retardation effect on bainite formation since it increases hardenability, it shifts the C curve to the longer times on the TTT diagram, but in bearing applications due to wear resistance requirement Cr is essential because it is a strong carbide former element. [22], [43]

CHAPTER 3

MATERIALS AND METHODS

3.1. Material

In this thesis study 100Cr6 (SAE 52100) steel grade is used. It is supplied from Ortadoğu Rulman Sanayi ve Ticaret A.Ş.

3.1.1. Spectral Analysis

Spectral analysis is performed in “Optical Emission Spectrometer WAS Foundrymaster” located in the Department and shown in Table 3.1.

Table 3.1. *Chemical composition of 100Cr6 raw material used*

Composition in Wt%									
C%	Mn%	Si%	P%	S%	Cr%	Mo%	Cu%	Al%	Ni%
1.01	0.368	0.314	0.018	0.0058	1.43	0.0365	0.0957	0.163	0.0695

3.2. Heat Treatment Processes

3.2.1. Heat Treatment Equipment

Protherm furnace is used for austenitization at elevated temperatures. Protherm salt bath is used for quenching the austenitized samples to desired temperatures and for isothermal treatment. It has 8.5 liter salt capacity and this high volume with respect to specimens is enough to minimize temperature fluctuations. The AS 135 Tempering Salt (PETROFER) is used in salt bath. It is composed of alkaline nitrites and nitrates. Its melting point is 135 °C and its working range is in between 160°C and 550 °C. The most useful property of this salt is it can be easily removed from the workpiece since it is water soluble. [44] Dry Heat Sterilizer/Oven is used for long isothermal heat

treatments and tempering. Its maximum working temperature is 250 °C. All the heat treatment equipment used for the thesis is shown in Figure 3.1.

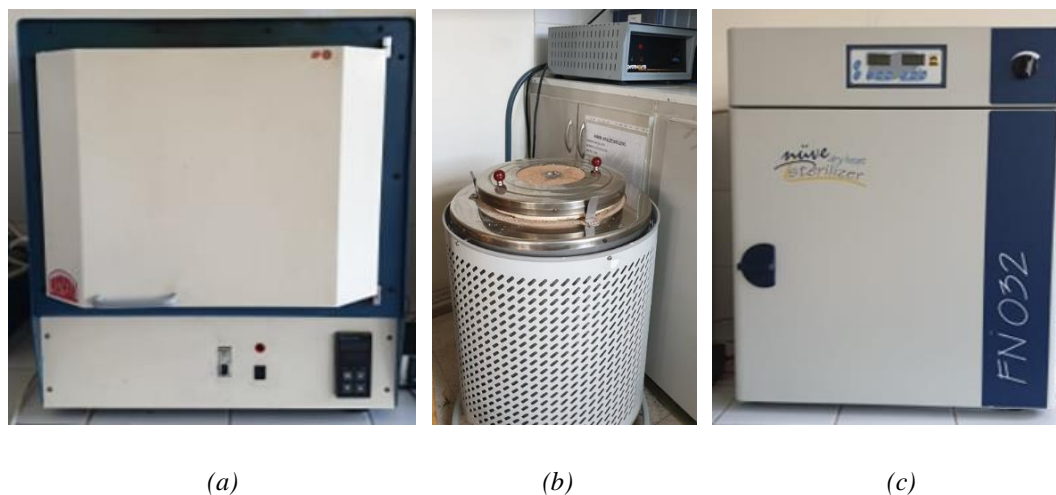


Figure 3.1. Heat treatment equipment used in this study (a) Protherm muffle furnace, (b) Protherm salt bath, (c) Dry heat oven.

In this study 100Cr6 bar having 35 mm diameter is used (Figure 3.2.a.). For heat treatment these bars are cut into half by using Metkon Metacut 251 Abrasive Cutter and the specimens with dimensions 17x15 mm are used (semi-rod) (Figure 3.2.b).



Figure 3.2. (a) the 100Cr6 bar and (b) the heat treatment specimen cut from it.

3.2.2. Heat Treatment Parameters

As mentioned before, three main austenitization temperatures are selected; 825 °C, 875 °C and 1000 °C. All the specimens are austenitized for 30 minutes. After austenitization, some of the specimens are quenched in oil at room temperature to obtain 100% martensitic structure whereas several others are isothermally treated for bainite formation. For isothermal heat treatment, the transformation temperature is selected as 200 °C to be certain about staying above the M_s and increasing transformation rate. Isothermal holding times are 1, 2, 4 and 6 days depending on the austenitization temperature. Moreover, some of the oil quenched and isothermally heat-treated specimens are tempered. For tempering two temperatures are selected: 180 °C, and 235 °C. 180 °C is a routine application in 100Cr6. However, it is known that most of the retained austenite transforms to martensite upon cooling to RT if tempering is carried out at 235 °C. Therefore, it can be assumed that after tempering at 235 °C, the specimens are nearly austenite free. Specimens are tempered for 90 minutes. Heat treatment operations are summarized in Table 3.2.

At the end of each heat treatment operation, specimens are cooled in air. For example, the specimen 825A-2-235T-180T in Table 3.2, the piece is first austenitized at 825 °C then quenched into the salt bath and after 2 days of isothermal heat treating the piece is cooled to room temperature in air. For tempering processes, first it is tempered at 235 °C for 90 minutes and again air cooled. The second step of tempering is that the specimen is held at 180 °C for 90 minutes and then air cooled. When the specimen is at room temperature the characterization is done.

Table 3.2. Process flows and sample identifications

Quenched and Tempered Specimens				
	Austenitization Temperature (°C)	Tempering (°C, 90 min.)		Sample ID
Oil Quenched	825	-		825A-Q
	875	-		875A-Q
	1000	-		1000A-Q
Quenched and Tempered	825	180		825A-Q-180T
		235		825A-Q-235T
		235+235		825A-Q-235T-235T
		235+180		825A-Q-235T-180T
	875	180		875A-Q-180T
		235		875A-Q-235T
		235+235		875A-Q-235T-235T
		235+180		875A-Q-235T-180T
	1000	180		1000A-Q-180T
	Isothermally Heat-Treated Specimens			
	Austenitization Temperature (°C)	Isothermally Holding Time (@200 °C, days)	Tempering (°C, 90 min.)	Sample ID
Isothermal Transformation	825	1	-	825A-1d
		2	-	825A-2d
	875	1	-	875A-1d
		2	-	875A-2d
	1000	4	-	1000A-4d
		6	-	1000A-6d
Isothermally Heat Treated and Tempered	825	1	180	825A-1d-180T
		2	180	825A-2d-180T
		2	235	825A-2d-235T
		2	235 +180	825A-2d-235T-180T
	875	1	180	875A-1d-180T
		2	180	875A-2d-180T
		2	235	875A-2d-235T
		2	235 +180	875A-2d-235T-180T
	1000	4	180	1000A-4d-180T
		4	235	1000A-4d-235T
		6	180	1000A-6d-180T

3.3. Microstructural Characterization

Microstructural examination of the specimens is performed by using both optical and scanning electron microscopes (SEM). Sample preparation process is the same for both microscopes. First, the heat-treated specimens are cut in the middle to eliminate the decarburized region as shown in Figure 3.3.a and then the piece shown in Figure 3.3.b was mounted into bakelite for easy handling.

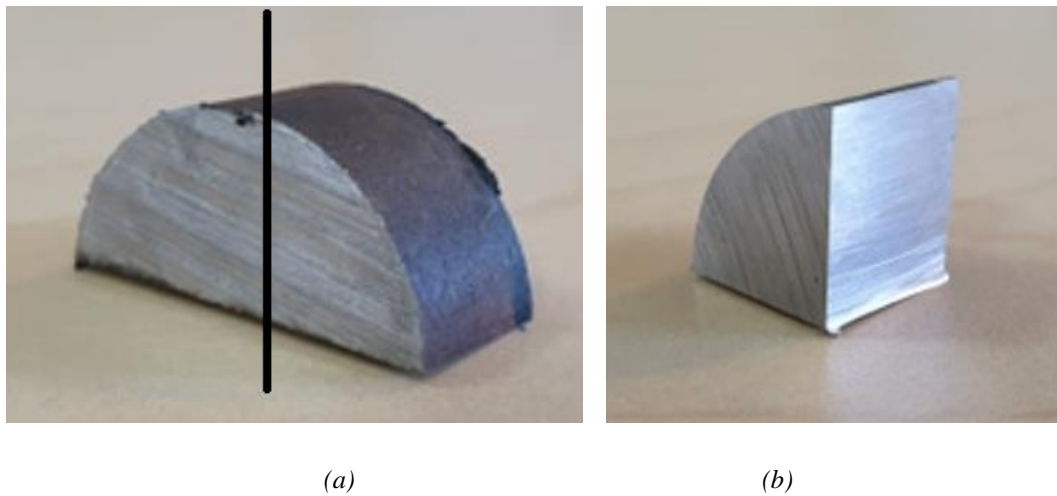


Figure 3.3. Preparation of a metallographic specimen

Mounted specimens are ground, polished and etched following the standard metallographic procedures.[45] Metkon Ecopress 100, Metkon Gripo 2V Grinder, and Mecapol P 230 Polisher are used for mounting, grinding and polishing respectively.

In polishing 6 μm and 1 μm of Diapat-P water based polycrystalline diamond suspension are used. For microstructural observation, samples are etched with 2% nital solution. Optical and SEM examinations are conducted by Huvitz Digital Microscope HDS-5800 and FEI 430 Nano Scanning Electron Microscope respectively.

3.4. Image Analysis

Accurate determination of carbide percentages is very important in calculating retained austenite volume fractions because in XRD plots carbide peaks cannot be differentiated due to overlapping. That is why in calculations, carbide percentage is directly used.

It is known that isothermal treatment and tempering does not have a crucial effect on carbide dissolution. Only austenitization temperature affects it. [11] In order to examine three different temperature effect, only the oil quenched specimens are concerned. 825A-Q, 875A-Q and 1000A-Q is prepared by standard metallographic specimen preparation procedures and etched with 2% nital solution. In order to calculate the volume fraction of carbides accurately, five images at a magnification of 1000x are taken randomly from each specimen by using optical microscope. Then 500x500 pixels (71x71 μm) are cut from each well-contrasted image. Finally, the area fraction of undissolved alloy carbides are computed by using a freeware image processing program, ImageJ.

3.5. X-Ray Diffraction Analysis

For identification and calculating volume fractions of the ferrite and retained austenite phases, X-Ray diffraction (XRD) measurements are performed using Bruker D8 Advance diffractometer. XRD pattern is obtained by using $\text{Cu-K}\alpha$ radiation with a wavelength of 1.5418 \AA at an operation voltage of 40 kV with a current of 30 mA. The specimens are scanned between 2θ s of 30° - 150° at a scanning rate of $1^\circ/\text{min}$.

The specimens for XRD analysis are prepared according to standard metallographic specimen preparation procedures. However, no etching is necessary, and specimens must be thinner than 5mm. Therefore, as polished specimens with thickness of 1.5 mm and 10x10 mm are prepared (Figure 3.4). This thickness is obtained by using IsoMet 5000 Liner Precision Saw.



Figure 3.4. The XRD measurement specimen of 100Cr6 from different angles

From XRD patterns integrated intensities and 2θ s of peaks are gathered. According to the ASTM E975-13 standard, ratio of volume fraction of ferrite over volume fraction of retained austenite were calculated.[46]

While calculating retained austenite volume fraction Equation 5 is used where R is a parameter which is proportional to the theoretical integrated intensity, $|F|^2$ is structure factor times its complex conjugate, p is the multiplicity factor of the (hkl) reflection, LP is the Lorentz Polarization factor, e^{-2M} is the Debye-Waller or temperature factor which is a function of θ and v is the volume of the unit cell. [46]

$$R(hkl) = \frac{|F|^2 p LP e^{-2M}}{v^2} \quad \text{Eq. 5}$$

After calculated R values, Equation 6 is used to calculate volume fractions where $I_\alpha(hkl)$ is the integrated intensity per angular diffraction peak (hkl) of the α -phase, $I_\gamma(hkl)$ is the integrated intensity per angular diffraction peak (hkl) of the γ -phase, $R_\alpha(hkl)$ and $R_\gamma(hkl)$ is the parameter that belongs to α and γ phases calculated via Equation 5, V_α is the volume fraction of the α -phase and V_γ is the volume fraction of γ -phase.

$$\frac{I_\alpha(hkl)}{I_\gamma(hkl)} = \frac{R_\alpha(hkl)V_\alpha(hkl)}{R_\gamma(hkl)V_\gamma(hkl)} \quad \text{Eq. 6}$$

After calculated R values, Equation 6 is used to calculate volume fractions where $I_{\alpha}(hkl)$ is the integrated intensity per angular diffraction peak (hkl) of the α -phase, $I_{\gamma}(hkl)$ is the integrated intensity per angular diffraction peak (hkl) of the γ -phase, $R_{\alpha}(hkl)$ and $R_{\gamma}(hkl)$ is the parameter that belongs to α and γ phases calculated via Equation 5, V_{α} is the volume fraction of the α -phase and V_{γ} is the volume fraction of γ -phase.[46]

The values used in calculations:

- Lattice parameters [46] (required to calculate volume of the unit cell)
 - α -iron, body centered cubic structure, unit-cell dimension is 2.8664 Å
 - γ -iron, face centered cubic structure, unit-cell dimension is 3.60 Å
- Wavelength, λ , is 1.5418 Å and constant for Bruker D8 Advance diffractometer.[47]
- Integrated intensities are collected from XRD plots.
- Multiplicity factor, p , is retrieved from Appendix 9 of Elements of X-ray Diffraction [47]
- Lorentz Polarization Factor, LP, is retrieved from Appendix 10 of Elements of X-ray Diffraction [47]
- Debye-Waller or temperature factor, e^{-2M} , is calculated where $M=B(\sin^2\theta)/\lambda^2$ by taking $2B=0.71$ according to the standard.
- Structure factor times its complex conjugate, $|F|^2$, is calculated by using atomic scattering factor according to the Equation 7 and 8. [47] Atomic scattering factor is retrieved from Appendix 8 of Elements of X-ray Diffraction [47]

$$F = f e^{2\pi i(h+k+l)} \quad \text{Eq. 7}$$

$$|F|^2 = f e^{2\pi i(h+k+l)} * f e^{-2\pi i(h+k+l)} \quad \text{Eq. 8}$$

For calculations, only (200) peaks of ferrite and austenite peaks are considered.

An example calculation of the specimen 1000A-Q is given.

Table 3.3. The data for calculation of retained austenite volume fraction of 1000A-Q

	hkl	Integrated Intensity	p	θ	LP	((sinθ)/λ)²	f	F	 F ²	e^{-2M}	R
α	200	0.676656	6	32.5	4.84	0.121	14.48	14.48	209.65	0.92	10.98
γ	200	0.445984	6	25.4	8.42	0.077	16.31	16.31	266.10	0.95	5.87

By using Equation 6; the ratio of volume fractions(V_{α}/V_{γ}) is calculated as 0.811.

Since carbide peaks are not seen due to overlapping, their volume fraction value is added to the calculations. The volume fraction of undissolved alloy carbides in 100A-Q is 0.97% (indicated in Table 4.2) In the calculations the volume fraction of carbides is denoted as V_C .

$$V_{\alpha} + V_{\gamma} + V_C = 100$$

$$V_C=0.97 \quad V_{\alpha} = V_{\gamma} * 0.811$$

So retained austenite volume fraction of 1000A-Q (V_{γ}) is 54.67

3.6. Hardness Measurement

Emco Universal Digital Hardness Testing Machine is used for hardness measurement. Tests are carried out on Vickers scale and 30 kg of load is applied to the specimens. The specimens for hardness test are prepared according to standard metallographic specimen preparation procedures. However, no etching is applied, the specimens are tested in as-polished condition for precision.

3.7. Tensile Testing

Tensile test specimens are prepared according to the ASTM E8/E8M-16a standard. [48] The specimens are dog bone shaped (Figure 3.5.), with the inner radius of 7mm and 40 mm gauge length. For every heat treatment path to be tested, three different specimens are prepared. For tensile tests, INSTRON 5582 Universal Testing with the maximum load capacity 10000 kg is used.



Figure 3.5. Tensile Test Specimen of 100Cr6 steel

CHAPTER 4

RESULTS

The aim of this thesis is to study the effect of microstructure on mechanical properties of 100Cr6 steel. For this purpose, different ratios of martensite-bainite phase mixtures are obtained by applying different heat treatment parameters. Heat treatment parameters does not only affect the morphology of bainite and martensite but also affect the volume fraction of undissolved carbides and retained austenite as well. For this purpose, several austenitization and tempering temperatures were selected. (Table 3.2)

4.1. Transformation Mechanism of Bainite in 100Cr6 Steel

The calculated TTT diagrams of the 100Cr6 steel are obtained using JMatPro software. Change in austenitization temperature results in change in dissolved carbon in matrix, because the amount of dissolution of carbides is different for each austenitization temperature. This change in carbon concentration directly affects the heat treatment parameters and that is why these extra TTT diagrams are required for each austenitization temperature. In this study three different austenitization temperatures are selected: 825 °C, 875 °C, and 1000 °C. TTT diagrams for each austenitization temperature are shown through Figure 4.1, to Figure 4.3.

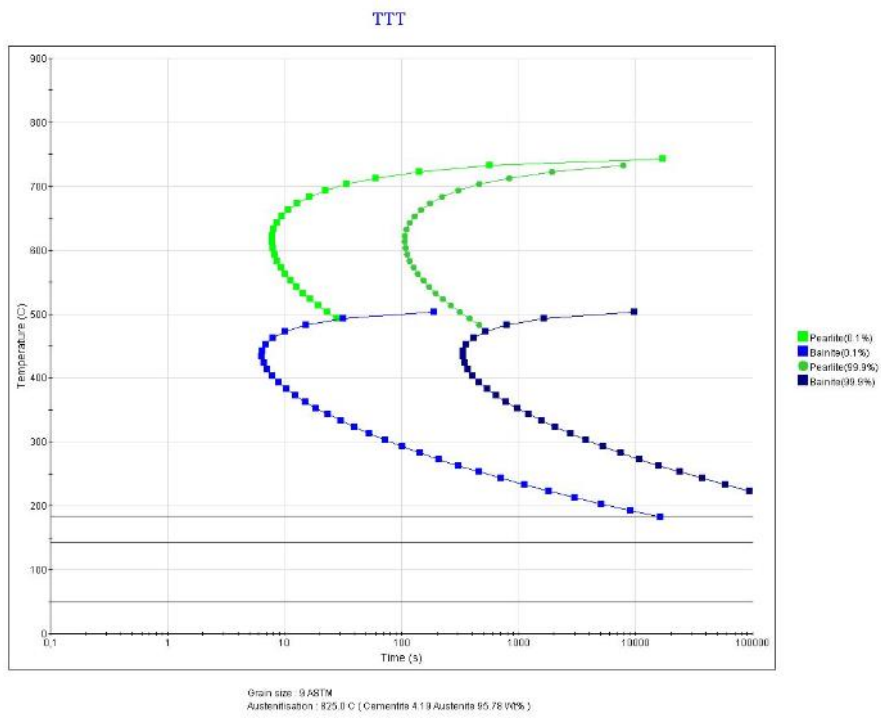


Figure 4.1. TTT diagram of 100Cr6 austenitized at 825 °C constructed by using JMatPro.

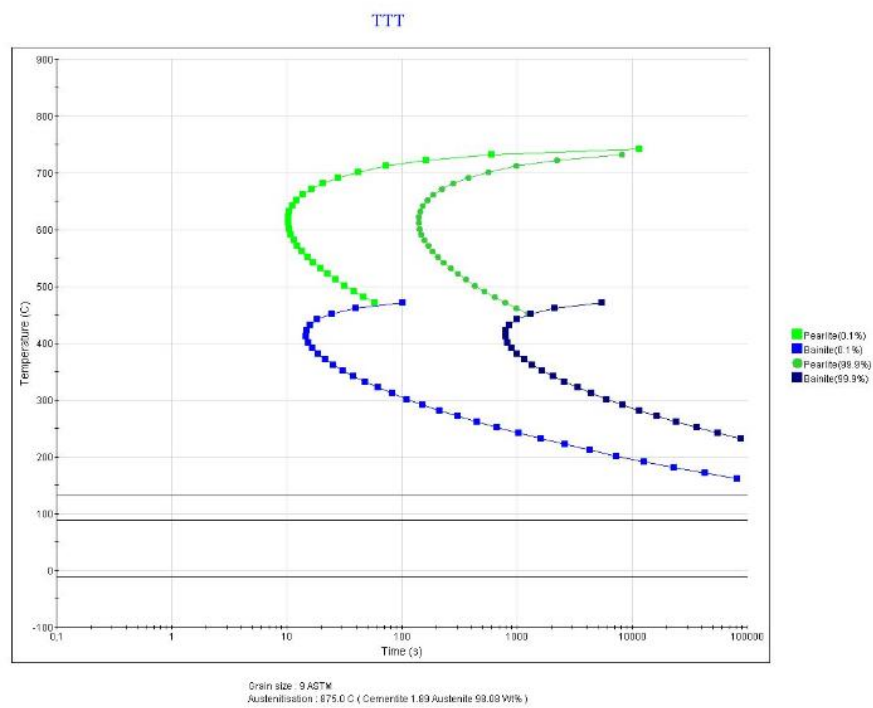


Figure 4.2. TTT diagram of 100Cr6 austenitized at 875 °C constructed by using JMatPro.

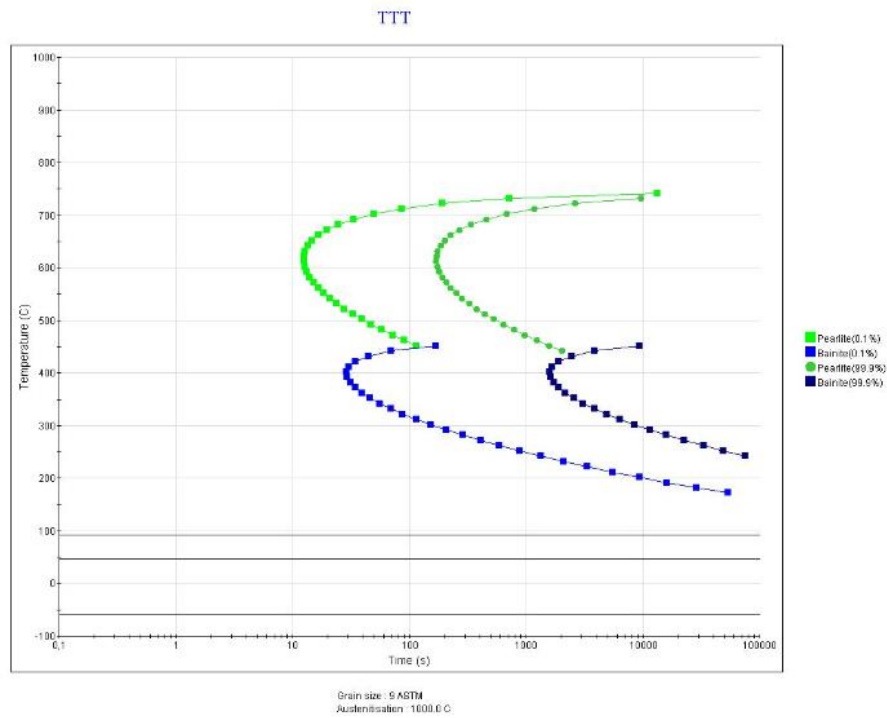


Figure 4.3. TTT diagram of 100Cr6 austenitized at 1000 °C constructed by using JMatPro.

Table 4.1. The information gathered from the TTT diagrams constructed by JMatPro

Austenitization Temperature (°C)	Martensite Start Temperature (M_s) (°C)	1% Bainite Time (hour)	100% Bainite Time (hour)
825	145	1.1	27
875	140	1.1	27
1000	128	2.7	144

The information gathered from Figure 4.1, Figure 4.2, and Figure 4.3 are summarized in Table 4.1 and heat treatment parameters are determined by using Table 4.1.

In this study, the specimens are austenitized at either 825 °C, 875 °C or 1000 °C. Since carbide dissolution is different in each austenitization temperature. After austenitization several specimens are quenched in oil to obtain 100% martensitic structure, whereas several others are isothermally treated for bainite formation. For

isothermal heat treatment, the transformation temperature is selected as 200 °C to assure bainite transformation with no martensite phase for all austenitization temperatures. According to Table 4.1 the 1% bainite and 100% bainite times are similar for the specimens austenitized at 825 °C and 875 °C. Therefore, an isothermal transformation of 1 day was chosen to obtain a mixture of bainite-martensite whereas a 2 days transformation time would give 100% bainitic structure. However, for the specimen which was austenitized at 1000°C, 1% bainite and 100% bainite times are 1.1 hour and 6 days respectively. Therefore 4 days is chosen to observe the effect of incomplete bainitic transformation, on the other hand, a 6 days transformation time would give 100% bainite. For tempering, two temperatures were selected; 180 °C and 235 °C. A tempering operation at 235 °C causes conditioning of retained austenite and hence all the retained austenite transforms to martensite. [11]

4.2. Microstructural Characterization

4.2.1. Microstructural Development in Oil Quenched Samples

In Figure 4.4 the microstructures of as quenched samples austenitized at 825 °C and 875 °C. Figure 4.4.a is the micrograph of 825A-Q and Figure 4.4.b is the micrograph of 875A-Q . They both consist of undissolved alloy carbides, martensite, and retained austenite phases. Carbides seem as white spherical particles. Retained austenite cannot be resolved in these specimens.

In Figure 4.5 the microstructure of the specimen austenitized at 1000 °C (1000A-Q) is seen. In the optical micrograph, dark regions are martensite and the light regions are retained austenite (Figure 4.5.a) In the SEM image, the dark martensite needles are seen and in between them retained austenite presents (Figure 4.5.b) martensite needles appear darker than the retained austenite. Also, alloy carbides could not be detected as most of them are dissolved in the matrix.

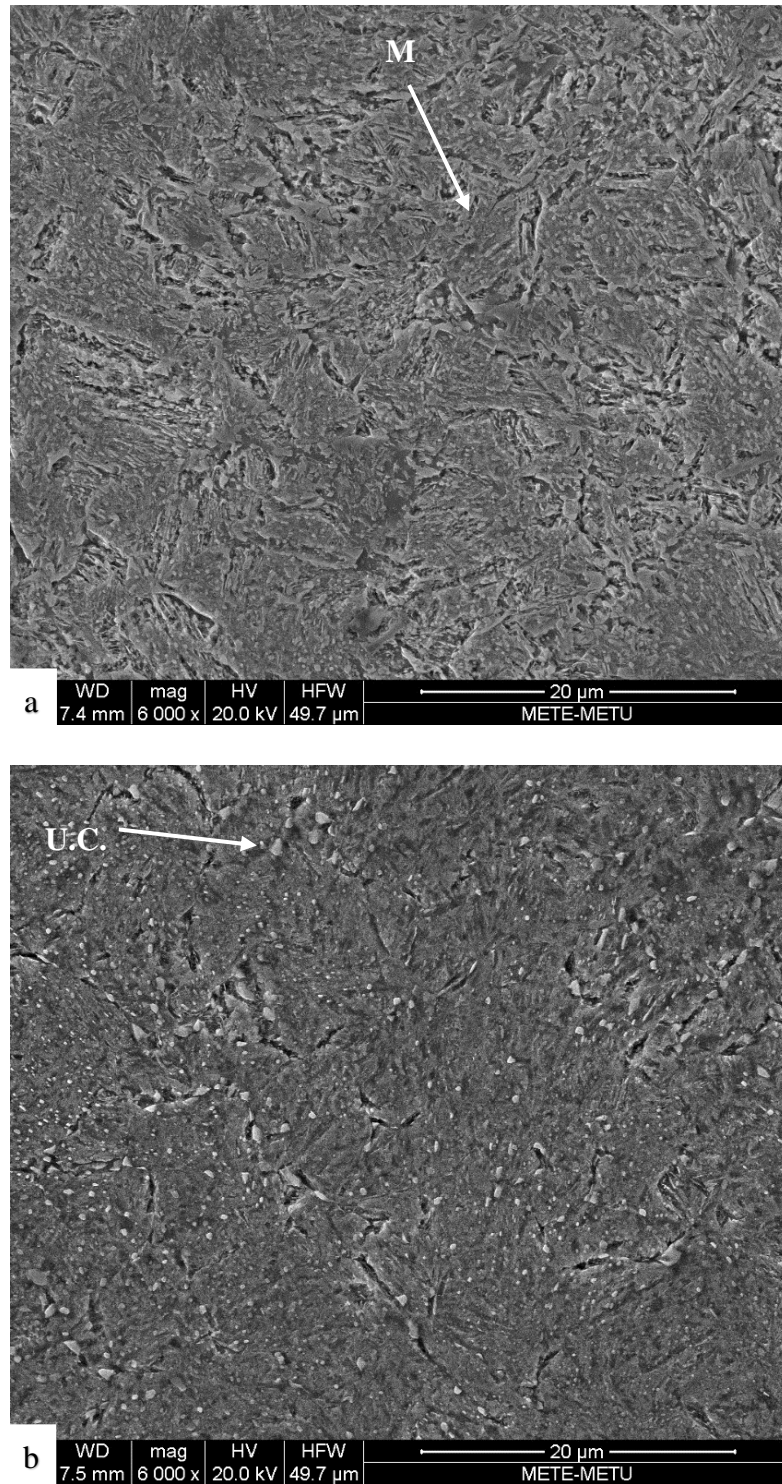


Figure 4.4. SEM image of the specimen (a) 825A-Q, (b) 875A-Q; undissolved carbides in martensitic matrix

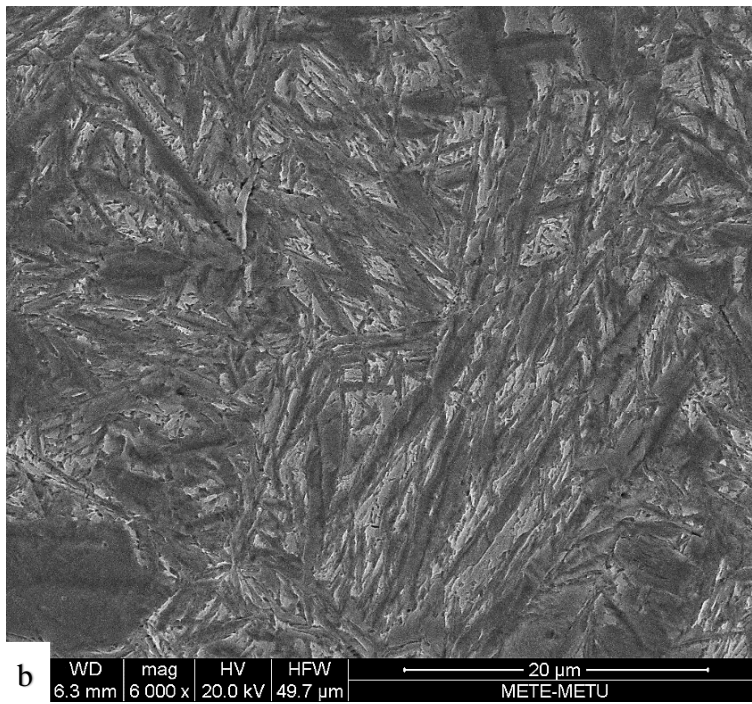
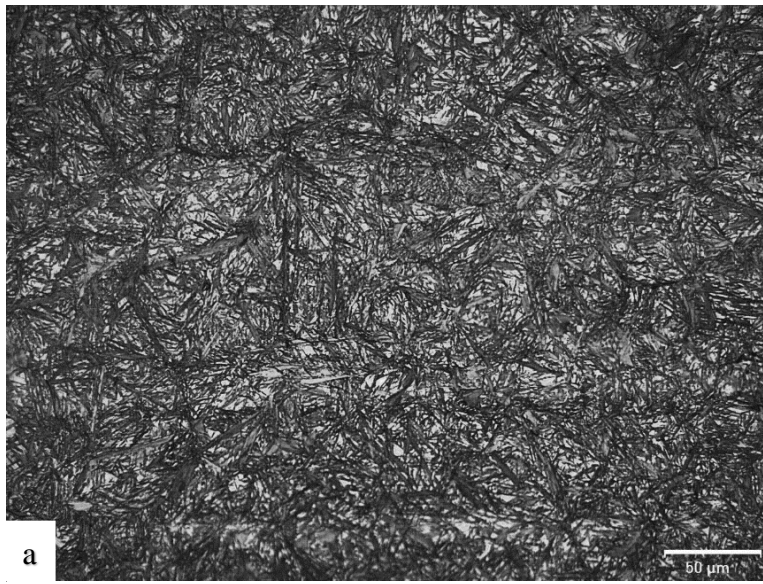


Figure 4.5. (a) Optical micrograph of the specimen 1000A-Q. Martensite needles in retained austenite (white matrix) can be seen. (b) SEM image of specimen 1000A-Q. Austenite between the martensite needles can be resolved as light contrasted areas.

4.2.2. Microstructural Development in Isothermally Heat-Treated Samples

Isothermal transformation temperature is selected as 200 °C for all the specimens.

4.2.2.1. Microstructural Development in Isothermally Heat-Treated Samples Austenitized at 825 °C

As mentioned in Table 4.1, the 1% bainite and 100% bainite transformation times are calculated as 1.1 hours and 27 hours respectively for austenitization at 825 °C.

The microstructures of 825A-1d and 825A-2d consist of martensite, bainite and alloy carbides. Retained austenite cannot be resolved. After an austenitization at 825 °C, the undissolved carbides are seen as small spherical particles embedded in the matrix (Figure 4.6 and Figure 4.7.)

Bainite phase is in the form of sheaves and martensite is seen as needle morphology. The difference is that, martensite seems as star-like and needles are disordered, on the other hand bainitic structure has a more ordered structure slightly similar to lamellar structure. (Figure 4.6.b and Figure 4.7.b)

The phases are shown on Figure 4.6 and Figure 4.7; where the letters M, and B denote martensite, and bainite respectively.

As far as the microstructure is concerned, a difference between the 825A-1d and 825A-2d specimens could not be detected. They both have very similar microstructure. However, in the following sections hardness values and retained austenite measurements will give a better information.

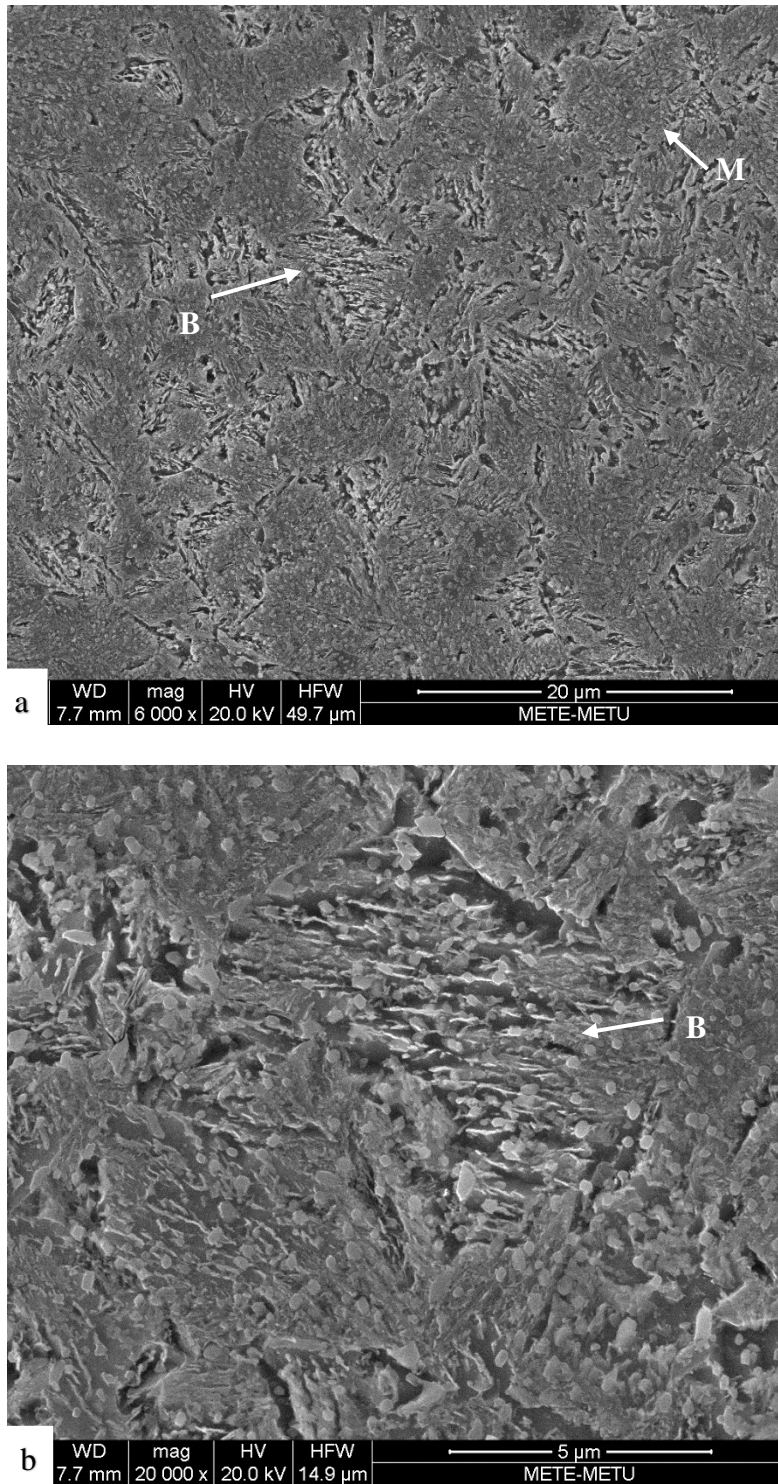


Figure 4.6. SEM image of 825A-1d, undissolved carbides in a matrix of bainite and martensite

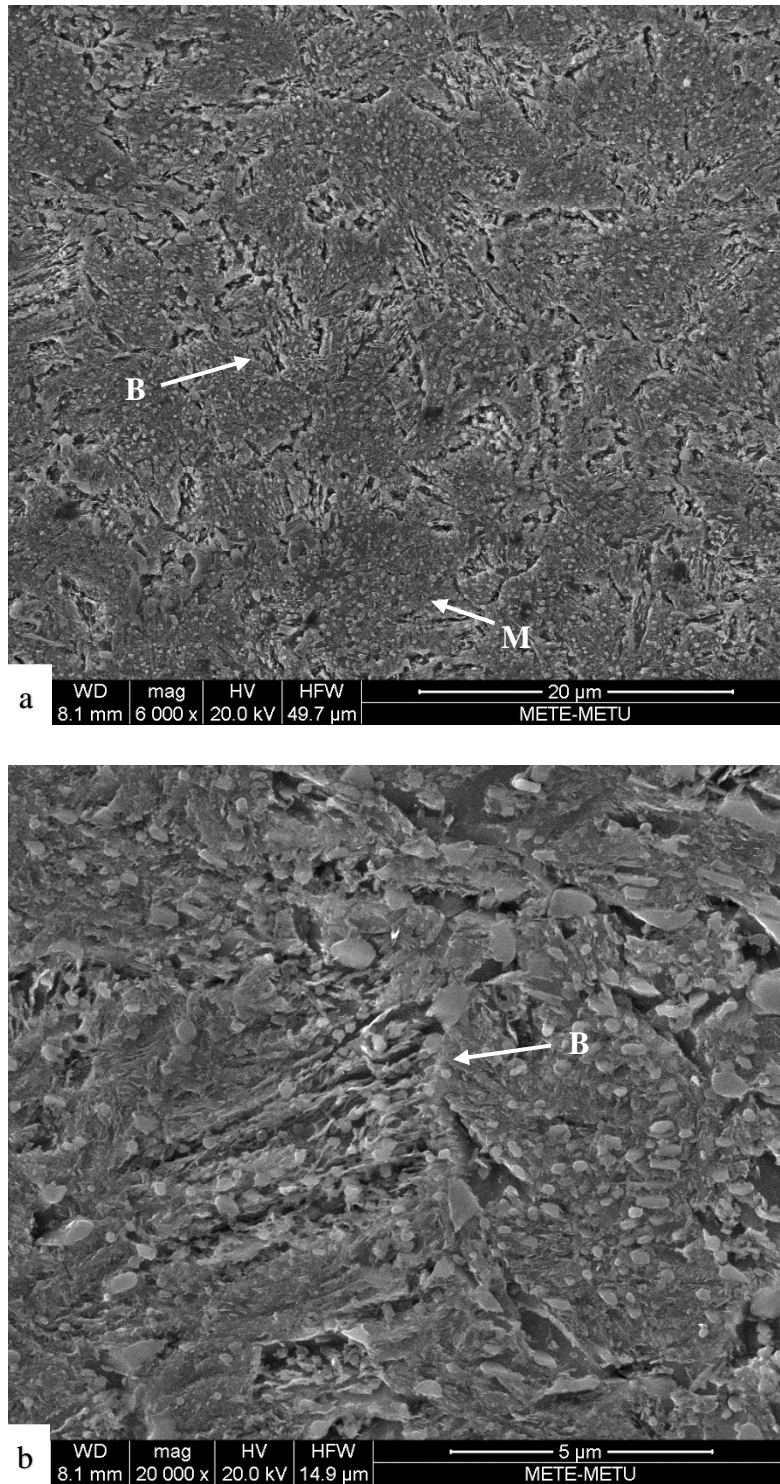


Figure 4.7. SEM image of the specimen 825A-2d, undissolved carbides in a matrix of bainite and martensite

4.2.2.2. Microstructural Development in Isothermally Heat-Treated Samples Austenitized at 875 °C

As mentioned in Table 4.1, the 1% bainite and 100% bainite transformation times are 1.1 hours and 27 hours respectively for austenitization at 875 °C.

The microstructures in Figure 4.8 and Figure 4.9 are similar to that of isothermally heat-treated specimens austenitized at 825 °C. There is no considerable difference between the micrographs given in Figure 4.8 (875A-1d) and Figure 4.9.(875A-2d) Fraction of bainitic ferrite in 875A-2d should increase with respect to the isothermally heat-treated specimen 875A-1d.

Moreover, in Figure 4.8.b and Figure 4.9.b carbide precipitates in the bainite can be observed. Undissolved alloy carbides (U.C.) are the ones which never dissolves during austenitization, and do not change during heat treatment and seem as white sphere like particles. However, carbide precipitation is the compound of carbon and iron in the bainitic ferrite and they precipitate in the ferrite in acicular morphology.

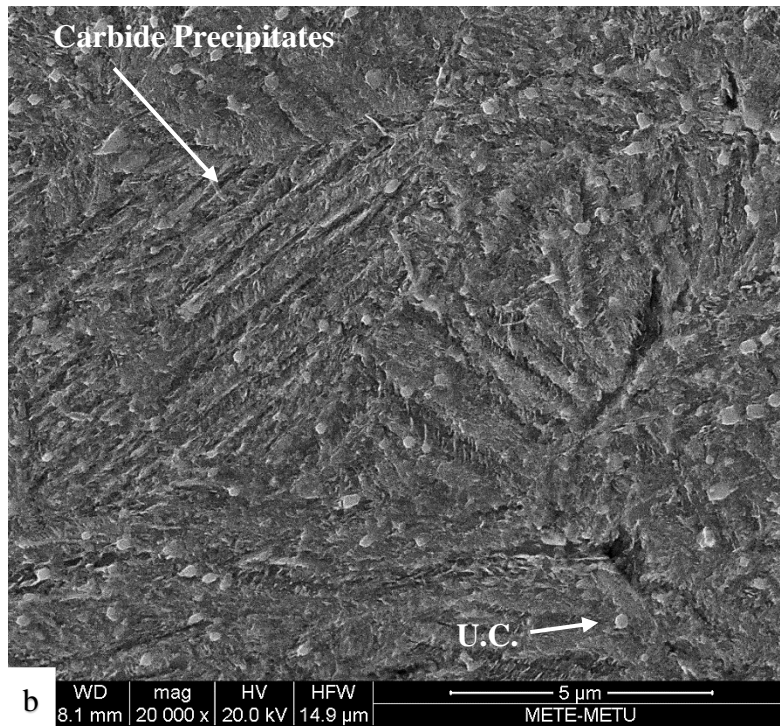
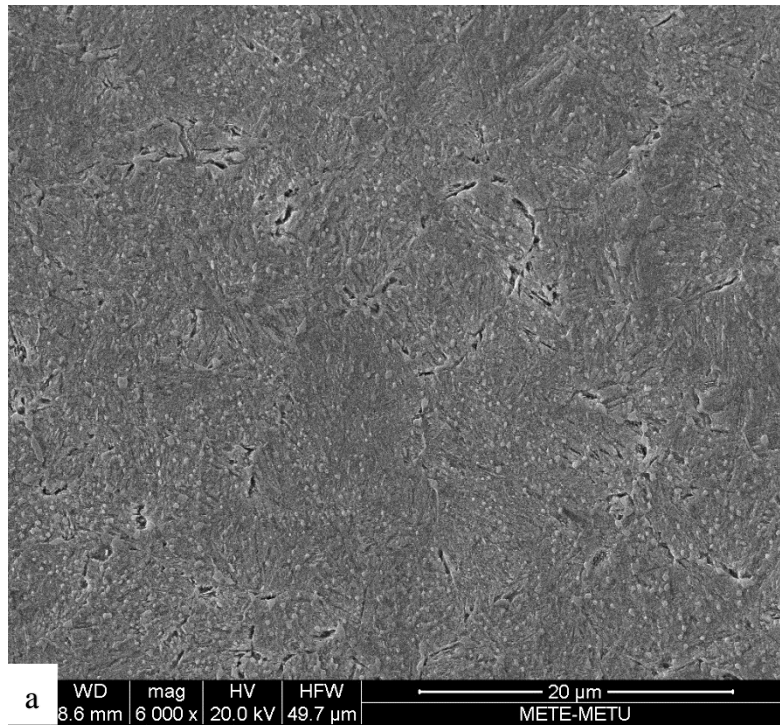


Figure 4.8. SEM image of the specimen 875A-1d, undissolved carbides in a matrix of bainite and martensite

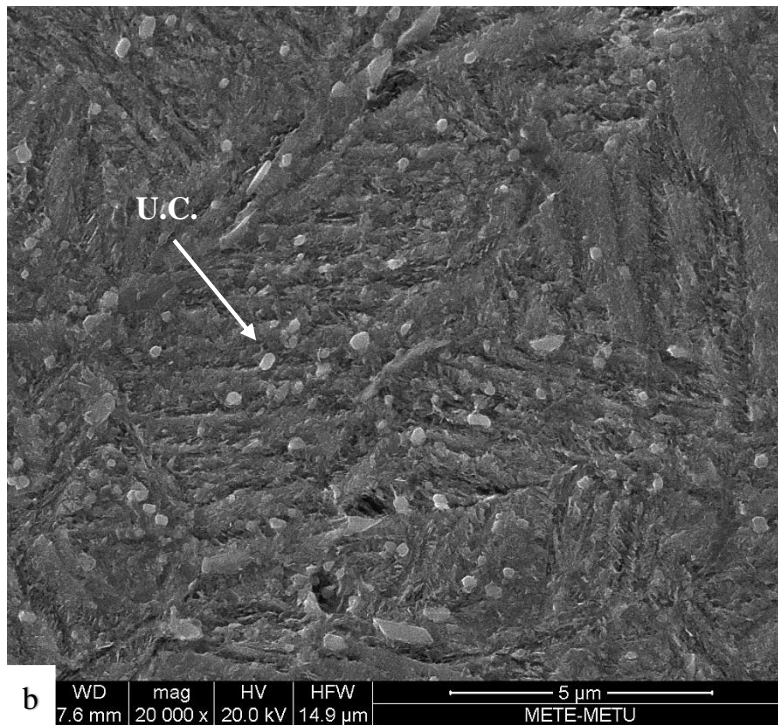
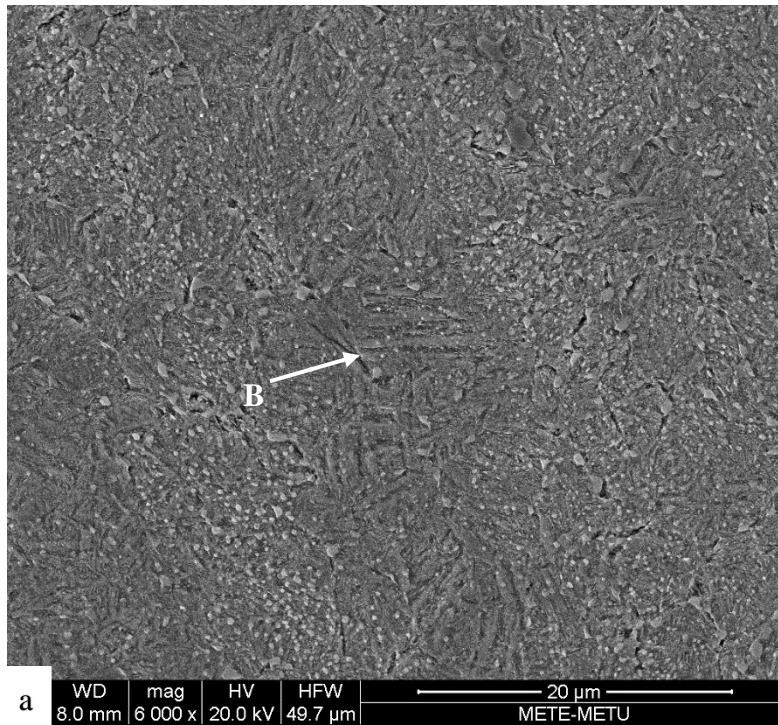


Figure 4.9. SEM image of the specimen 875A-2d, undissolved carbides in a matrix of bainite and martensite

4.2.2.3. Microstructural Development in Isothermally Heat-Treated Samples Austenitized at 1000 °C

As mentioned in Table 4.1, the 1% bainite and 100% bainite transformation times are 2.7 hours and 144 hours (6days) respectively for austenitization at 1000 °C.

The microstructures of 1000A-4d (Figure 4.10) and 1000A-6d (Figure 4.11) consist of retained austenite, bainite and martensite. However, it is difficult to differentiate these phases under SEM. The amount of bainite should increase as the transformation temperature is increased from 4days to 6days.

In the micrographs Figure 4.10 and Figure 4.11 the carbides precipitated in the bainitic ferrites has observed. Additionally, the undissolved alloy carbide precipitates (white spherical particles) are randomly distributed in the matrix. Most probably there is some amount of undissolved carbide in the specimens but since the austenitization temperature is high, they are small so that only be observed with 20000x magnification (Figure 4.10.b and Figure 4.11.b). Also, in Figure 4.11.b a blocky retained austenite is clearly seen. In some regions, austenite may have transformed into martensite that is why it is denoted as M/A.

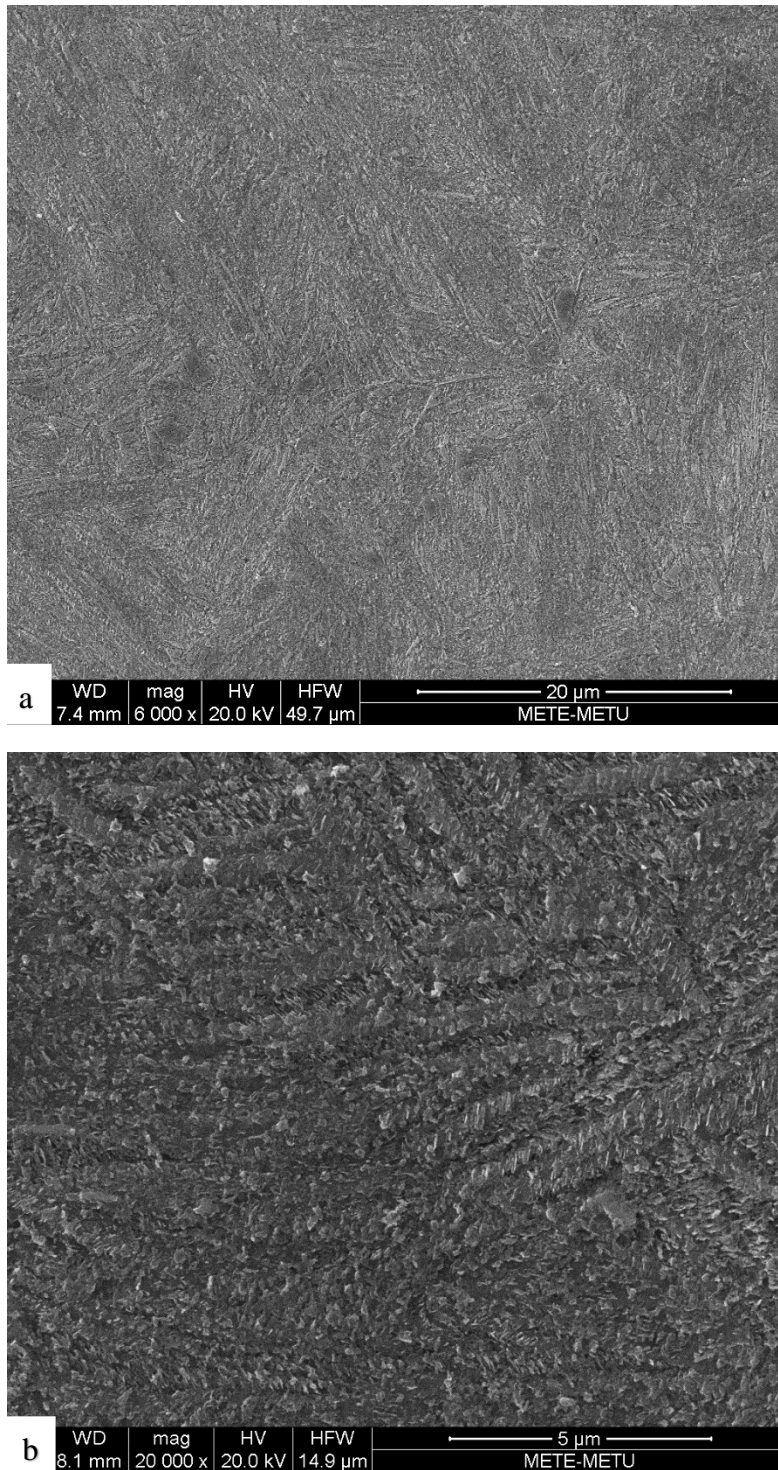


Figure 4.10. SEM image of the specimen 1000A-4d, bainite and martensite

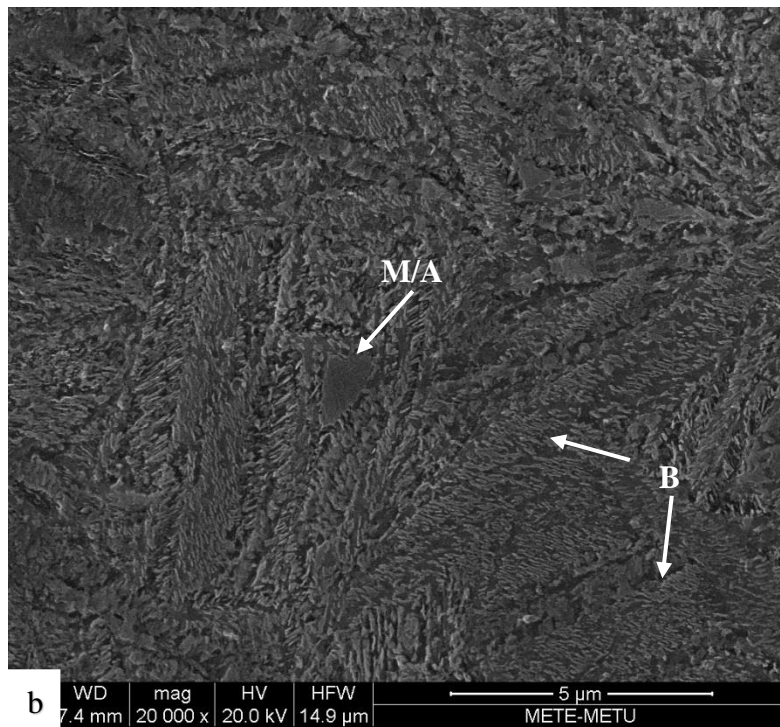
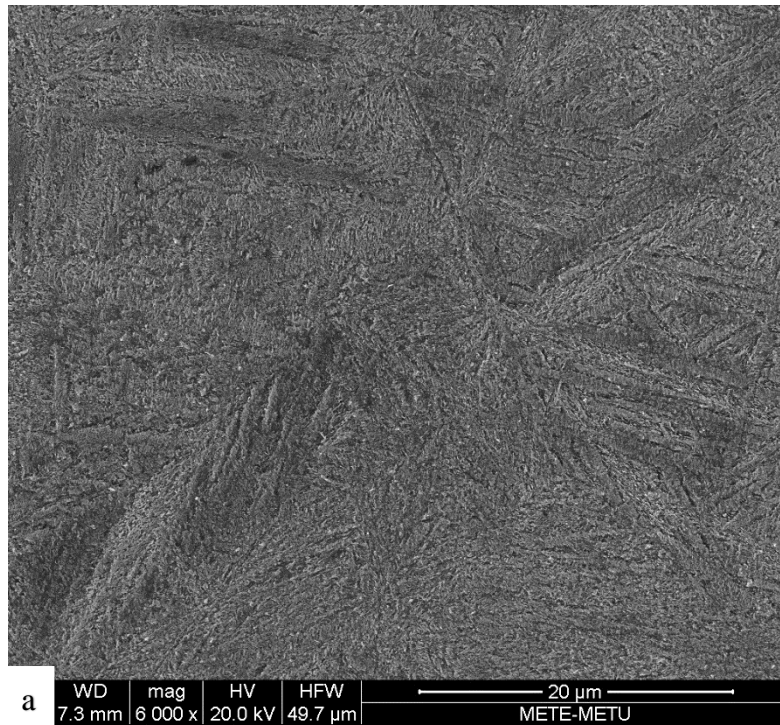


Figure 4.11. SEM image of the specimen 1000A-6d, bainite and martensite

4.2.3. Microstructural Development in Tempered Specimens

Specimens are tempered at either 180 °C or 235 °C for 90 minutes. The aim of tempering is to reduce brittleness of the martensite phase and hence make the steel commercially usable. [2]

It is known that tempering does not have a crucial role on carbide dissolution, and selected temperatures are not high enough to change the acicular morphology of bainite and martensite therefore a remarkable change in morphology is not expected. [11] That is why only the micrographs of oil quenched and tempered samples are given, it will be easy to compare martensitic morphology.

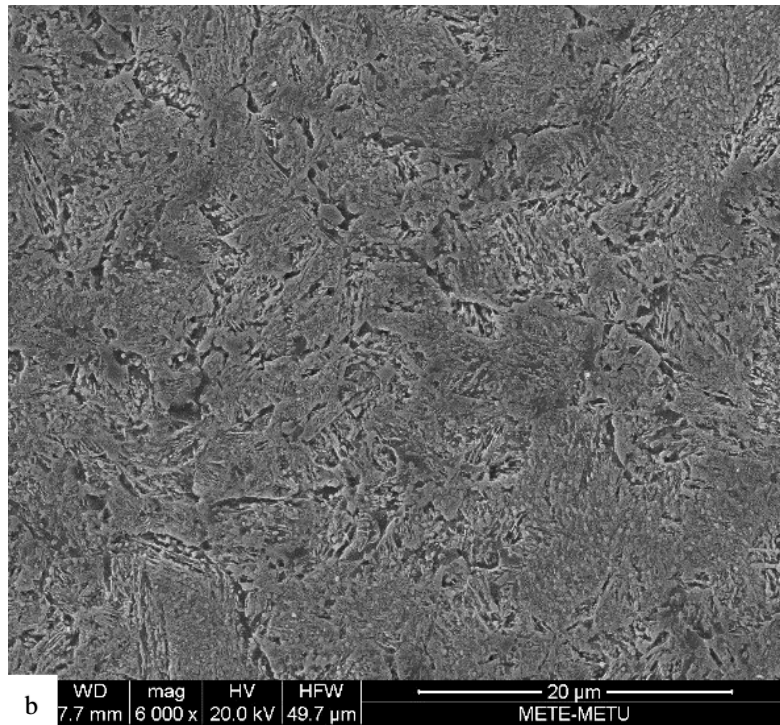
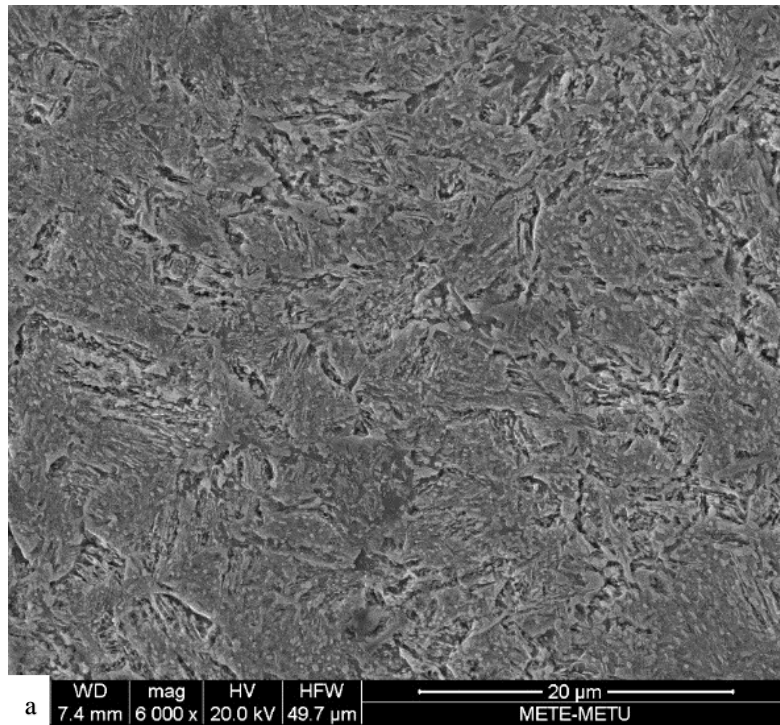


Figure 4.12. SEM image of the specimen (a) 825A-Q, undissolved carbides in martensite and (b) 825A-Q-180T, undissolved carbides in tempered martensite

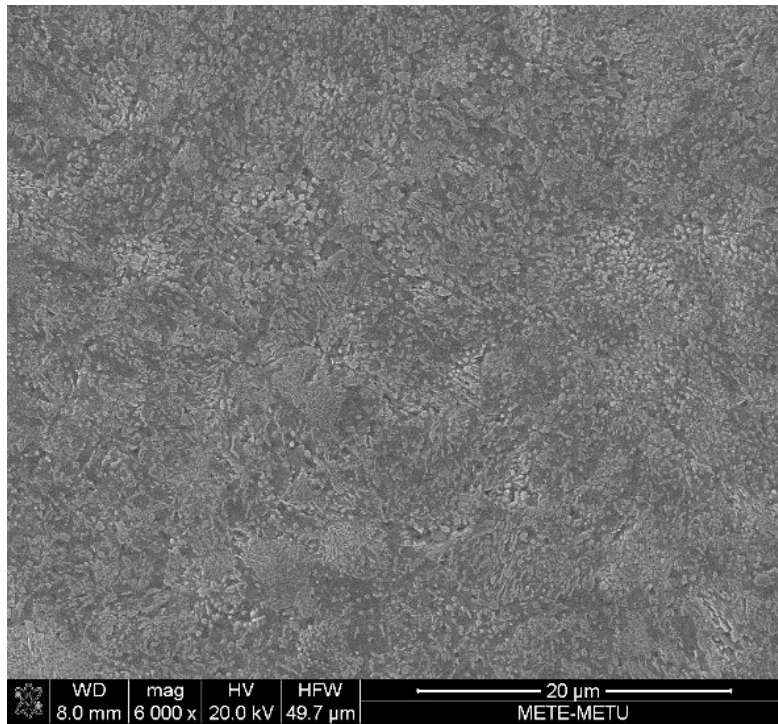


Figure 4.13. SEM image of the specimen 825A-Q-235T, undissolved carbides in tempered martensite

Figure 4.12 and Figure 4.13 are a comparison of as- quenched and the tempered specimens of austenitized at 825 °C. It is seen that tempering did not change the microstructure remarkably.

Similar comparison can be made for specimens which were austenitized at 875 °C and 1000 °C and tempered. (Figure 4.14, Figure 4.15, and Figure 4.16)

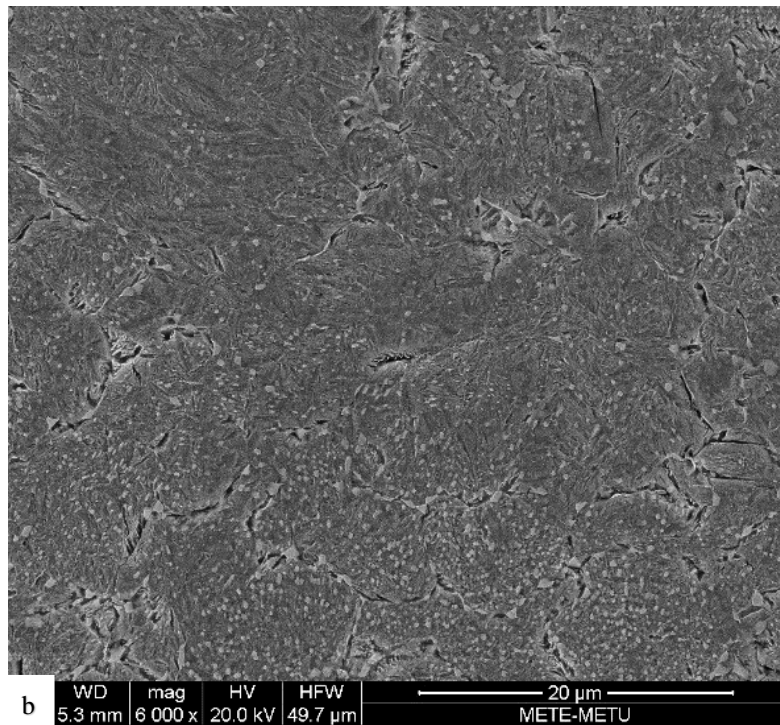
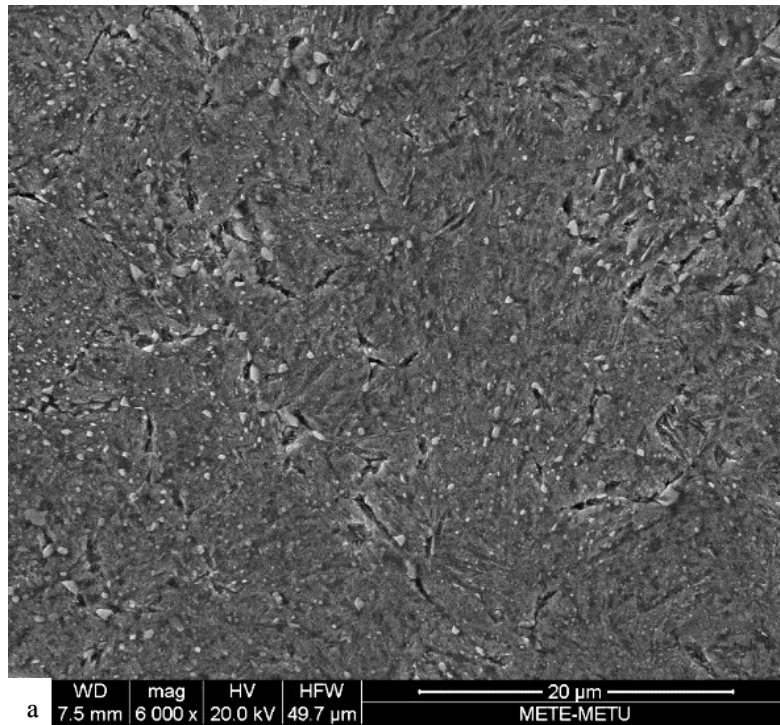


Figure 4.14. SEM image of the specimen (a)875A-Q, undissolved carbides in martensite and (b) 875A-Q-180T, undissolved carbides in tempered martensite

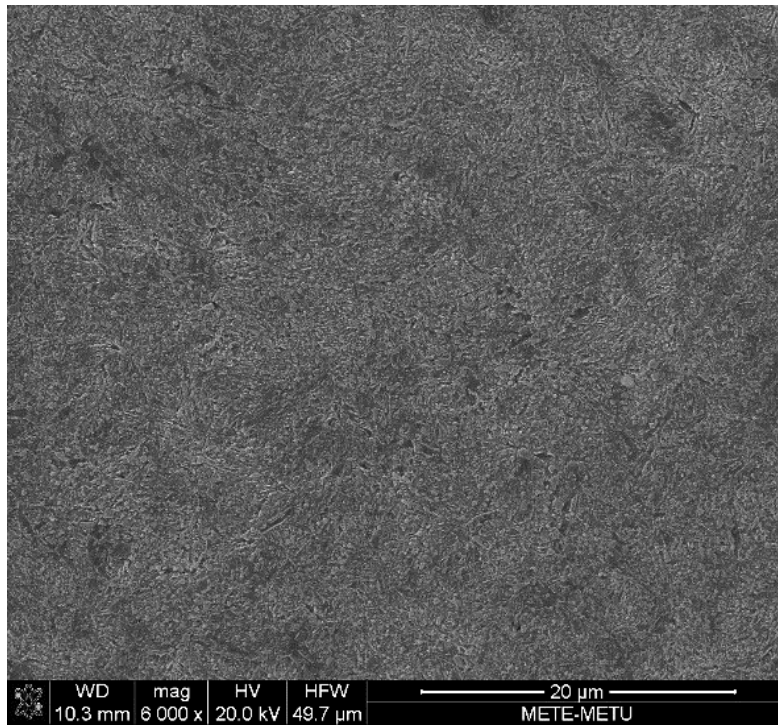


Figure 4.15. SEM image of the specimen 875A-Q-235T, undissolved carbides in tempered martensite

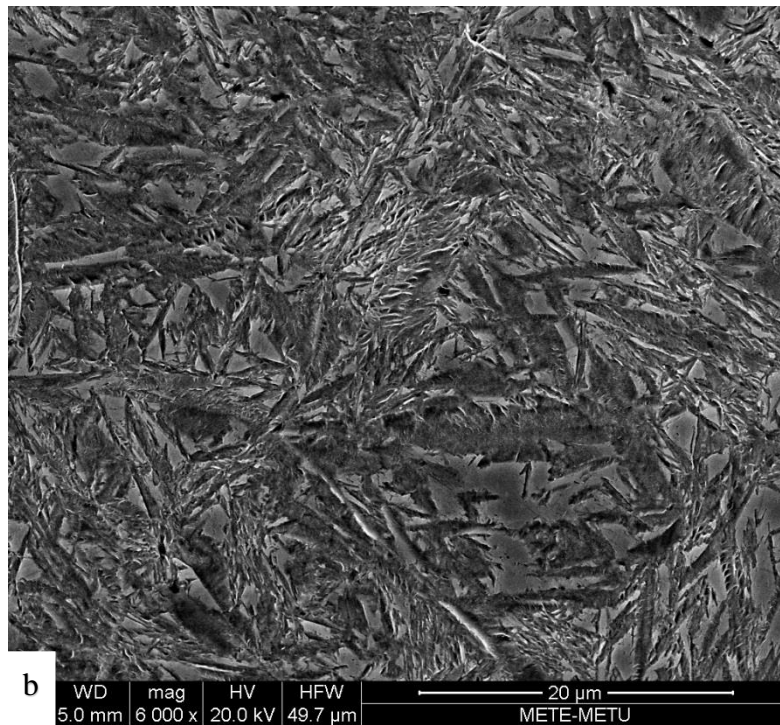
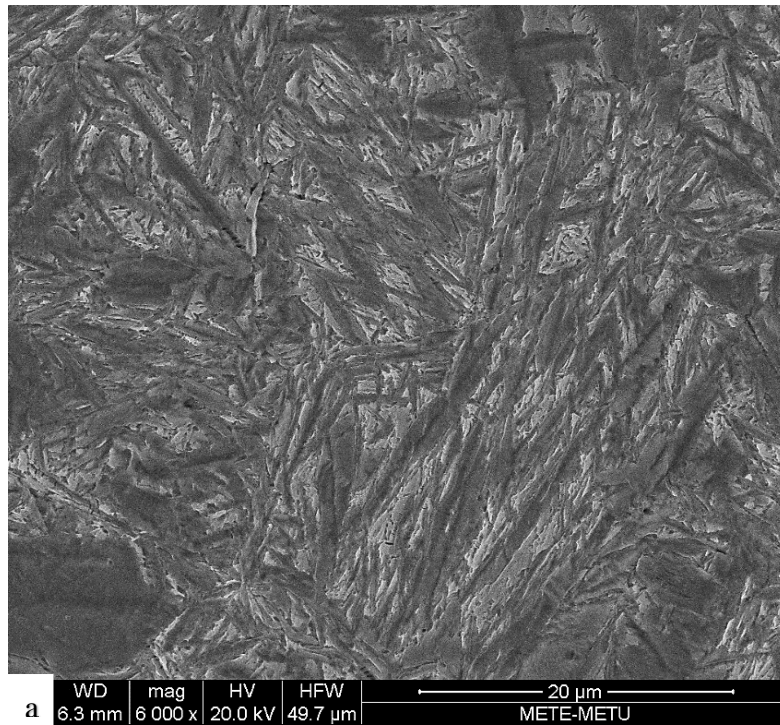


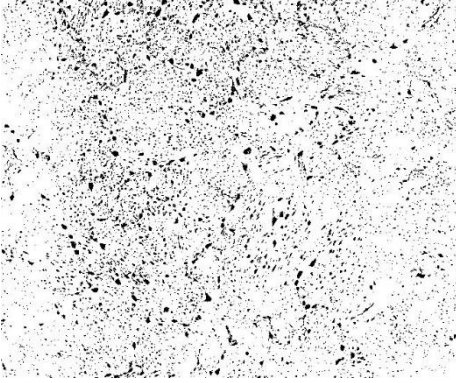
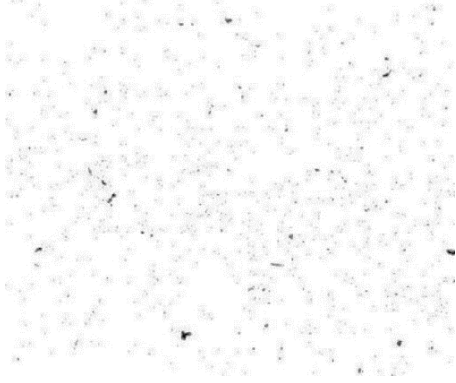
Figure 4.16. SEM image of the specimen (a) 1000A-Q, martensite and (b) 1000A-Q-180T, tempered martensite

As far as tempering is concerned, either 180 °C or 235 °C does not affect the microstructure. This is expected, because, any austenite transformed to martensite will not be etched easily. As a result, it will be difficult to differentiate fresh martensite from retained austenite. However, as seen in Figure 4.16.b, several martensite needles are etched at a faster rate indicating that these are formed during initial quenching.

4.3. Quantitative Analysis of Undissolved Alloy Carbides

The microstructures and quantitative analysis results of carbide percentages are given in Table 4.2 for three different austenitization temperatures. In the table black and white images are constructed by ImageJ and in the images dark spherical particles are carbides.

Table 4.2. *Quantitative Analysis of Undissolved Alloy Carbides Constructed by ImageJ*

Specimen	ImageJ Microstructure (500px-500px)	Volume Fraction of Undissolved Carbides
825A-Q		8.82 % (±0.3 %)
875A-Q		7.66 % (±0.5)
1000A-Q		0.97% (±0.09%)

4.4. Retained Austenite Measurements

In Table 4.3, the planes of ferrite and austenite peaks are given, and they are the same for all the XRD plots. The differences are integrated intensities and the ratio between the phases.

Table 4.3. *Planes and Peak Angles of Ferrite and Austenite Peaks*

Ferrite Peaks		Austenite Peaks	
Plane	2θ	Plane	2θ
(110)	44.66	(111)	43.58
(200)	65.01	(200)	50.79
(211)	82.31	(220)	74.69
(220)	98.91	(311)	90.70
(310)	116.35	(222)	95.96
(222)	137.09	(100)	118.16

Retained austenite percentages is given in Table 4.4 for all samples experimented in this thesis. The results which are lower than 1% are not reliable and because of this reason they are not given in the table. From Table 4.4, several results emerge: Firstly, as austenitizing temperature increases retained austenite volume fraction increases. Secondly, isothermal heat-treating decreases retained austenite volume fraction due to bainite transformation. As isothermal treating time increases, retained austenite volume fraction decreases. The third result is on tempering: Tempering at 180 °C did not affect retained austenite remarkably, on the other hand tempering at 235 °C significantly decreased the retained austenite volume fraction.

Table 4.4. Retained Austenite Analysis Results of All Samples

Quenched and Tempered Specimens					
Sample ID	As- quenched	Tempered at 180 °C	Tempered at 235 °C	Double Tempered at 235 °C	Double Tempered at 235 and 180°C
825A-Q	10.0	9.7	2.1	-	-
875A-Q	16.7	14.0	3.6	-	-
1000A-Q	54.7	53.0	-	-	-
Isothermally Heat-Treated Specimens					
Sample ID	Heat Treated	Tempered at 180 °C	Tempered at 235 °C	Double Tempered at 235 °C	Double Tempered at 235 and 180°C
825A-1d	5.9	4.5	-	-	-
825A-2d	1.6	1.1	-	-	-
875A-1d	8.7	7.1	-	-	-
875A-2d	1.8	1.5	-	-	-
1000A-4d	24.7	21.4	16.1	-	-
1000A-6d	6.0	5.7	-	-	-

For all the XRD plots (Figure 4.17, Figure 4.19, Figure 4.20, and Figure 4.21) martensite and ferrite peaks are indistinguishable from each other because their angles are too close to each other and the peaks overlaps. Because of this reason, only ferrite peaks were based on. Moreover, due to overlapping, carbide peaks cannot be seen. To overcome this difficulty, the carbide percentages are calculated and given in the previous section in Table 4.2.

4.4.1. Retained Austenite Analysis of Quenched Specimens

The specimens austenitized either at 825C, 875C or 1000C consist of undissolved alloy carbide, fresh martensite and retained austenite. The fraction of phases in each specimen is different and shown in Table 4.5. As seen, as austenitization temperature increases the amount of retained austenite increases.

Table 4.5. *Undissolved Carbides and Retained Austenite Volume Fractions of Oil Quenched Samples*

Sample ID	Austenitization Temperature (°C, 30 min.)	Volume Fraction of Undissolved Carbides (%)	Retained Austenite Fraction (%)
825A-Q	825	8.8 (± 0.3)	10.0
875A-Q	875	7.6(± 0.5)	16.7
1000A-Q	1000	0.9 (± 0.09)	54.7

The reason for the values in Table 4.5 is clearly seen on Figure 4.17. The retained austenite peaks are more distinguishable for the XRD plot of 1000A-Q. The distinguishability of the austenite peaks seems to increase as the austenitization temperature increases. This means the integrated intensity of the austenite phase increases and hence the ratio of volume fractions of ferrite over austenite decreases because ratio of integrated intensities and ratio of volume fractions are proportional. It should be noted that, not seeing significant peaks does not mean that the phase did not present. All the peaks mentioned in exist on the XRD plots and shown with their labels. For example, in 825A-Q plot on Figure 4.17, all austenite peaks present with the smaller intensities with respect to 875A-Q and 1000A-Q plots.

Moreover, in Figure 4.18, the graphical representation of Table 4.5 is seen. Two inference is made from the graph: as austenitization temperature increases, undissolved alloy carbides decreases and retained austenite volume fraction increases.

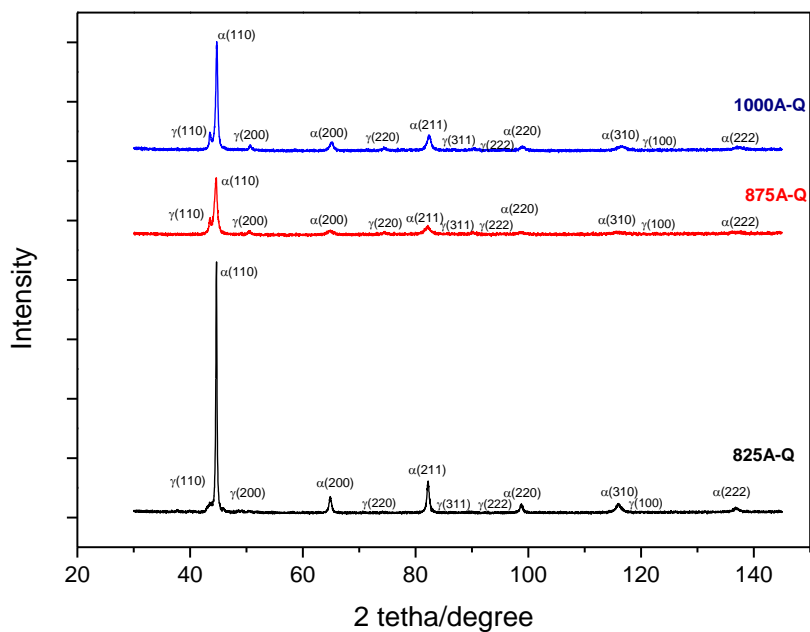


Figure 4.17. XRD data of oil quenched- tempered specimens: 825A-Q, 875A-Q, and 1000A-Q

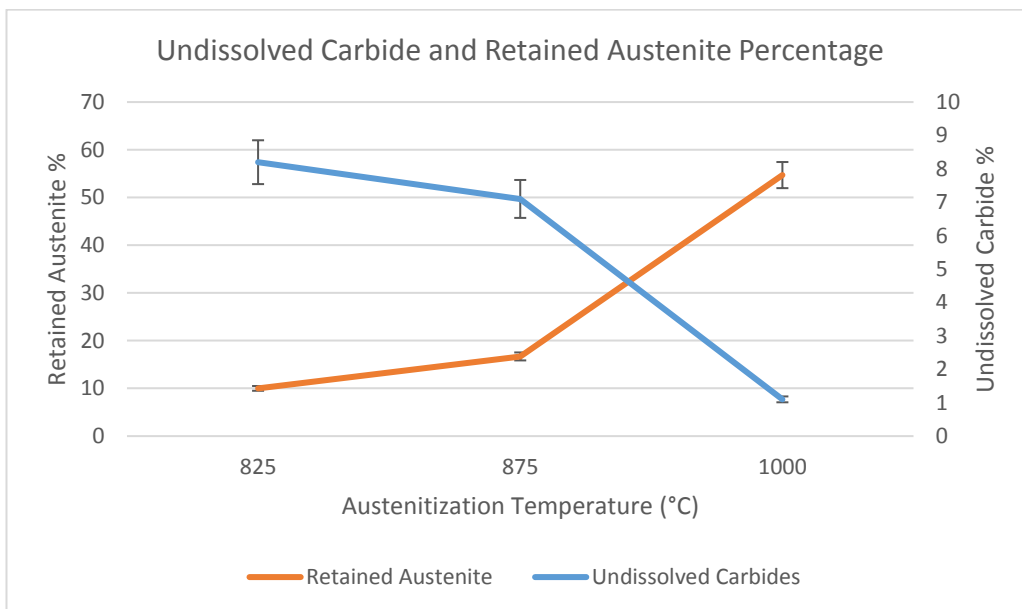


Figure 4.18. Graphical Representation of Undissolved Alloy Carbide and Retained Austenite Percentages of as-quenched specimens

4.4.2. Retained Austenite Analysis of Isothermally Heat-Treated Specimens

The XRD plots of as-quenched specimens and isothermally treated specimens were given for each austenitization temperature; 825 °C, 875°C and 1000 °C see Figure 4.19, Figure 4.20 and Figure 4.21 respectively. Austenite transformation to bainitic ferrite results in two change in these plots. First is the intensities of ferrite peaks increase, and the second intensities of austenite peaks decrease as isothermally treating time increases. All the isothermally heat-treated specimens consist of same phases, undissolved alloy carbides, bainitic ferrite, martensite and retained austenite. Volume fraction of undissolved carbides did not change with the isothermal holding time because it is only affected by the austenitization temperature.

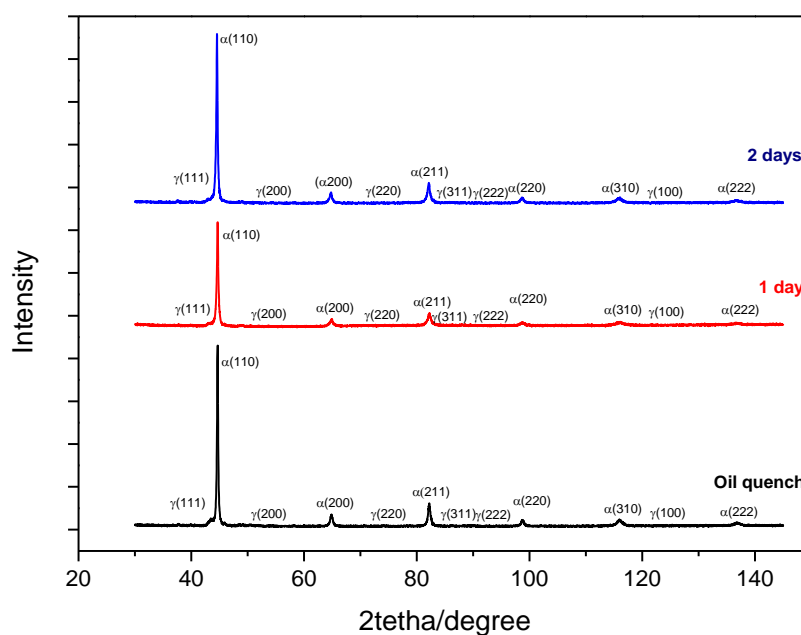


Figure 4.19. XRD data of untempered specimens of 825 °C austenitization: 825A-Q, 825A-1d and 825A-2d

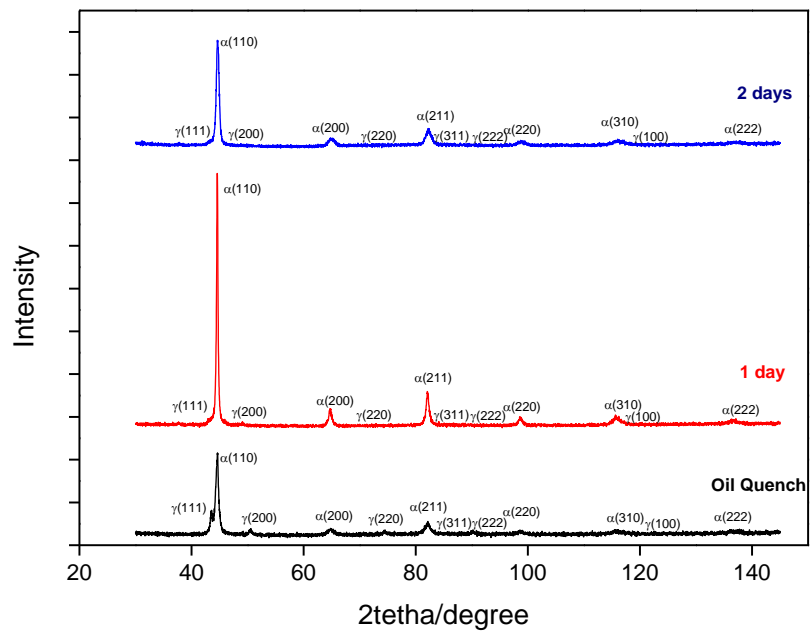


Figure 4.20. XRD data of untempered specimens of 875 °C austenitization: 875A-Q, 875A-1d and 875A-2d

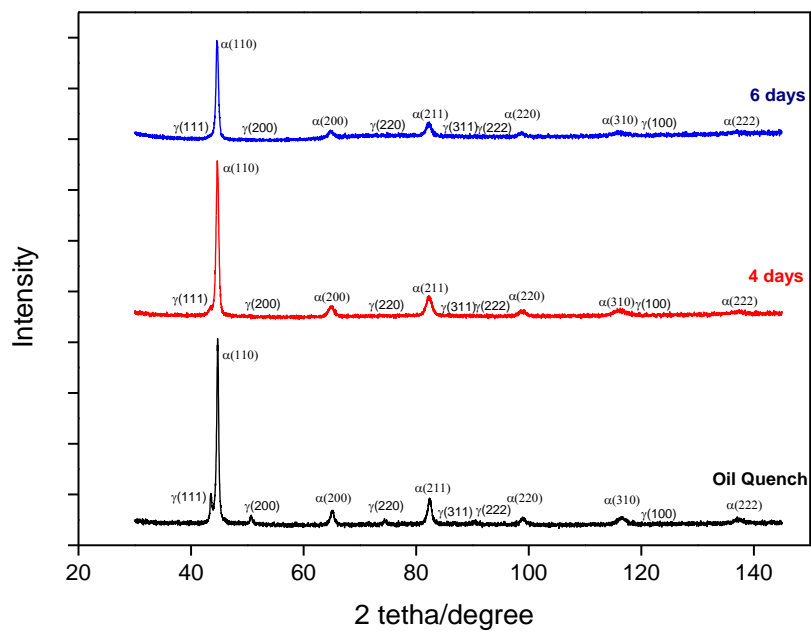


Figure 4.21. XRD data of untempered specimens of 1000 °C austenitization: 1000A-Q, 1000A-4d and 1000A-6d

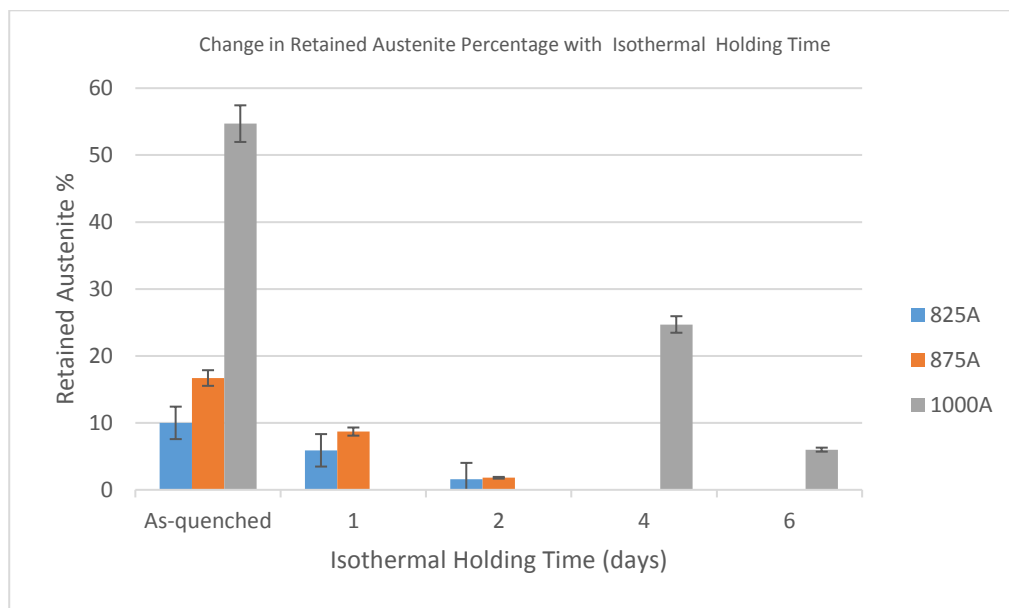


Figure 4.22. Graphical Representation of Retained Austenite Percentages of as-quenched and isothermally treated specimens for series of 825 °C, 875 °C and 1000 °C of austenitization.

The graph represented in Figure 4.22 summarize all the retained austenite contents. It can be observed that as isothermal treating time increases, the retained austenite fraction decreases for each austenitization temperature. Moreover, the specimen treated for longer times has more volume fraction of bainite because transformation has progressed more. It is also shown that retained austenite percentage is the highest for 1000 °C among the as-quenched specimens due to carbon dissolution. Additionally, the decrease in retained austenite for three group of specimens are because of bainite transformation progress.

4.4.3. Retained Austenite Analysis of Tempering Effect

The retained austenite calculations is given in Table 4.4. It is found that tempering at 180 °C has no remarkable effect on the volume fraction of retained austenite while volume fraction of retained austenite has remarkably decreased on the specimens tempered at 235 °C. It is most probably because of austenite re-conditioning. If tempering is carried out at a sufficiently high temperature austenite transforms into fresh martensite. [11],[41]

Double tempering is necessary because the fresh martensite formed with the tempering at 235 °C is brittle and detrimental for the usage. That is why only the specimens which were tempered at 235 °C is double tempered. The specimens which were double tempered, their tempering temperatures and retained austenite percentages are given in Table 4.4 .

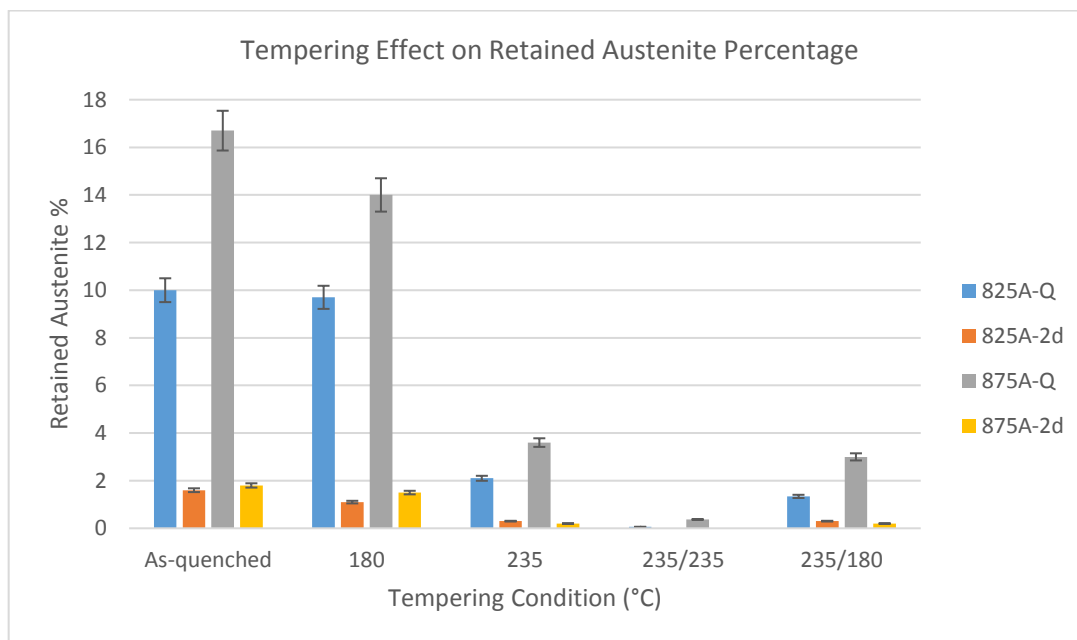


Figure 4.23. Graphical Representation of Tempering Effect on Retained Austenite on as-quenched and isothermally heat-treated specimens for 1 day and 2 days for 825 and 875 °C of austenitization

On Figure 4.23, there is a graphical representation of tempering effect on retained austenite volume percentage. To summarize these findings in word, tempering at 235 °C is more effective on retained austenite than tempering at 180 °C, and similarly for the case of double tempering, specimens whose second cycle of tempering were at 235 °C has less amount of retained austenite with respect to the specimens whose second tempering temperature was 180°C. However isothermally heat-treated specimens were double tempered at 235 °C and 180 °C because some amount of retained austenite is necessary in the service life of a product. In Table 4.4 the retained austenite values of double tempered specimens are not given because they are lower than 1%. XRD cannot measure the values under 1% that is why those calculations were not reliable and not given.

4.5. Mechanical Characterization

4.5.1. Hardness Measurements

Table 4.6. *Sample identifications, heat treatment procedure, resultant morphologies and the hardness values of all specimens*

Quenched and Tempered Specimens			
	Sample ID	Microstructure	Hardness (HV30)
Oil Quenched	825A-Q	M + RA + UC	673 (± 12)
	875A-Q	M + RA + UC	757 (± 4)
	1000A-Q	M + RA + UC	783 (± 2)
Quenched and Tempered	825A-Q-180T	TM + RA + UC	575 (± 6)
	825A-Q-235T	TM + RA + UC	482 (± 7)
	825A-Q-235T-235T	TM + RA + UC	405 (± 1)
	825A-Q-235T-180T	TM + RA + UC	448 (± 3)
	875A-Q-180T	TM + RA + UC	736 (± 3)
	875A-Q-235T	TM + RA + UC	566 (± 8)
	875A-Q-235T-235T	TM + RA + UC	453 (± 5)
	875A-Q-235T-180T	TM + RA + UC	550 (± 1)
	1000A-Q-180T	TM + RA + UC	637 (± 3)
Isothermally Heat-Treated Specimens			
	Sample ID	Microstructure	Hardness (HV30)
Isothermal Transformation	825A-1d	B + M + RA + UC	611 (± 10)
	825A-2d	B + M + RA + UC	597 (± 4)
	875A-1d	B + M + RA + UC	657 (± 9)
	875A-2d	B + M + RA + UC	645 (± 5)
	1000A-4d	B + M + RA + UC	720 (± 8)
	1000A-6d	B + M + RA + UC	549 (± 5)
Isothermally Heat Treated and Tempered	825A-1d-180T	B + TM + RA + UC	527 (± 7)
	825A-2d-180T	B + TM + RA + UC	562 (± 3)
	825A-2d-235T	B + TM + RA + UC	552 (± 7)
	825A-2d-235T-180T	B + TM + RA + UC	520 (± 1)
	875A-1d-180T	B + TM + RA + UC	636 (± 3)
	875A-2d-180T	B + TM + RA + UC	625 (± 6)
	875A-2d-235T	B + TM + RA + UC	612 (± 2)
	875A-2d-235T-180T	B + TM + RA + UC	593 (± 3)
	1000A-4d-180T	B + TM + RA + UC	666 (± 4)
	1000A-4d-235T	B + TM + RA + UC	654 (± 6)
	1000A-6d-180T	B + TM + RA + UC	535 (± 2)

The hardness values of all specimens together with the resultant microstructures is given in Table 4.6.

The hardness values of the as-quenched and quenched and tempered specimens are plotted in Figure 4.24. As austenitizing temperature increases from 825 °C to 1000 °C, the as-quenched hardness values increase. This result is expected because as the austenitization temperature increases, the carbide dissolution increases; as do carbon content of the austenite to be heat treated. Since the strength of martensite is directly related with the carbon content of the austenite, hardness of the martensite increases.

Tempering effect on hardness of oil quenched specimens is also presented in Figure 4.24 for the samples which are austenitized at 825 °C, 875°C and 1000°C. As expected with tempering hardness values has decreased in all the specimens. Moreover, as tempering temperature increases for the same tempering period (for this study 90 minutes) hardness values has decreased more.

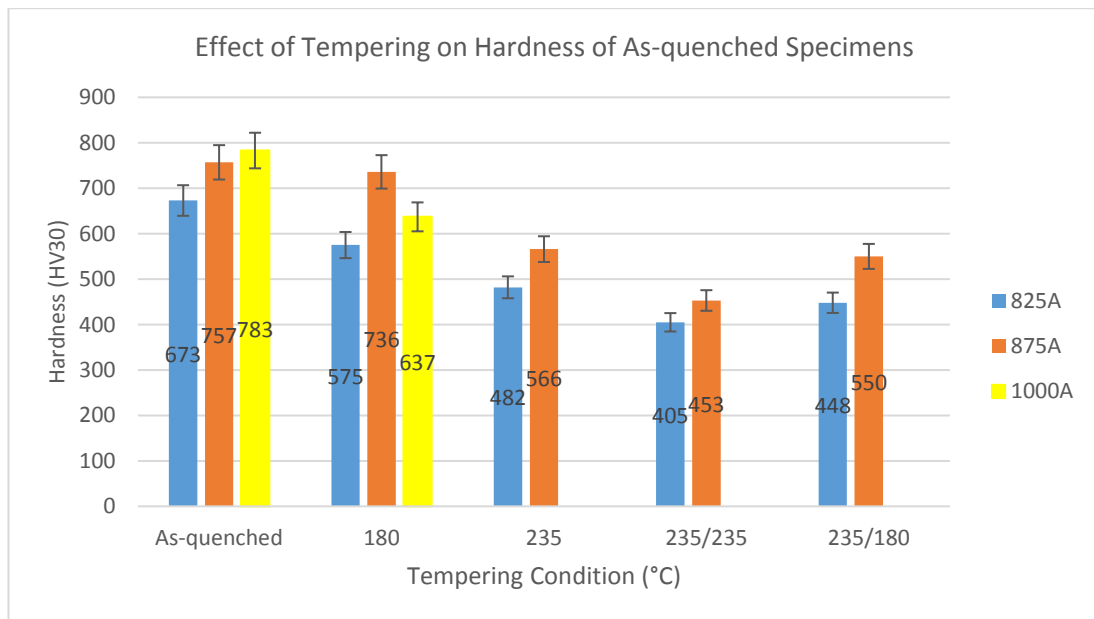


Figure 4.24. Hardness values of as-quenched specimens with different austenitization temperatures and tempering effect on hardness values of as-quenched specimen

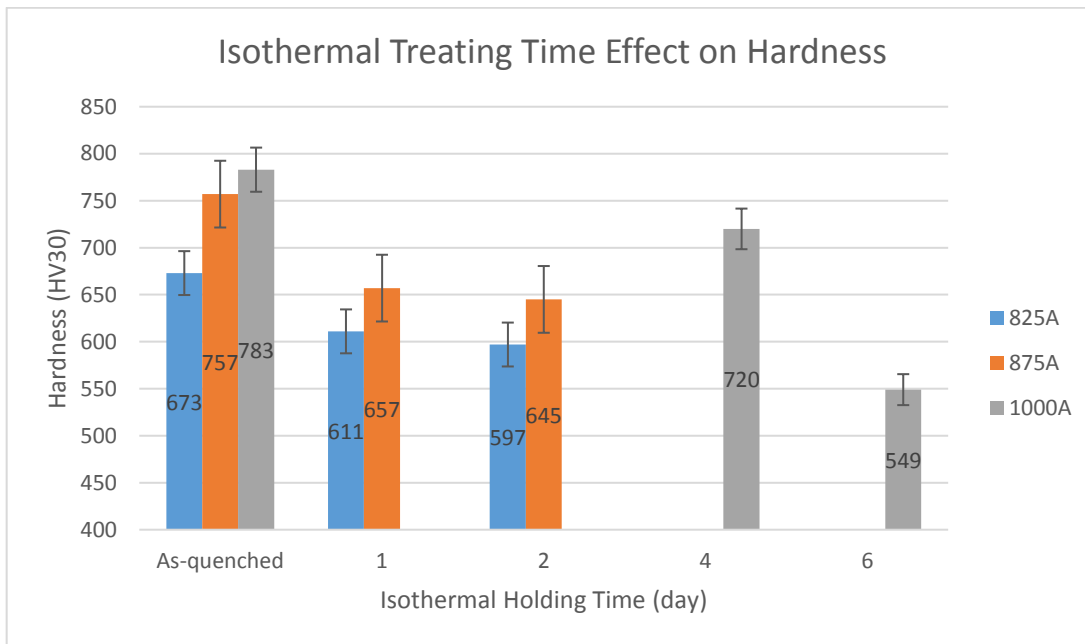


Figure 4.25. Hardness values of as-quenched and isothermally heat-treated specimens with different austenitization temperatures

As far as bainitic specimens are concerned, the variation of hardness upon isothermal treatment times are shown in Figure 4.25. It is seen that as-quenched specimens are harder than isothermally treated specimens and as isothermal treating time increases hardness decreases. The former is because of bainite being softer than martensite. By isothermal heat treating, bainite transformation starts and steel becomes softer with respect to the as quenched specimens which consist of martensite and retained austenite. The latter is because of progress of bainite reaction. As isothermal treating time increases, more austenite transforms into bainite this causes, less retained austenite fraction and more bainite fraction in the final microstructure. Bainite is harder than retained austenite.

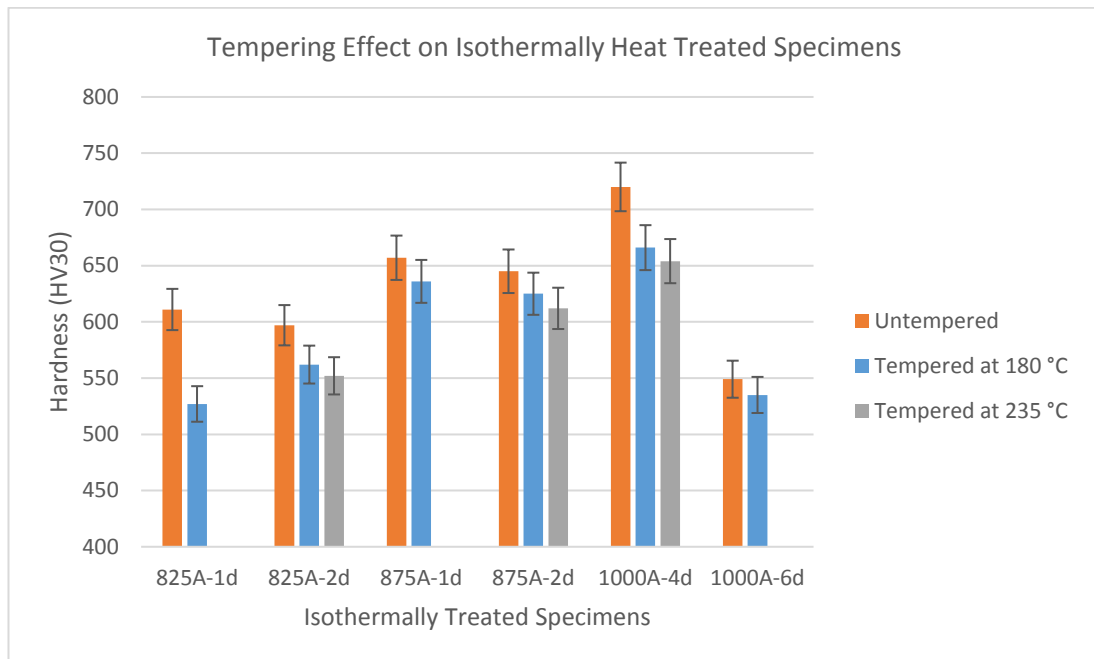


Figure 4.26. Graphical Representation of Tempering Effect on Isothermally Heat-Treated Specimens of Different Austenitization Temperatures

In Figure 4.26, the graph shows that tempering decreases hardness and as the tempering temperature increases, hardness decreases more for the same tempering period. The great softening is not observed. The reason for that hardness of bainite does not change considerably if tempering is performed below 450 °C.[49] During tempering fresh martensite softens and if the temperature is above 200 °C some amount of retained austenite reconditions to martensite upon cooling to room temperature. [39], [41] It should be noted that martensite softening is dominant mechanism rather than austenite recondition because hardness values decreases by tempering at 235 °C.

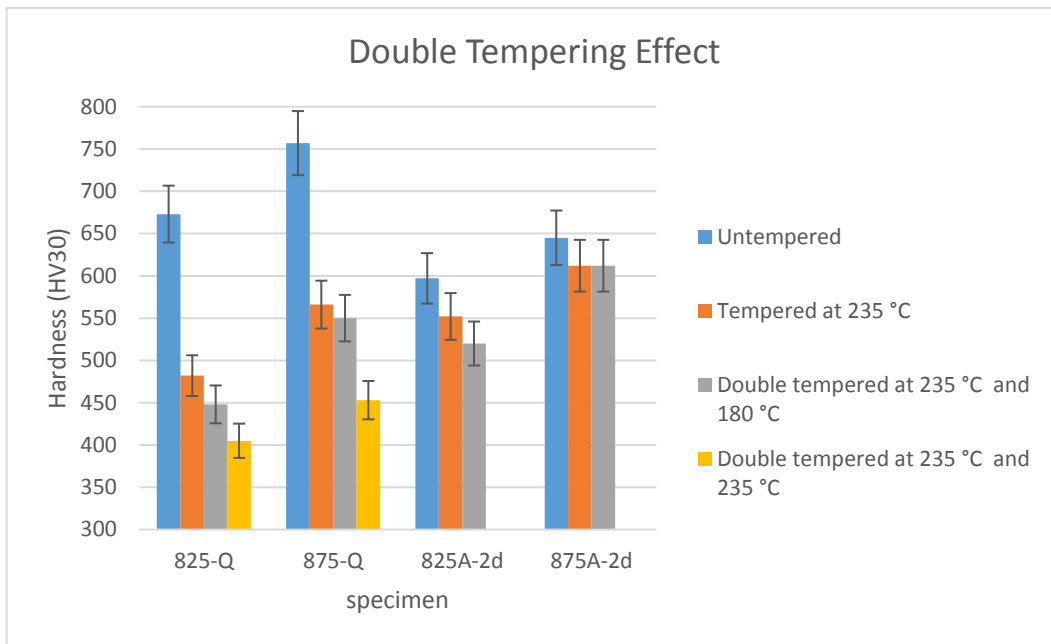


Figure 4.27. The effect of double tempering and its comparison with the tempering effect on the oil quenched and isothermally treated specimens of different austenitization temperatures

The double tempering effect and its comparison with tempering effect is seen on Figure 4.27 for oil quenched and isothermally treated specimens for 2 days. Double tempering was only performed to the specimens which were austenitized at 825 °C and 875 °C. The temperature in the first cycle of double heat treatment is 235 °C for all the samples because the purpose of double tempering is to relieve stresses and soften the fresh martensite formed by austenite re-conditioning during cooling to room temperature from 235 °C. Figure 4.27 also shows that the hardness values decrease more in the specimens of 235/235 °C cycle than 235/180 °C cycle. This is because of the fundamental principle of tempering: as tempering temperature increases the material softens more.

4.5.2. Tensile Tests

For tensile tests, the samples which can have a commercial use are chosen. The tensile test results are given in Table 4.7.

Table 4.7. Tension test results of the specimens

Quenched and Tempered Specimens	
Sample ID	UTS (MPa)
875A-Q-180T	613
Isothermally Treated Specimens	
Sample ID	UTS (MPa)
825A-2d-180T	2061 (\pm 218)
875A-2d	930 (\pm 288)
875A-2d-180T	1408 (\pm 490)

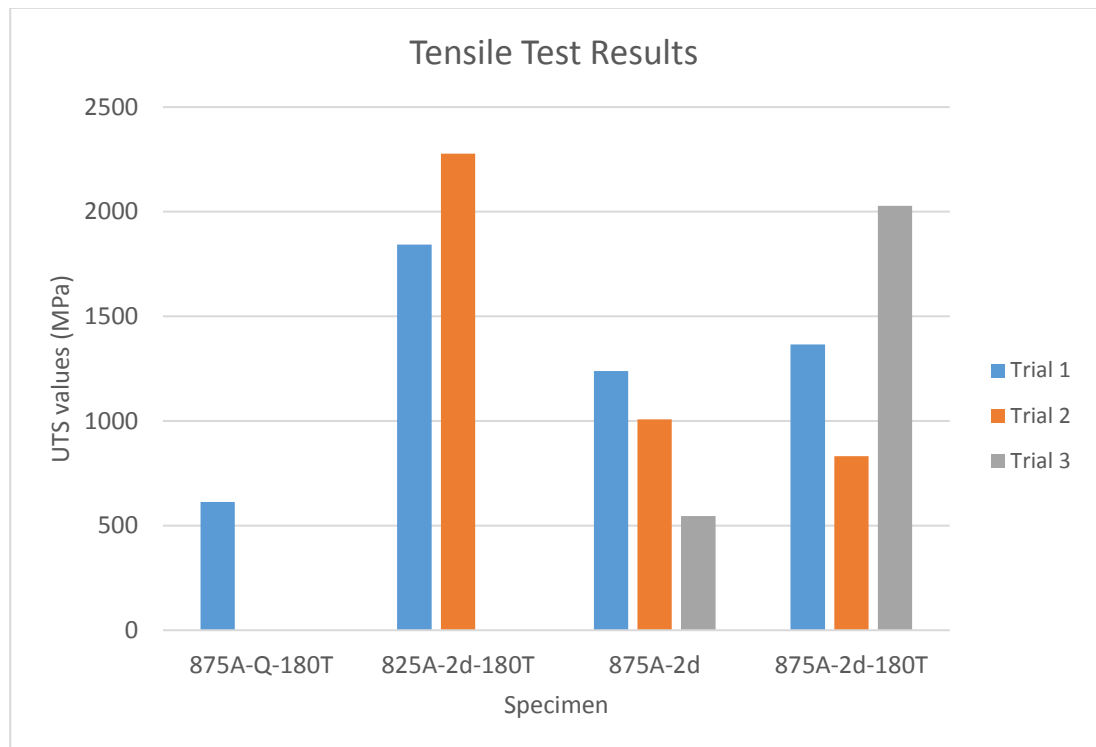


Figure 4.28. Tensile test results of the specimen in every trial.

As seen in Figure 4.28 the scatter in tensile test results are high. The quenched and tempered specimens of 875 °C austenitization group yielded very low values than expected: They should be around 2000MPa or high but could not exceed 1000 MPa. Similarly, the specimen austenitized at 825 °C, isothermally treated for 2 days and tempered at 180 °C yielded a tensile strength at around 2000MPa which was again close to that of 100% bainitic specimens. However, the 100% bainitic specimens of 875 °C and 1000 °C yielded low UTS values unexpectedly.

The fracture surfaces of the specimens show brittle morphology. The brittleness may cause a large scatter in the tensile data. In Figure 4.29, the hardness and the UTS values of the specimens which were austenitized at 825 °C and 875 °C, are plotted. A direct correlation between the hardness and UTS values could not be found. It is known that the hardness values of the specimens austenitized at 875 °C are higher than that of 825 °C austenitization but their UTS values have an opposite trend.

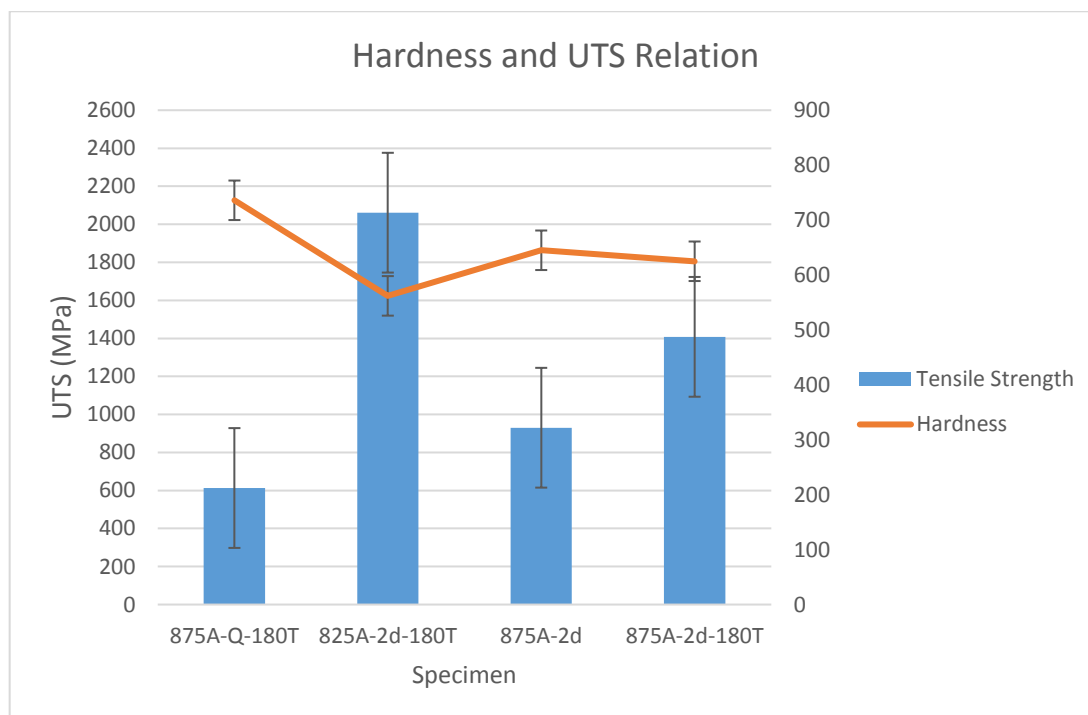


Figure 4.29. Graphical representation of hardness and UTS relations of as quenched and tempered specimens of austenitization at 825°C and 875°C

CHAPTER 5

DISCUSSION

In this study the 100Cr6 bearing steel is heat treated under different conditions and in this chapter, the experimental results will be discussed.

Spectral analysis result of 100Cr6 was identical with the chemical composition in the literature. (Table 3.1) The microstructure of as-received 100Cr6 is consist of alloy carbides on ferritic pearlitic matrix.

5.1. Microstructural Characterization

From the retained austenite analysis and quantitative analysis of alloy carbides, it can be concluded that all the oil quenched specimens consist of undissolved alloy carbides, martensite and retained austenite. Also, all the isothermally treated specimens consist of martensite, bainite, undissolved alloy carbide and retained austenite.

5.1.1. Microstructural Characterization of As-quenched Specimens

On Figure 4.4, the microstructures of as-quenched specimens of 825 and 875 °C austenitization are so similar. There is no observable difference in undissolved carbide fraction on the micrographs because the amount of undissolved carbide is not remarkably different from each other. 825A-Q has 8.82% undissolved carbide and 875A-Q has 7.66% undissolved carbide in the structure. However, increased carbon dissolution in the specimen 875A-Q, has led to more austenite retains. There is no retained austenite can be seen on the micrographs however from the XRD analysis, it is known that there are 10.0% and 17.0% volume fraction of retained austenite respectively. (Table 4.4)

On the other hand, for 1000A-Q, undissolved alloy carbides cannot be seen on the micrographs (Figure 4.5). The undissolved alloy carbide content is less than 1% in the

structure. This can be attributed to the dissolution of all carbides in the matrix. Moreover, retained austenite phase is much more apparent in 1000A-Q due to the high carbon content of the matrix which result from carbide dissolution. The martensite fraction of the final microstructure only depends on the temperature of quenching medium. If the temperature of quenching medium is just in the middle of M_s and M_f and then resultant microstructure consist 50% martensite and 50% retained austenite. In the specimens austenitized at 1000 °C, carbon content of austenite has increased more with respect to 825A-Q and 875A-Q and hence M_s and M_f has decreased more. All three specimens (825A-Q, 875A-Q and 1000A-Q) has quenched into the oil at room temperature as a result of carbon dissolution, less fraction of martensite and more fraction of retained austenite has formed in 1000A-Q with respect to 825A-Q and 875A-Q.

5.1.2. Microstructural Characterization of Isothermally-Treated Specimens

The difference in between the structures of as-quenched specimens and isothermally treated specimens is the bainite morphology because bainite only forms with isothermal treating. Isothermally treated specimens have less amount of retained austenite in their structure with respect to as-quenched specimens because austenite transforms into bainite. Moreover, all isothermally treated specimens have martensite phase in this study because the calculated TTT diagrams are used in the design of the experiments. This can be expected since there can be some shift in real phase boundaries. If 100% bainite transformation boundary would be crossed, there would be no martensite structure in the specimen.

In order to differentiate bainite and martensite morphologies general appearance is important. Bainitic ferrite grow as parallel sheaves however martensite needles have a random distribution. Additionally, carbide precipitates are a tool to differentiate bainite and martensite. Since silicon content of 100Cr6 is not enough to prevent carbide precipitation and due to low transformation kinetics, carbon is both ejected to the neighboring austenite and precipitate in ferrite newly formed. In martensite

needles, carbide precipitation is not seen. Carbide precipitates are clearly seen on the Figure 4.8.

For each austenitization temperature, if isothermally heat-treated samples are compared with each other, the difference in volume fraction of bainitic ferrite cannot be observed. However, by retained austenite volume fraction, it can be deduced that longer isothermal heat treatment results in higher bainitic ferrite fraction in the final morphology. For example, the specimen 825A-1d has 5.9% volume fraction of retained austenite, while 825A-2d has 1.6 % volume fraction of retained austenite this is because there is more time for bainite reaction in the case for heat treating 825A-2d. This relation is valid for the specimens 875A-1d – 875A-2d and 1000A-4d - 1000A-6d.

While comparing bainite morphology of 825 °C, 875°C and 1000°C of austenitization, their carbide dissolution must be concerned. Their undissolved alloy carbide amounts are 8.82%, 7.66% and 0.97% respectively so that the austenite carbon concentration of the specimens which are austenitized at 1000 °C is the highest. This has two effects on the microstructures, the sheaves of bainitic ferrite becomes thicker as the austenitizing temperature increases. For example, while comparing 1000 °C austenitization and 825 °C austenitization, the M_s values are 128 °C and 145 °C respectively. (Table 4.1) Therefore the transformation temperature (200 °C) is less close to the M_s for 1000 °C austenitization than 825 °C austenitization. That is why the bainite sheaves that formed after 825 °C austenitization has finer morphology. Second effect is that there should be more retained austenite as austenitizing temperature increases because increased carbon content has shifted the C curve to the right on the TTT diagram so that with the same transformation time there will be more untransformed austenite in the specimens austenitized at 1000 °C. Moreover, not only M_s but also the M_f temperature has decreased so that air cooling may not be enough to cross M_f and there will be more volume of retained austenite in the final microstructure. These deductions are consistent with both microstructures (Figure 4.6 to Figure 4.11) and retained austenite volume fractions. (Table 4.4).

5.1.3. Microstructural Characterization of Tempered Specimens

Tempering does not have a crucial role on carbide dissolution and selected temperatures which were 180 °C and 235 °C are not high enough to change morphology, that is why microstructures of tempered specimens will not be discussed.

5.2. Retained Austenite Measurements

In Table 4.4, result of retained austenite measurements that belong to all specimens are given. From the table, it can be concluded that, as austenitizing temperature increases the retained austenite volume fraction increases. Isothermal treating decreases retained austenite volume fraction. Tempering at 180 °C does not have a considerable influence on retained austenite while tempering at 235 °C decreases retained austenite remarkably.

In Figure 4.18, the retained austenite volume fraction of as-quenched specimens and relation with carbide dissolution is seen. As mentioned before, as austenitizing temperature increases, the carbide dissolution increases, and this decreases martensite start and finish temperatures. Therefore, an increase in austenitizing temperature results in increase in retained austenite volume fraction.

In Figure 4.22, it is shown that, retained austenite volume fractions are smaller in isothermally treated specimens than as-quenched specimens for each austenitization temperature. It is also seen that, as isothermal treating time increases, the volume fraction of retained austenite decreases. This is because of bainitic transformation. By isothermal treating austenite transforms into bainitic ferrite and cementite. Moreover, as isothermal treating time increases, more austenite undergoes bainite transformation and there will be less amount of austenite to be retained in the final microstructure.

Moreover, tempering treatment applied to the specimens to relieve stresses and increase toughness of fresh martensite and recondition to austenite. Tempering at 180 °C reduces retained austenite volume fractions but not in remarkable amounts. This small decrease is most probably because of carbon diffusion from martensite to

austenite and eventually ϵ -carbide precipitation. It should be noted that these precipitations are so low in amount and size that they do not result in an observable change in metallographic counting of carbides. [2], [11], [13] By tempering at 180 °C, only the martensite tempered, and retained austenite structure is not affected. However, tempering at 235 °C remarkably decreases the volume fraction of retained austenite such that they are lower than 1%. Podder and Bhadeshia have proved that after tempering which is performed at a temperature above 200 °C, during cooling to the room temperature some of the austenite transforms into fresh martensite because of increase in carbon concentration.[41] This phenomenon which is conditioning explains why the retained austenite volume fraction significantly decreases after tempering at 235 °C.

Since fresh martensite is not suitable for utilization due to its brittle character a second cycle of tempering is essential for the specimens which are tempered at 235 °C. In Figure 4.23, effect of both tempering and double tempering on retained austenite can be seen. First cycle of double tempering is performed at 235 °C but the double tempered specimens can be separated into two according to their second cycle temperature 180 °C and 235 °C. All tempering treatments are performed for 90 minutes.

For the samples which are double tempered 180 °C and 235 °C, the retained austenite volume fractions have decreased but not as much as the first tempering at 235 °C. This is because retained austenite is not suitable to transform into fresh martensite this time due to carbon diffusion happens in the second cycle of tempering even though the temperature is above 200 °C. For the samples which are double tempered 235 °C and 180 °C retained austenite volume fractions do not change significantly. One common result has been observed for the two groups of specimens which is by tempering stress relief of fresh martensite and hence softening of material have observed. This will be proven by hardness results.

5.3. Mechanical Characterization

5.3.1. Hardness Measurements

The hardness values of all the specimens are given in Table 4.6.

The specimen 1000A-Q has the highest hardness value among the as-quenched specimens. This is because increased carbon content of the austenite to be transformed because of carbon dissolution. Strength of martensite is directly related with the carbon concentration so that the austenite with the highest carbon concentration transforms into the strongest martensite. Additionally, 1000A-Q is the specimen that has the highest amount of retained austenite. It shows the highest hardness value despite of retained austenite is the softest phase. This is because hardness of martensite phase is so high that, it dominates the retained austenite.

As mentioned before, as quenched specimens consist of martensite and retained austenite while isothermally treated specimens consist of bainite, martensite and retained austenite phase mixture. Since martensite is harder than bainite, the hardness values of isothermally treated specimens are smaller than that of as-quenched specimens for the same austenitization temperature. Similarly, as isothermal treating time increases, bainite fraction increases and hence there is less amount of austenite retains to transform into martensite upon cooling to room temperature. Therefore, longer isothermal treatments lead to smaller hardness values. Figure 4.25 shows that with isothermal heat treatment and increasing isothermal treating time, hardness decreases for each austenitization temperature. Moreover, for the same isothermal treating time, for example 825A-1d and 875A-1d, the specimen which are austenitized at higher temperature shows higher hardness.

Figure 4.24 and Figure 4.26 shows the effect of tempering on hardness of as-quenched specimens and isothermally treated specimens respectively. Tempering periods are the same and 90 minutes for all tempered specimens. The difference is tempering temperature. Tempering process decreases hardness however, as the tempering temperature increases, hardness decreases more. That is why the specimens which are

tempered at 180 °C shows higher hardness values than the specimens which are tempered at 235 °C. It should be noted that, the hardness of the specimens tempered at 235 °C decrease despite of austenite reconditions. This is because the only small fraction of the structure reconditions and transforms into fresh martensite and softening of structure becomes dominant over austenite conditioning.

Still, fresh martensite is detrimental for commercial use so that the specimens which are tempered at 235 °C, are tempered once more. The effect of double tempering on hardness has shown in Figure 4.24 and Figure 4.27. As expected, hardness values decrease with the second cycle of tempering. This decrease is higher for tempering at 235 °C when comparing to 180 °C. To conclude, the specimens which the second cycle of double tempering is at 235 °C yields the lowest hardness values.

5.3.2. Tensile Test

The tensile test results are given in Table 4.7. Unfortunately, the results are not comparable to each other. The fracture surface of the tensile tests specimens shows brittle morphology. The scattering UTS data is most probably because of this brittle character. Most of the specimens have fractured long before they reach expected UTS values.

CHAPTER 6

CONCLUSION

In this study 100Cr6 steel was heat treated to obtain bainitic and martensitic microstructures by austempering and oil quenching. Moreover, tempering was performed for comparison. Microstructural and mechanical properties of phases were investigated. Additionally, retained austenite volume fraction was calculated and its effects on mechanical properties were concerned.

1. In quenched specimens, as austenitization temperature increases, retained austenite volume fraction increases due to carbide dissolution.
2. In consistent with the calculated TTT diagrams, either 100% bainitic or bainitic-martensitic microstructures could be obtained.
3. Isothermally treated bainitic specimens always yielded lower hardness values than their quenched counterparts. Also, their amount of retained austenite is much lower
4. Tempering at 180 °C does not affect the retained austenite volume fraction whereas tempering at 235 °C significantly decreases retained austenite volume fraction due to austenite reconditioning.
5. An austenitization at 1000 °C dissolve most of the carbides and upon quenching and the specimen become very brittle.
6. Probably due to the high hardness and brittleness of the specimens, there is a large scatter in tensile test results. Only the specimen which is austenitized at 825 °C yielded reasonable UTS values.

REFERENCES

- [1] *ASM Handbook Vol.1 Properties and Selection: Iron Steels and High Performance Alloys*, 10th ed., vol. 1. ASM International, 1990.
- [2] *ASM Handbook Vol.4 Heat Treating*, vol. 4. ASM International, 1991.
- [3] C. Garcia-Mateo and F. G. Caballero, “Understanding the Mechanical Properties of Nanostructured Bainite,” in *Handbook of Mechanical Nanostructuring*, M. Aliofkhaezai, Ed. Wiley, 2016, pp. 35–59.
- [4] W. D. Callister and D. G. Rethwisch, *Material Science and Engineering: An Introduction*. New York: Jhon Wiley & Sons, 2007.
- [5] D. J., E. Jezierska, K. Rozinatowski, and W. Swiatnicki, “Characterization of Nanobainitic Structure Obtained in 100CrMnSi6-4 Steel After Industrial Heat Treatment,” *Arch. Metall. Mater.*, vol. 59, no. 4, pp. 1637–1640, 2014.
- [6] *ASM Handbook Vol. 9 Metallography: An Introduction, Metallography and Microstructures*, vol. 9. ASM International, 2004.
- [7] F. G. Caballero, C. Garcia-Mateo, and H. K. D. H. Bhadeshia, “Very Strong Bainitic Steels,” vol. 3, 1992.
- [8] M. Soliman and H. Palkowski, “Development of the low temperature bainite,” *Arch. Civ. Mech. Eng.*, vol. 16, no. 3, pp. 403–412, 2016.
- [9] J.-Y. Chae, “Application of Lower Bainite Microstructure for Bearing Steels and Acceleration of Transformation Kinetics,” Pohang University of Science and Technology, 2012.
- [10] “ASTM 52100 Bearing Steel | 1.3505 | 100Cr6 | SUJ2 | EN31.” [Online]. Available: <http://www.astmsteel.com/product/52100-bearing-steel-aisi/>. [Accessed: 15-Apr-2019].
- [11] Z. Özgeneci, “The Effect of Retained Austenite and Carbide Distribution on The Wear Resistance of Bearing Steel,” Middle East Technical University.
- [12] C. A. Stickels, “Carbide Refining Heat Treatments for 52100 Bearing Steel.,” *Met. Trans.*, vol. 5, no. 4, pp. 865–874, 1974.
- [13] H. K. D. H. Bhadeshia and R. Honeycombe, *Steels: Microstructure and Properties*, 3rd ed. 2006.
- [14] E. J. Pavlina and C. J. Van Tyne, “Correlation of Yield strength and Tensile strength with hardness for steels,” *J. Mater. Eng. Perform.*, vol. 17, no. 6, pp. 888–893, 2008.
- [15] G. F. Vander Voort, *Atlas of Time-Temperature Diagrams for Irons and Steels*.

- ASM International, 1991.
- [16] Z. Öztürk, “An Investigation of Bainitic Transformation in Low Carbon Alloy and High Carbon Railway Steels,” Middle East Technical University, 2018.
 - [17] F. C. Campbell, Ed., *Elements of Metallurgy and Engineering Alloys*. ASM International, 2008.
 - [18] H. K. D. H. Bhadeshia, *Physical Metallurgy of Steels*, Fifth Edit., vol. 1. Elsevier B.V., 2014.
 - [19] J. Trzaska, “CALCULATION OF CRITICAL TEMPERATURES BY EMPIRICAL FORMULAE,” *Arch. Metall. Mater.*, vol. 61, no. 2, pp. 981–986, 2016.
 - [20] G. Krauss and A. R. Marder, “The Morphology of Martensite in Iron Alloys,” *Metall. Mater. Trans.*, vol. 2, no. September, pp. 2343–2357, 1971.
 - [21] H. K. D. H. Bhadeshia, *Bainite in Steels: Transformations, Microstructure and Properties*, 2nd ed. IOM Communications Ltd, 2001.
 - [22] J. W. Christian and H. K. D. H. Bhadeshia, “Bainite in Steels,” *Metall. Mater. Trans.*, vol. 21A, pp. 767–797, 1990.
 - [23] R. F. H. F. Hemann, K. R. Kinsman, and H. I. Aaronson, “A Debate on the Bainite Reaction,” *Metall. Mater. Trans.*, vol. 3, no. May, pp. 1077–1094, 1972.
 - [24] H. K. D. H. Bhadeshia, “The Bainite Transformation : Unresolved Issues,” *Mater. Sci. Eng.*, vol. 273–275, pp. 58–66, 1999.
 - [25] H. K. D. H. Bhadeshia, “High Performance Bainitic Steels,” *Mater. Sci. Forum*, vol. 500–501, pp. 63–74, 2005.
 - [26] *ASM Handbook Vol.20 Materials Selection and Design*, vol. 20. ASM International, 1997.
 - [27] F. C. Campbell, “Nonequilibrium Reactions—Martensitic and Bainitic Structures,” in *Phase Diagrams: Understanding the Basics*, 2012, pp. 303–338.
 - [28] X. C. Xiong, B. Chen, M. X. Huang, J. F. Wang, and L. Wang, “The effect of morphology on the stability of retained austenite in a quenched and partitioned steel,” *Scr. Mater.*, vol. 68, no. 5, pp. 321–324, 2013.
 - [29] C. Sidoroff, M. Perez, P. Dierickx, and D. Girodin, “Advantages and Shortcomings of Retained Austenite in Bearing Steels: a Review,” *Bear. Steel Technol. 10th Vol. Adv. Steel Technol. Roll. Bear.*, vol. 10, no. January, pp. 1–37, 2014.
 - [30] N. Luzginova, L. Zhao, and J. Sietsma, “Evolution and thermal stability of retained austenite in SAE 52100 bainitic steel,” *Mater. Sci. Eng. A*, vol. 448,

- no. 1–2, pp. 104–110, 2007.
- [31] B. Avishan, M. Tavakolian, and S. Yazdani, “Two-step austempering of high performance steel with nanoscale microstructure,” *Mater. Sci. Eng. A*, vol. 693, no. March, pp. 178–185, 2017.
- [32] G. Krauss, “Bainite—An Intermediate Temperature Transformation Product of Austenite,” in *Steels-Processing, Structure, and Performance, Second Edition*, ASM International, 2015, pp. 99–112.
- [33] L. Fielding, “The Bainite Controversy,” *Mater. Sci. Technol.*, vol. 29, no. 4, pp. 383–399, 2013.
- [34] Z. Lawrynowicz and A. Barbacki, “Features of Bainite Transformation in Steels,” *Adv. Mater. Sci.*, vol. 2, no. November, pp. 5–32, 2002.
- [35] F. G. Caballero, M. K. Miller, and C. Garcia-Mateo, “Carbon supersaturation of ferrite in a nanocrystalline bainitic steel,” *Acta Mater.*, vol. 58, no. 7, pp. 2338–2343, 2010.
- [36] H. K. D. H. Bhadeshia and C. Cb, “Nanostructured bainite,” *Proc. R. Soc.*, no. October 2009, pp. 3–18, 2010.
- [37] H. K. D. H. Bhadeshia and A. R. Waugh, “Bainite: An atom-probe study of the incomplete reaction phenomenon,” *Acta Metall.*, vol. 30, no. 4, pp. 775–784, 1982.
- [38] M. K. Miller, P. A. Beaven, S. S. Brenner, and G. D. W. Smith, “An atom probe study of the aging of iron- nickel- carbon martensite,” *Metall. Trans.*, vol. 14, no. 5, pp. 1021–1024, 1983.
- [39] S. H. Talebi, M. Jahazi, and H. Melkonyan, “Retained Austenite Decomposition and Carbide Precipitation during Isothermal Tempering of a Medium-Carbon Low-Alloy Bainitic Steel,” *MDPI*, 2018.
- [40] S. Matas and R. F. Heheman, “Retained Austenite and Tempering of Martensite,” *Nature*, vol. 187, no. 4738, pp. 685–686, 1960.
- [41] A. S. Podder and H. K. D. H. Bhadeshia, “Thermal stability of austenite retained in bainitic steels,” *Mater. Sci. Eng. A*, vol. 527, no. 7–8, pp. 2121–2128, 2010.
- [42] N. V Luzginova, L. Zhao, and J. Sietsma, “Bainite Formation Kinetics in High Carbon Alloyed Steel,” *Mater. Sci. Eng. A*, vol. 482, pp. 766–769, 2008.
- [43] F. G. Caballero and H. K. D. H. Bhadeshia, “Acceleration of Low-temperature Bainite,” *ISIJ Int.*, vol. 43, no. 11, pp. 1821–1825, 2003.
- [44] “As 135 Product Information.”
- [45] G. Petzow, “Metallographic Etching 2nd Edition: Techniques for

- Metallography, Ceramography, Plastography,” pp. 60–61, 2000.
- [46] ASTM, “ASTM E975-13 Standard Practice for X-Ray Determination of Retained Austenite in Steel with Near Random Crystallographic Orientation,” *Astm*, vol. 03, pp. 1–7, 2009.
- [47] B.D.Cullity and S.R.Stock, *Elements of X-ray Diffraction*, 3rd ed. 2001.
- [48] ASTM, “ASTM Standard E8/E8M-16a: Standard Test Methods for Tension Testing of Metallic Materials,” *ASTM Int.*, vol. ASTM Stds., no. Designation: E8/E8M-16a, pp. 1–28, 2013.
- [49] C. Garcia-Mateo, M. Peet, F. G. Caballero, and H. K. D. H. Bhadeshia, “Tempering of hard mixture of bainitic ferrite and austenite,” *Mater. Sci. Technol.*, vol. 20, no. 7, pp. 814–818, 2004.